Characterization of peroxiredoxins and plasmoredoxin of the malarial parasite *Plasmodium falciparum*

Inaugural-Dissertation

zur Erlangung des Grades

Doktor der Naturwissenschaften

- Dr. rer. nat. -

des Fachbereichs Biologie und Chemie, FB08

der Justus-Liebig-Universität Gießen

vorgelegt von

Kathrin Pauli

geboren in Aachen

-2020-

The present thesis was performed during the period of September 2015 to December 2019 at the Institute for Nutritional Sciences, Chair of Biochemistry and Molecular Biology, Interdisciplinary Research Centre, Justus Liebig University, Gießen, Germany. The thesis was supervised by Prof. Dr. med. Katja Becker and Prof. Dr. rer. nat. Albrecht Bindereif.

The thesis defense examination committee was composed of:

Prof. Dr. med. Katja Becker

Prof. Dr. rer. nat. Albrecht Bindereif

Prof. Dr. med. Eveline Baumgart-Vogt

Prof. Dr. rer. nat. Ritva Tikkanen

Declaration

I declare that I have completed this dissertation single-handedly without the unauthorized help of a second party and only with assistance acknowledged therein. I have appropriately acknowledged and cited all text passages that are derived verbatim from or are based on the content of published work of others, and all information relating to verbal communications. I consent to the use of an anti-plagiarism software to check my thesis. I have abided by the priciples of good scientific conduct laid down in the charter of the Justus Liebig University Giessen "Satzung der Justus-Liebig-Universität Gießen zur Sicherung guter wissenschaftlicher Praxis" in carrying out the investigations described in the dissertation.

Eidesstattliche Erklärung

Ich erkläre: Ich habe die vorgelegte Dissertation selbstständig und ohne unerlaubte fremde Hilfe und nur mit den Hilfen angefertigt, die ich in der Dissertation angegeben habe. Alle Textstellen, die wörtlich oder sinngemäß aus veröffentlichen Schriften entnommen sind, und alle Angaben, die auf mündlichen Auskünften beruhen, sind als solche kenntlich gemacht. Ich stimme einer evtl. Überprüfung meiner Dissertation durch eine Antiplagiat-Software zu. Bei den von mir durchgeführten und in der Dissertation erwähnten Untersuchungen habe ich die Grundsätze guter wissenschaftlicher Praxis, wie sie in der „Satzung der Justus-Liebig-Universität Gießen zur Sicherung guter wissenschaftlicher Praxis" niedergelegt sind, eingehalten.

Gießen, 2020

_____

Kathrin Pauli

Acknowledgements

I would like to take this opportunity to thank **Prof. Dr. Katja Becker** for her supervision and unreserved support in the preparation of my doctoral thesis. Her very encouraging and always friendly manner has been very valuable over the past years.

I would like to thank **Prof. Dr. Albrecht Bindereif** for taking over the second supervision of my doctoral thesis.

Furthermore, I would like to thank **Dr. Stefan Rahlfs**, **Dr. Christina Brandstädter** and **Dr. Julia Hahn** for their helpfulness and support in the past.

Special thanks go to **Dr. Karin Fritz-Wolf**, for the endless and enthusiastic discussions and the outstanding professional support.

Many thanks also for the helpfulness of all past and present employees of the **AG Becker**, especially I would like to thank **Michaela**, **Marina**, **Norma**, and **Kim** for their support and the discussions.

Furthermore, I would like to thank **Dr. Kathrin Buchholz** for the pleasant time in our office and for all the interesting discussions.

A very special thank you goes to **Katharina Schuh**, for the funny, also sad and very challenging years, in which a great friendship has developed and which have demanded a lot from us, especially in private life.

Finally, I would like to thank **my family** from the bottom of my heart, who have supported me in every situation in life and have always believed in me.

Summary

Malaria, one of the most severe infectious diseases, is caused by five pathogenic *Plasmodium* species: *P. malariae, P. vivax, P. knowlesi, P. berghei* and *P. falciparum*. The latter, causing severe anaemia and cerebral malaria, accounts for the majority of malaria infections in Sub-Saharan Africa. The malarial parasite possesses two redox systems: the thioredoxin system and the glutathione system, both comprising a cascade of redox-active proteins. As *P. falciparum* lacks catalase and glutathione peroxidase, the parasite is in need of maintaining the intracellular redox balance which is provided by enzymes such as peroxiredoxins.

Peroxiredoxins (Prxs) are thiol peroxidases involved in fundamental processes of life by providing antioxidant defense and by contributing to cellular redox regulation. Prxs are tightly regulated, occur in different oligomerization states, and reduce hydrogen peroxide, organic hydroperoxides, and peroxynitrite by thiol-based enzyme-substitution mechanisms. The unicellular eukaryotic malaria parasite *Plasmodium falciparum* possesses five Prxs including cytosolic Prx1a and Prx6, mitochondrial Prx1m, apicoplast Prx5, and nuclear PrxQ. Furthermore, the parasite imports human erythrocyte Prx2 into its cytosol to enhance its antioxidant capacity.

In this thesis, the contributions of conserved amino acids located closely to the active site, at the dimer/dimer interface, or at the monomer/monomer interface to the catalytic cycle of *Plasmodium* peroxiredoxins were assessed. In-depth site directed mutagenesis studies on *Pf*Prx1a indicated that the substitution of the conserved residue Tyr42 results in a complete loss of peroxidase activity, presumably because the mutated enzyme cannot form the catalytic essential higher oligomers anymore. Loss of Arg125 also led to a drastic decrease in activity, although the dynamic shift from decamer to dimer was intact.

P. falciparum possesses a large repertoire of small redox-active proteins which have a thioredoxin sequence similarity and belong to the group of the thioredoxin superfamily. Plasmoredoxin (Plrx), has been identified by the Becker group and on the basis of databank information, Plrx seems to be unique for *Plasmodium* species.

To continue, the accessibility of individual cysteine residues of *Pf*Prxs and *Pf*Plrx to *S*-glutathionylation and *S*-nitrosation, post-translational modification involved in regulation of protein structure and function, was studied. *Pf*Prx1a, *Pf*Prx1m, *Pf*Prx5, *Pf*PrxQ, and *Pf*Plrx are identified as targets for post-translational modifications.

For further in-depth analysis of the susceptible cysteine residues, cysteine mutants of *Pf*Prx1a (C50S/C74A, C74A/C170S, C50S/C170S, C50S/C74A/C170S), *Pf*Prx5 (C117S, C143S, C117S/C143S), and *Pf*PrxQ (C56S, C103S, C56S/C103S) were glutathionylated. For *Pf*Prx1a, all cysteines were found to be glutathionylated with particular susceptibility of Cys74 and Cys50. Both cysteines of *Pf*Prx5 were glutathionylated, with a slight preference for Cys117 (C_P of Prx5) over Cys143. For *Pf*PrxQ, solely the peroxidatic cysteine Cys56 was found to bind glutathione. All wild type Prxs were analyzed for their glutathionylation sites via mass spectrometry. This method confirmed glutathionylation of all three cysteines in *Pf*Prx1a, and both cysteines in *Pf*Prx5. Although Western Blot analysis had indicated only Cys56 of *Pf*PrxQ as target of glutathionylation, mass spectrometry (MS) showed that also the resolving cysteine Cys103 might be accessible. For *Pf*Prx1m, MS indicated the peroxidatic (C152) and the resolving (C187) cysteine as glutathionylation sites.

*Pf*Plrx wild type enzyme and cysteine mutants *Pf*Plrx^{C3S}, *Pf*Plrx^{C63S}, and *Pf*Plrx^{C115S} were analyzed for their glutathionylation sites via mass spectrometry and the *S*-glutathionylation of the two active site cysteines C60 and C63 could be shown.
Furthermore, *Pf*Prxs and *Pf*Plrx are accessible for *S*-nitrosation.

This data provides further insight into the complex catalysis of these redox-active enzymes and points to potential novel target sites for specific enzyme inhibitors.

Zusammenfassung

Malaria, eine der schwersten Infektionskrankheiten, wird durch fünf pathogene Plasmodium-Arten verursacht: *P. malariae*, *P. vivax*, *P. knowlesi*, *P. berghei* und *P. falciparum*. Letzterer verursacht schwere Anämie und zerebrale Malaria und ist für die Mehrzahl der Malariainfektionen in Afrika südlich der Sahara verantwortlich. Der Malariaparasit besitzt zwei Redoxsysteme: das Thioredoxinsystem und das Glutathionsystem, die beide eine Kaskade von redoxaktiven Proteinen enthalten. Da es *P. falciparum* an Katalase und Glutathionperoxidase mangelt, muss der Parasit das intrazelluläre Redox-Gleichgewicht aufrechterhalten, das durch Enzyme wie Peroxiredoxine bereitgestellt wird. Peroxiredoxine (Prxs) sind Thiolperoxidasen, die an grundlegenden Lebensprozessen beteiligt sind, indem sie für die antioxidative Abwehr sorgen und zur zellulären Redoxregulation beitragen. Prxs sind streng reguliert, treten in verschiedenen Oligomerisierungszuständen auf und reduzieren Wasserstoffperoxid, organische Hydroperoxide und Peroxynitrit durch Thiol-basierte Enzym-Substitutionsmechanismen. Der einzellige eukaryotische Malariaparasit *Plasmodium falciparum* besitzt fünf Prxs, darunter zytosolisches Prx1a und Prx6, mitochondriales Prx1m, apikoplastisches Prx5 und nukleäres PrxQ. Darüber hinaus importiert der Parasit das humane Peroxiredoxin 2 (hPrx2) aus dem Erythrozyten in sein Zytosol, um seine antioxidative Kapazität zu erhöhen.

In dieser Arbeit wurden die Beiträge konservierter Aminosäuren, die sich nahe am aktiven Zentrum, an der Dimer/Dimer-Grenzfläche oder an der Monomer/Monomer-Grenzfläche befinden, am katalytischen Zyklus von Peroxiredoxinen von *P. falciparum* untersucht. Eingehende ortsgerichtete Mutagenesestudien an *Pf*Prx1a zeigten, dass die Substitution des Aminosäurerestes Tyr42 zu einem vollständigen Verlust der Peroxidaseaktivität führt, vermutlich weil das mutierte Enzym die katalytisch essentiellen höheren Oligomere nicht mehr bilden kann. Der Verlust von Arg125 führte ebenfalls zu einem drastischen Rückgang der Aktivität, obwohl die dynamische Verschiebung vom Decamer zum Dimer intakt war.

P. falciparum besitzt ein großes Repertoire kleiner redox-aktiver Proteine, die aufgrund ihrer Sequenzähnlichkeiten zu Gruppe der Thioredoxin-Superfamilie gehören. *Plasmoredoxin* (Plrx), wurde innerhalb der Arbeitsgruppe von Prof. Katja Becker identifiziert, und auf der Grundlage von Datenbankinformationen scheint Plrx einzigartig für Plasmodium-Arten zu sein.

Es wurde zudem die Zugänglichkeit einzelner Cysteinreste von *Pf*Prxs und *Pf*Plrx für die *S*-Glutathionylierung und *S*-Nitrosierung, posttranslationale Modifikationen, die an der Regulation der Proteinstruktur und -funktion beteiligt sind, untersucht. *Pf*Prx1a, *Pf*Prx1m, *Pf*Prx5, *Pf*PrxQ und *Pf*Plrx wurden als Ziele für post-translationale Modifikationen identifiziert. Zur weiteren eingehenden Analyse wurden die Cysteinmutanten von *Pf*Prx1a (C50S/C74A, C74A/C170S, C50S/C170S, C50S/C74A/C170S), *Pf*Prx5 (C117S, C143S, C117S/C143S) und *Pf*PrxQ (C56S, C103S, C56S/C103S) glutathionyliert. Bei *Pf*Prx1a waren alle Cysteine glutathionyliert, wobei eine besondere Anfälligkeit für Cys74 und Cys50 festgestellt wurde. Beide Cysteine von PfPrx5 waren glutathionyliert, mit einer leichten Präferenz für Cys117 (CP von Prx5) gegenüber Cys143. Bei *Pf*PrxQ wurde nur das C_P Cys56 als glutathionbindendes Cystein gefunden. Alle Wildtyp-Prxs wurden mittels Massenspektrometrie auf ihre Glutathionylierungsstellen analysiert. Diese Methode bestätigte die Glutathionylierung aller drei Cysteine in *Pf*Prx1a und beider Cysteine in *Pf*Prx5. Obwohl die Western-Blot-Analyse nur Cys56 von *Pf*PrxQ als Ziel der Glutathionylierung angezeigt hatte, zeigte die Massenspektrometrie (MS), dass auch das C_R Cys103 zugänglich sein könnte. Für *Pf*Prx1m zeigte die MS das C_P (C152) und das C_R (C187) als Glutathionylierungsstellen an.

*P*lasmoredoxin und die Cysteinmutanten *Pf*Plrx^{C3S}, *Pf*Plrx^{C63S} und *Pf*Plrx^{C115S} wurden mittels Massenspektrometrie auf ihre Glutathionylierungsstellen hin analysiert, und die *S*-Glutathionylierung der beiden Cysteine C60 und C63 an der aktiven Stelle konnte gezeigt werden. Darüber hinaus konnte gezeigt werden, dass *Pf*Prxs und *Pf*Plrx für die *S*-Nitrosierung zugänglich sind.

Diese Daten geben weitere Einblicke in die komplexe Katalyse dieser redoxaktiven Enzyme und weisen auf mögliche neue Angriffspunkte für spezifische Enzyminhibitoren hin.

List of Content

List of Tables

List of Figures

List of Abbreviations

Å	Ångström
ATP	Adenosine triphosphate
Bp	Base pair
BSA	Bovine serum albumin
C_P	Peroxidatic cysteine
C_R	Resolving cysteine
DNA	Deoxyribonucleic acid
DNase	Deoxyribonuclease
DTT	1,4-dithiothreitol
E. coli	*Escherichia coli*
ε	Molar extinction coefficient
FF	Fully folded
FPLC	Fast protein liquid chromatography
GLP	Glutaredoxin like protein
GR	Glutathione reductase
Grx	Glutaredoxin
GSH	Glutathione
GSNO	Nitrosoglutathione
GSSG	Glutathione disulfide
H_2O	Water
H_2O_2	Hydrogen peroxide
IPTG	Isopropyl-β-D-thiogalactopyranoside
kDa	Kilodalton
K_M	Michaelis constant
LB	Lysogeny broth
LU	Locally unfolded
Ni-NTA	Nickel nitrilotriacetic acid
NO	Nitric oxide
NOS	Nitric oxide synthase
OD	Optical density
PCR	Polymerase chain reaction
Pf	*Plasmodium falciparum*
pK_a	Logarithmic acid dissociation constant
Plrx	Plasmoredoxin
Prx	Peroxiredoxin
PVDF	Polyvinylidene difluoride
ROS	Reactive oxygen species
SDS	Sodium dodecyl sulphate
SDS-PAGE	Sodium dodecyl sulphate-polyacrylamide gel electrophoresis
St	*Salmonella typhimurium*
TCEP	Tris(2-carboxyethyl)phosphine
TEMED	N,N,N`N,N`-tetramethylethylenediamine
Tris	Tris-(hydroxymethyl)-aminomethane
Trx	Thioredoxin
TrxR	Thioredoxin reductase
U	International unit
V_{max}	Maximum reaction rate
Xc	*Xanthomonas campestris*

Abbreviations of amino acids

amino acid	3 letter code	1 letter code
alanine	Ala	A
arginine	Arg	R
asparagine	Asn	N
aspartic acid	Asp	D
cysteine	Cys	C
glutamic acid	Glu	E
glutamine	Gln	Q
glycine	Gly	G
histidine	His	H
isoleucine	Ile	I
leucine	Leu	L
lysine	Lys	K
methionine	Met	M
phenylalanine	Phe	F
proline	Pro	P
selenocysteine	Sec	U
serine	Ser	S
threonine	Thr	T
tryptophan	Trp	W
tyrosine	Tyr	Y
valine	Val	V

1. Introduction

1.1 Malaria

1.1.1 Malarial infections

Malaria is still one of the most deadly infectious disease. The global distribution of malaria infections is uneven. Due to stable health systems and economic growth the disease was eliminated in temperate areas in Western Europe and North America. However, malarial infections have a broad distribution in the tropics and subtropics. According to the 2019 Malaria Report published by the World Health Organization (WHO), the global prevalence of the malarial infection has decreased from 251 million in 2010 to 221 million in 2013. As visualized in figure 1, the malaria case incident rate dropped from 71 to 57 cases per 1000 population at risk, but is still high in sub-Saharan Africa (WHO 2019).

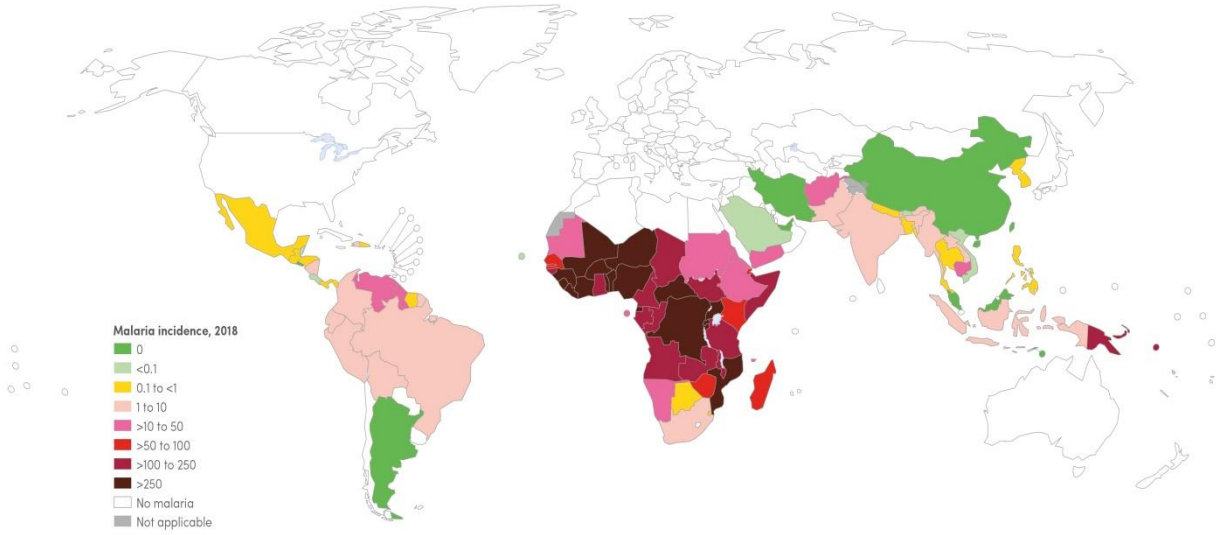

Figure 1: Map of malaria case incidence rate, by country (WHO, 2019).

One of the targets for the millennium development goal by the WHO was to reduce the mortality rate in children under the age of 5 years by two thirds until 2015. In the year 2018, 405.000 malaria deaths occurred; 67% of these deaths were children under the age of 5 (WHO 2019)

Malaria is transferred through an infected female *Anopheles* mosquito. About 400 species of *Anopheles* exist, whereas 60 occur as potential malaria vectors and 30 of

these species are of major importance for malarial infections. The eukaryotic single-celled malaria parasite belongs to the genus *Plasmodium.* Over 100 species of *Plasmodium* are able to infect various animal species including birds and reptiles. Of these parasite species the following five are capable of infecting humans: *Plasmodium vivax, Plasmodium malariae*, *Plasmodium knowlesi*, *Plasmodium ovale*, and *Plasmodium falciparum* (Cox-Singh *et al*. 2008; Schlitzer 2008; Tuteja 2007). The asexual intraerythrocytic cycle of *Plasmodium* is responsible for the malaria-typical clinical symptoms and diseases. The sporozoite-, liver- and gametocyte stadium are asymptomatic. The development of symptoms differs according to species from 6 - 30 days after the infection by an infected *Anopheles* (WHO 2019). The acute illness is marked by fever, headache, vomiting, sweating, with periodic bounds of fever being the main symptom for all malaria infections. These bounds are synchronic with the parasites life cycle, which is accompanied by bursting erythrocytes. The life cycle of *P. vivax* and *P. ovale* lasts 48 hours and underlies a three-day rhythm (Malaria tertiana), whereas *P. malariae* has a 72 hour cycle, resulting in a four-day rhythm for Malaria quartana. The most severe form of the malaria disease is Malaria tropica, with *P. falciparum* causing irregular bounds of fever. According to data published by the WHO, the majority of the malarial infections in sub-Saharan Africa were triggered by *P. falciparum* in year 2018. The symptoms can vary from fever and shivering to diarrhoea and respiratory distress. The severe form of the malarial infection is complex and can additionally trigger pathogenic processes such as anaemia and kidney failure. An infection with *P. falciparum* is especially dangerous for pregnant women and young children. The parasite is a determinant for prenatal mortality and increased mortality in the new born as it infects the placenta (Andrews and Lanzer 2002). The complications of the disease differ depending on the exposure and the age of the patient, but cerebral malaria can occur independent of the age, with coma and acidosis as the most severe manifestation (Beeson *et al*. 2002; Idro *et al.* 2010). Without therapy, a *P. falciparum* infection with manifested blood schizogeny can lead to death after a few days.

1.1.2 Life cycle of *Plasmodium*

Plasmodium parasites have a complex life cycle involving the human and mosquito hosts. Figure 2 represents the life cycle of *Plasmodium* mainly divided into the human liver stage, the human blood stage and the mosquito stage (Winzeler 2008). The life

cycle proceeds as sexual stage in mosquito host, and asexually in the human host. The life cycle begins when an infected female *Anopheles* mosquito injects its saliva in preparation for an upcoming blood meal. The injected saliva contains a small number of sporozoites, the motile form of the parasite, which immigrate into the human host's skin remaining at the endothelium for several hours or days. The sporozoites are slowly released into the blood stream and travel to the liver where they penetrate the hepatocytes. Within the hepatocytes the liver stage proceeds asymptomatically and the sporozoites of *Plasmodium* replicate, increasing in number up to 100.000 fold (Tuteja 2007). The duration of this phase varies from 2 days in *P. berghei* to 6-15 days in human pathogen species.

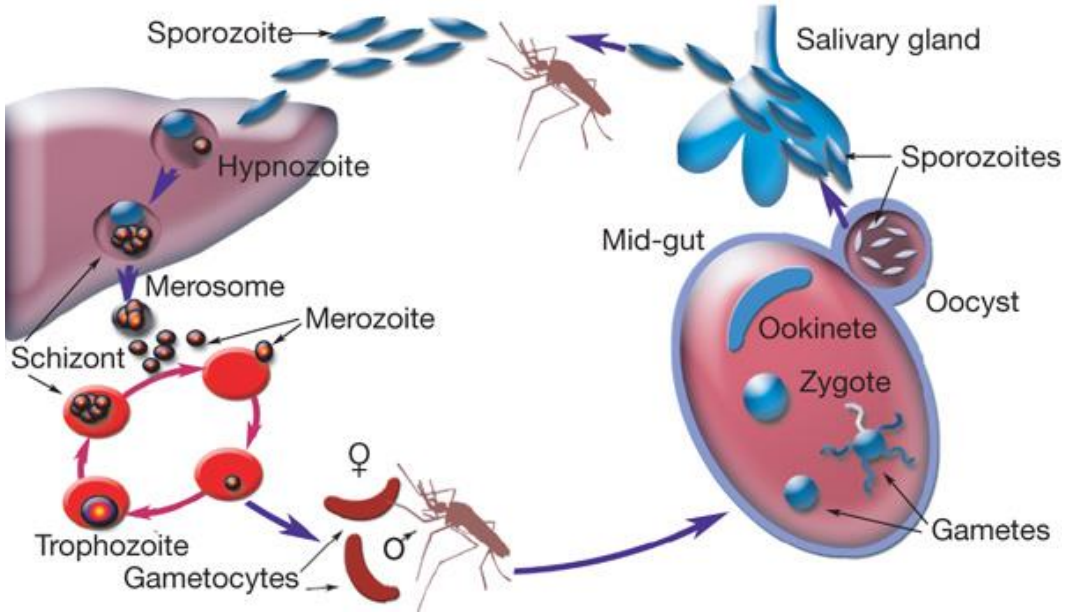

Figure 2: The life cycle of *Plasmodium* parasites. Mainly divided into the human liver stage, human blood stage and mosquito stage, the life cycle begins with the injection of sporozoites from the mosquito's saliva into the human host's skin. After penetrating the hepatocytes, sporozoites develop into tissue schizonts revealing merozoites which invade erythrocytes replicating asexually in a 48-hour cycle. Gametocytes, the sexual form, are taken up by the mosquito and infect the mosquito host (Winzeler 2008).

Within this time mature sporozoites develop into tissue schizonts, containing thousands of merozoites, the blood stage of the parasite. Having entered the blood stream in the parasitic vacuole, the merozoites develop into mature schizonts (Winzeler 2008; Tuteja 2007).

The parasites develop through different stages. The early trophozoite is often referred to as the ring stage due to the typical morphology. The parasite enlargement

at this stage is based on a very active metabolism, including the glycolysis of a large amount of glucose and the proteolysis of haem of the erythrocytes into amino acids. The end of the trophic stage results in the formation of schizonts containing approximately 20 merozoites which are released into the blood stream after lysis of the erythrocyte to invade another red blood cell (RBC) (Tuteja 2007). The parasite utilizes the erythrocytic haemoglobin as an important source for amino acids, although the by-product haem cannot be metabolized. Since haem is toxic for the parasite, it gets polymerized to haemozoin (malaria pigment) and accumulates in the parasite's vacuole (Goldberg and Slater 1992). The release of the merozoites into the blood circulation is accompanied with increasing body temperature. A small number of merozoites in the erythrocytes differentiate to micro- and macrogametocytes, the sexual forms, which are of importance for infecting the next mosquito host. The asexual forms of the parasite are pathogenic, affecting numerous organs. The sexual forms are non-pathogenic for the human host but are taken up by mosquitos, where they infect the mosquito host by producing sporozoites, making the mosquito infectious for humans (Aravind *et al.* 2003; Tuteja 2007).

1.1.3 Fighting malaria

The WHO describes malaria as entirely preventable and treatable. In the 17. Century Chinin was the first effective agent against *P. falciparum*-malaria. From the 1950s onward, chloroquine and amodiaquin were substances of choice for the treatment against every variant of malarial infections. Shortly after the introduction of chloroquine as antimalarial drug, resistances developed in malaria endemic countries Colombia and Venezuela (Wellems and Plowe 2001; YOUNG and MOORE 1961) and spread to South America, south East Asia, india and the eastern regions of Africa. Thailand was the first country to widely distribute Mefloquine as malaria drug treatment, and, with rising resistances, the therapy was accompanied by artesunate. This drug combination (artemisinin-based combination therapy) was found to be very effective, resulting in decreased incidences of *P. falciparum*-malaria. The currently used antimalarial drugs are subdivided into seven drug classes, namely 4-aminoquinolines, arylaminoalcohols, 8-aminoquinolines, artemisinins, antifolates, inhibitors of the respiratory chain, and antibiotics (Schlitzer 2008). The WHO recommends the treatment of uncomplicated *P. falciparum*-malaria with artemisinin – based combination therapy (ACTs) as a first-line treatment (WHO 2019). Artemisinin possesses a peroxide structure, losing stability in the presence of iron ions and

producing radicals. ACTs are a common drug therapy combining an artemisinin-derivative with an antimalarial drug. Due to the combination of the fast-acting artemisinin with a longer half-life drug, the elimination of all parasite stages is ensured. First drug resistance of *P. falciparum* against artemisinin has been detected in five countries of South East Asia (Cambodia, Laos, Myanmar, Thailand, Vietnam). However, as long as the partner drug in the combined therapy is locally effective, artemisinin-derivatives remain effective (WHO 2019). With regard to antimalarial drug development, the redox metabolism represents the most promising approach as the parasite is highly sensitive to oxidative stress. This can be achieved by the development of enzyme specific inhibitors, which are capable of paralysing the parasites anti-oxidative defence (Budde and Flohé 2003; Krauth-Siegel *et al.* 2005). This phenomenon is underlined by the fact, that a glucose-6-phosphate-dehydrogenase deficiency (G6PD deficiency) in human gives a degree of protection against malaria. The G6PD deficiency is a congenital deficiency of the enzyme due to mutation of the G6PD gene, which is located on the X-chromosome. The physiological function of the enzyme in the pentose phosphate cycle is the conversion of glucose-6-phosphate to D-glucono-1,5-lakton-6-phosphate accompanied by the formation of reduced Nicotinamide adenine dinucleotide phosphate (NADPH). NADPH is a cofactor of the enzyme glutathione reductase, which is of major importance to maintain the reduced intracellular milieu by reducing glutathione disulfide to glutathione. The enzyme G6PD is therefore indispensable for the recycling of oxidized Nicotinamide adenine dinucleotide phosphate ($NADP^+$) to NADPH and responsible for the perpetuation of the anti-oxidative capacity in human and parasite, since the parasite uses the host´s NADPH for its own anti-oxidative defence (Eckman and Eaton 1979). The effects of G6PD deficiency vary from absence of symptoms to haemolytic anaemia. Worldwide, about 200 Million people are affected by this gene mutation, predominantly in malaria-endemic regions, implying a coevolution of G6PD deficiency and malaria (Clarke *et al*. 2017; Nguetse *et al*. 2016; Atamna *et al.* 1994; Becker *et al*. 2005; Hunt and Stocker 1990). Due to the increasing resistances, antimalarial drug development is crucial and remains a challenge. Therefore, novel drugs should be sufficient for eliminating all strains and should be suitable for sensitive groups such as pregnant women and children. Possible novel approaches for drug development are blood stage gametocytes as

they transfer the infection from the human host to the mosquito (Lucantoni *et al*. 2013).

In the past years a lot of effort has been put into the development of anti-malarial vaccines and some candidates have been identified for targeting the parasite´s blood stage (Salamanca *et al*. 2019). The majority of vaccine candidates are in phase I trials, had an acceptable safety profile and strong immunogenicity when exposed to homologous parasite strains (Salamanca *et al*. 2019). However, the candidates' efficacy dropped when being exposed to heterologous strains, again showing the urgency for improvement of antimalarial vaccinations (Metzger *et al.* 2020; Salamanca *et al*. 2019). The most advanced vaccine available is the pre-erythrocytic subunit vaccine RTS,S/ ATS01 (Ballou *et al*. 1985). During phase III testing and an 18 month follow-up the total effectiveness of the vaccine varied from 5-45 %, depending on age and case definition (Metzger *et al*. 2020). However, a vaccine with 75 % and more effectiveness, as required by the WHO, is momentarily out of reach (Salamanca *et al*. 2019; Metzger *et al*. 2020).

1.2 Peroxiredoxins

1.2.1 Importance of peroxiredoxins

Peroxiredoxins (Prxs) are very efficient cysteine-peroxidases and are of major importance in antioxidant, regulatory and signalling systems (Gretes *et al*. 2012), and play an important role in detoxifying hydrogen peroxide, organic hydroperoxides and peroxynitrite (Chae *et al.* 1994; Rahlfs and Becker 2001; Richard *et al*. 2011; Djuika *et al.* 2013). Prxs form a very widely spread family of enzymes, presumably evolved from an ancestor protein with the typical thioredoxin fold (Chae *et al.* 1994; Copley *et al.* 2004). Prxs are abundant proteins accounting for approximately 0.1 – 1 % of soluble proteins in most cells and tissues (Chae *et al.* 1999). In human, the highest concentration (5,6 mg/ml RBC) of Prx2 was found in erythrocytes (Moore *et al*. 1991; Low *et al*. 2008). The importance of Prxs in cell homeostasis is underlined by the observations of the overexpression of some Prxs in human breast and lung cancer (Chang *et al.* 2001; Tehan *et al*. 2013). Additionally, knock out of the most abundant Prx1 in mice led to the development of malign tumours and haemolytic anaemia (Neumann *et al*. 2003). The depletion of mitochondrial human Prx3 (hPrx3) is

suggested to promote increasing levels of intracellular hydrogen peroxide (H_2O_2) and has sensitizing effects on cell-induced apoptosis (Chang *et al*. 2004). Furthermore, hPrx5, also located in the mitochondria, inhibited apoptosis (Zhou *et al*. 2000), and protects mitochondrial DNA from oxidative damage caused by H_2O_2 (Banmeyer *et al.* 2005). The six human peroxiredoxins play important roles in the central nervous system and in inflammatory diseases. High levels of hPrxI were observed in glia cells and neuronal cells as a result of haemorrhagic stress (Nakaso *et al.* 2000) and exposure to haemin (Nakaso *et al.* 2003). Moreover, hPrx3 levels correlate with human age, showing lower protein levels in brain samples of elderly (Park *et al.* 2016; Chen *et al.* 2003; Krapfenbauer *et al.* 2003) and has altered expression levels in neurodegenerative diseases (Krapfenbauer *et al*. 2003; Kim *et al.* 2001). Huh *et al.* 2012 also showed, that hPrx3 has a beneficial role in inflammatory diseases, since hPrx3 deficiency increased abnormal lipid accumulation in adipose tissue, due to increased ROS (Huh *et al.* 2012). To continue, the expression of hPrx4 is increased in Rheumatoid Arthritis patients, which showed that hPrx4 inhibts inflammatory diseases by suppressing oxidative stress and inflammatory signalling (Chang *et al*. 2009; Park *et al*. 2016).

1.2.2 Structure and catalytic cycle of peroxiredoxins

The Prx family is structurally distinguished into 3 types including the typical 2-Cys peroxiredoxin, the atypical 2-Cys peroxiredoxin and the 1-Cys peroxiredoxin (Wood *et al*. 2003b). The classification of the different Prx family members is determined by the number of the active site cysteines involved in the catalytic cycle. The complete catalytic cycle of Prxs can be subdivided into the main steps of peroxidation, resolution and recycling, with steps 2 and 3 requiring local conformational changes (Figure 3)(Hall *et al*. 2011; Gretes *et al*. 2012; Perkins *et al*. 2014; Wood *et a*l. 2002). For the first step of the cycle, the starting position of the Prx is in a fully folded (FF) active state. The peroxidatic cysteine of the Prx is in its reduced thiolate form and has the ability to react directly with peroxide substrates. During the step of peroxidation, a nucleophilic attack by the thiolate of the peroxidatic cysteine (C_P) on the peroxide is carried out, releasing the corresponding alcohol or water. Cysteines with a basic environment surrounded by His, Lys or Arg residues, as present in typical 2-Cys Prxs, undergo a greater deprotonation resulting in higher reaction rates with H_2O_2 under sulfenic acid formation (Peskin *et al*. 2016; Forman *et al*. 2004).

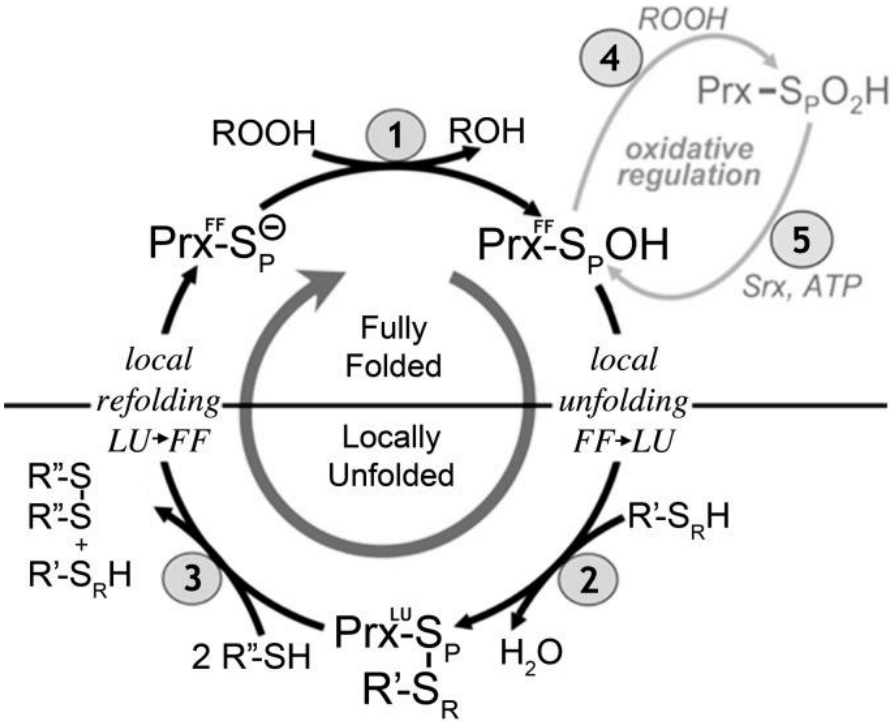

Figure 3: The Prx catalytic cycle. Peroxide reduction by Prxs involves the three main steps of reduction, resolution and recycling. Two protein conformations are involved in the catalysis: FF (fully folded active-site) and LU (locally unfolded, disulfide between peroxidatic and resolving cysteines). The resolving cysteine can be supplied by a different protein (1-Cys mechanism) or by a second Cys within the same Prx (Gretes *et al.* 2012).

The thiol of the C_P itself is oxidized to sulfenic acid. The following step of resolution is characterised through the attack on the sulfenic acid by a resolving thiol. In case of a 2-Cys mechanism the resolving thiol is on the peroxiredoxin itself, whereas 1-Cys Prxs rely on other proteins or molecules. The active site of the Prx is locally unfolded (LU) for the resolution step that resolves when the sulfenic acid is exposed to form a disulfide bridge with the resolving thiol. In the case of a 2-Cys mechanism, an intramolecular disulfide bridge is formed, whereas in the case of a 1-Cys peroxiredoxin, the disulfide bridge is built intermolecularly. In the last step of the catalytic cycle, the disulfide bridge between the peroxidatic and the resolving cysteine is reduced by a cysteine thiol of an additional protein, e.g. glutaredoxin or thioredoxin. Completing the cycle, the active site refolds to the FF conformation, which is the required position for the reduction of peroxide substrates (Wood *et al*. 2002). A number of Prxs are sensitive to hyperoxidation of the peroxidatic sulfenic acid. Hyperoxidation can occur when a second peroxide molecule reacts with the sulfenic acid to form cysteine sulfinic acid (Wood *et al.* 2002). In many organisms the sulfinic acid of the peroxidatic cysteine can be reactivated by an adenosine triphosphate

(ATP)-dependent reduction with sulfiredoxin. However, a gene encoding sulfiredoxin appears to be non-existent in protozoan parasites (Gretes *et al.* 2012).

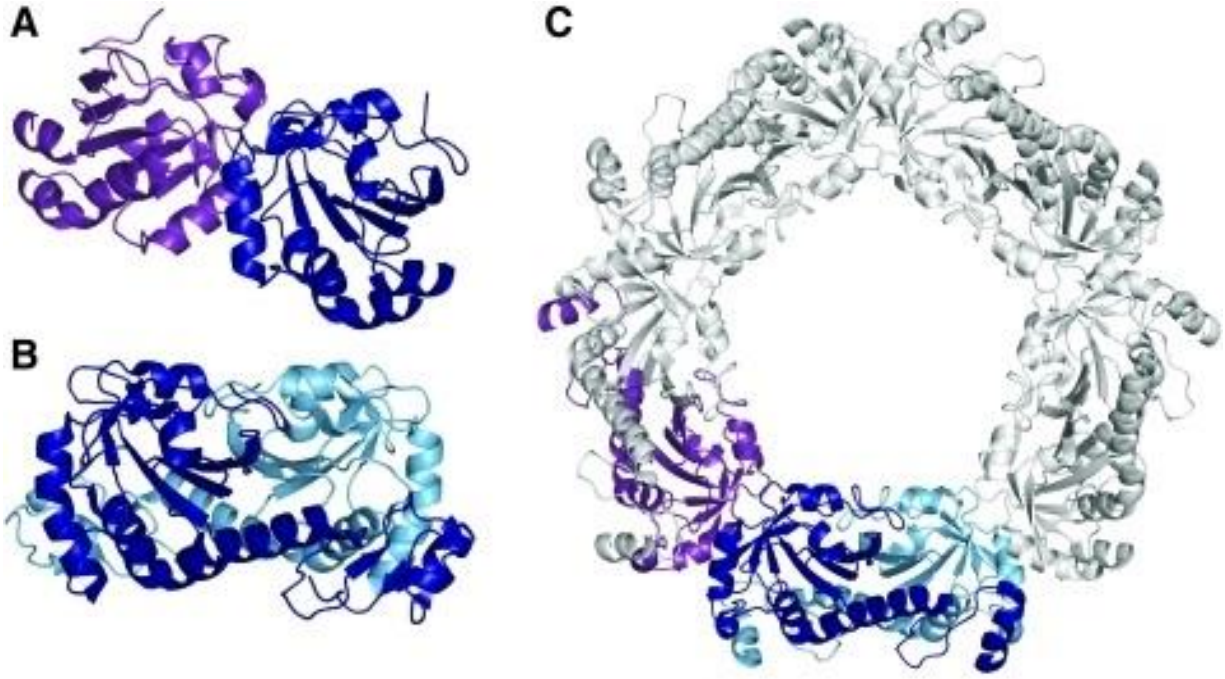

Figure 4: Quaternary structures of Prxs. Monomeric structure can form A-type dimers (A) or B-type dimers (B). Some Prxs form decameric structures through the interaction of four to six B-type dimers over the A-type interface (C) (Hall *et al.* 2011).

Almost all Prxs are known to form dimers, and a variety of subfamilies form decameric or dodecameric oligomer structures. Prxs that are present and active as monomers have only been observed in the BCP subfamily. As mentioned in numerous studies (Wood *et al.* 2003; Karplus and Hall 2007; Sarma *et al*. 2005), oligomeric Prxs are formed by associations involving two interfaces. One interface involves the association of the central ß-sheet of two Prx chains, the other interface is an association of a helix packing against the counterpart of the other subunit (Karplus and Hall 2007). These interfaces are referred to as B-type interface (for ß-sheet based) and A-type interfaces (“alternate” or “ancestral”) (Sarma *et al.* 2005).

For most Prxs building B-type dimers, oligomers are formed with up to six B-type dimers associating through the A-type interface to form a ring-like structure (Figure 4, C). It is suggested that during the catalytic cycle of the Prxs, dissociation at the A-type interface occurs, causing a transition from an oligomeric to dimeric structure linked to the redox state. Reduced and hyperoxidized Prxs reveal a decameric structure with the A-type interface stabilising the fully folded active site of the Prx.

The formation of a dimeric structure is therefore linked to an oxidized state of the Prx with a formed disulfide bridge destabilizing the A-type interface (Hall *et al*. 2011; Wood *et al.* 2002).

1.2.3 Other amino acid residues participating in catalysis and oligomerization

The C_P, located at the enzymes active site, is completely conserved among all members of the peroxiredoxin family, with a selenocysteine-containing Prx in *Eubacterium acidaminophilum* being one exception (Söhling *et al*. 2001). The exact mechanism of the removing of the proton from the peroxidatic Cys and which residue could be responsible for this role, is still to be elucidated. The Prx active site possesses a conserved structure, with two of the most highly conserved amino acid residues threonine (Thr) and arginine (Arg) appearing to act directly with the peroxidatic cysteine during catalysis (Figure 5). In a few Prxs, the Threonine proximal to the peroxidatic Cys is naturally substituted by a Serine. In Prx5, the hydroxyl group of the Thr side chain was shown to be of importance, since a Serine replacement did not alter activity, whereas the substitution of Thr by Valine inactivated the enzyme (Wood *et al*. 2003a; Flohé *et al.* 2002). Moreover, numerous studies revealed the conserved Arg residue being indispensable for Prx catalysis, since the substitution altered the Cp reactivity (Montemartini *et al.* 1999; Tairum *et al*. 2012; Tairum *et al*. 2016; Nelson *et al*. 2018; Schröder *et al*. 2000; König *et al.* 2003). Mutagenesis of this residue in *Crithidia fasiculata* (Montemartini *et al.* 1999) and *Leishmania donovani* (Flohé *et al.* 2002) resulted in inactive enzymes. A substitution to alanine in *Salmonella typhimurium* (*S. typhimurium*) AhpC, a typical 2-Cys peroxiredoxin, did not affect the enzymes reactivity (Nelson *et al.* 2018). Furthermore, in *P. falciparum* Prx6 a substitution of a conserved active site proximal histidine to tyrosine increased the enzyme activity four- to six- fold (Feld *et al*. 2019).

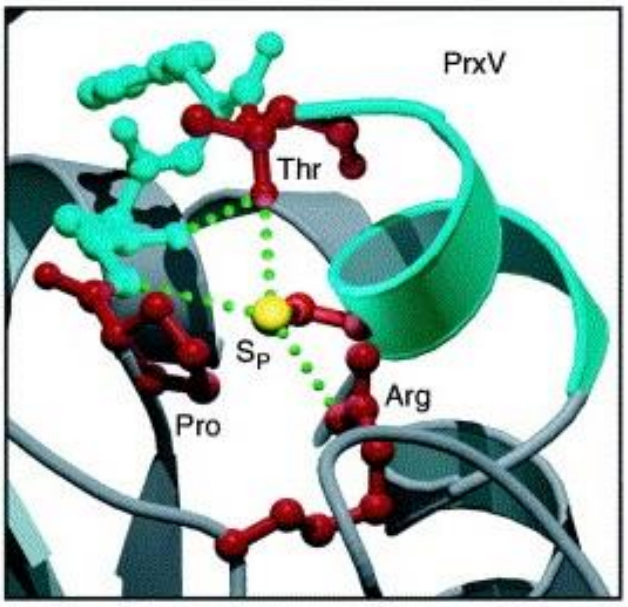

Figure 5: Conserved structure of Prx active sites. Conserved Cys, Pro, Arg and Thr are shown in red. Dotted green lines indicate the hydrogen bonding network between the conserved amino acids (Wood *et al.* 2003).

The formation of decamers from dimers via the enzymes A-type interfaces is a property of some typical 2-Cys peroxiredoxins. Numerous studies have enlightened the importance of conserved amino acids contributing to oligomerization and activity of the enzyme (Loberg *et al.* 2019; Nelson *et al.* 2018; Sarma *et al.* 2005; Parsonage *et al.* 2005). In yeast Prx, aromatic residues at the dimer-dimer interface were identified to have an impact on decamer formation and activity, since mutations showed a 10-fold to 100-fold lower reactivity with H_20_2 (Loberg *et al.* 2019). Tairum *et al*. indicated a threonine destabilizing the decameric structure in the enzymes oxidized state due to steric hindrance (Tairum *et al*. 2016). Moreover, in *S. typhimurium* a substitution of Thr to isoleucine (Ile) disrupted the decamer, whereas a mutation to Val had a stabilizing effect on the decamer formation (Nelson *et al*. 2018).

1.3 Redox-metabolism in *Plasmodium falciparum*

The glutathione and thioredoxin systems are of major importance for maintaining an intracellular redox balance. As shown in figure 6, both systems depend on the reducing agent NADPH provided mainly by the pentose phosphate shunt. NADPH reduces thioredoxin reductase (TrxR), which delivers electrons to its substrate thioredoxin (Trx). Trx then reduces protein disulfides (Holmgren and Bjornstedt

1995). NADPH also provides electrons for the glutathione system by reducing glutathione reductase (GR). GR reduces oxidized glutathione (GSSG) by generating two molecules of reduced glutathione (GSH), which can provide electrons to oxidized glutaredoxin (Grx) (Holmgren 1978).

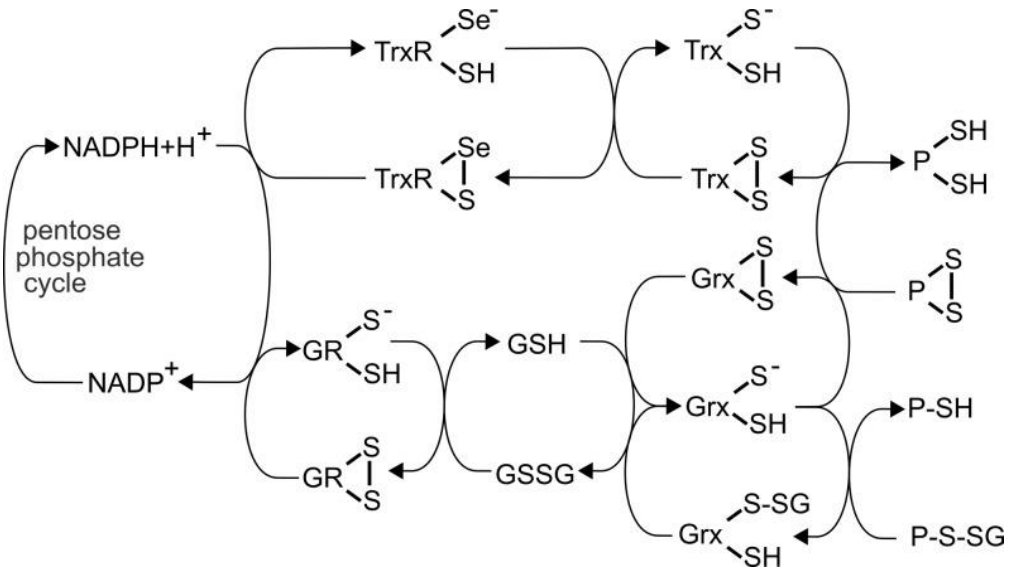

Figure 6: Electron flow from NADPH to substrates via the Trx and GSH/Grx systems. The electrons are provided by NADPH for both pathways. NADPH reduces TrxR, which delivers electrons to Trx. Trx reduces protein disulfides. NADPH also reduces GR which reduces GSSG by generating two molecules of GSH. GSH provides electrons to oxidized glutaredoxin (Hanschmann *et al*. 2013).

1.3.1 Thioredoxin system in *P. falciparum*

The parasite *P. falciparum* is highly adapted to oxidative stress. Due to the rapid development and spread of merozoites in an environment containing high oxygen tension the parasite is in need of an effective anti-oxidative system. Besides, as the parasite digests a large amount of haemoglobin within the red blood cells, a considerable amount of prooxidative haem iron is produced, requiring detoxification (Rahlfs and Becker 2001; Becker *et al.* 2004). In *P. falciparum* the thioredoxin system plays a crucial role in the defence against oxidative stress, especially since the parasite lacks catalase, glutathione peroxidase and sulfoxide reductase (Sztajer *et al.* 2001; Clarebout *et al.* 1998). The system comprises a variety of proteins including an NADPH–dependent TrxR, Trx, and peroxiredoxins (Prxs) (Kanzok *et al*. 2000). The

latter removes harmful peroxides with electron donation provided by Trx and TrxR (Rahlfs and Becker 2001).

Thioredoxin reductase

The malarial parasite *P. falciparum* possesses two TrxR isoforms located in the mitochondria and in the cytosol (Jortzik and Becker 2012; Kehr *et al*. 2010). TrxR reduces its major substrate Trx, which is highly dependent on the activity of the enzyme (Berndt *et al.* 2008). *Pf*TrxR was shown to be essential for the intraerythrocytic stages of *P. falciparum* and therefore a possible target for antimalarial drugs (Krnajski *et al*. 2002). The differences of hTrxR and *Pf*TrxR regarding their seleno-based and thiol-based catalytic mechanism was proposed for specific drug design (Becker *et al*. 2000). The gold-based auranofin was shown to inhibit *Pf*TrxR and therefore the growth of the parasites *in vivo* (Sannella *et al.* 2008), but the compound also inhibited human TrxR (Urig und Becker 2006). The inhibition of *Pf*TrxR was found to be non-competitive regarding both substrates Trx and NADPH, showing no interaction of the inhibitor neither with the C-terminal redox centre of TrxR nor with the NADPH binding site (Andricopulo *et al.* 2006). Interestingly, in contrast to *P. falciparum*, a systematic phenotype analysis throughout the life cycle of *Plasmodium berghei* excluded an essential function for TrxR for any of the developmental stages (Buchholz *et al*. 2010). These differences could be due to differences in the redox system of *P. berghei* and *P. falciparum*.

Thioredoxin

The functions of Trx are mainly characterized by modifications in the redox status of protein targets by its active site cysteine structure. The malarial parasite possesses three classical Trx and two thioredoxin-like proteins, the latter cannot be reduced by TrxR (Jortzik and Becker 2012; Krnajski *et al*. 2001). *Pf*Trx1 is located to the cytosol (Kehr *et al*. 2010) and has the ability to directly reduce oxidized glutathione (Kanzok *et al.* 2000). In addition, *Pf*Trx1 supports maintaining the redox balance by directly detoxifying H_2O_2, tert-butylhydroperoxide, and cumene hydroperoxides (Rahlfs *et al*. 2003) and reduces Trx-dependent peroxiredoxins (Rahlfs and Becker 2001).

1.3.2 Glutathione system in *P. falciparum*

Glutathione

Glutathione (GSH) is the major redox buffer of most aerobic cells. The ratio between GSH and GSSG varies between 10:1 and 100:1. Oxidized glutathione (GSSG) is a result of a variety of reactions and is toxic to the cell above concentrations of 100 µM (Becker *et al*. 2003b). GSH has an estimated concentration of about 2 mM in the cytosol of trophozoites, which is remarkably higher than NADPH (<100 µM) and Trx (10 µM) (Becker et al. 2003b). The GSH:GSSG ratio is maintained on the side of the reduced form catalyzed by GR. Despite functioning as a redox buffer, GSH is an effective cofactor for a variety of proteins including glutathione-dependent peroxidases and Grxs. The glutathione metabolism of *Plasmodium* infected erythrocytes is not limited to its redox and antioxidant functions, but is also involved in drug resistance (Becker *et al.* 2004; Harding *et al*. 1996). *Plasmodium* parasites possess a functional glutathione synthesis pathway. When the parasitic *de novo* synthesis of GSH is inhibited, half of the amount of cellular glutathione is lost within a short period of time, suggesting a high dependency of the parasitized cell on the *de novo* synthesis of GSH. Increased oxidative stress in *Plasmodium*-infected erythrocytes can be due to a lack of intracellular glutathione (Meierjohann *et al.* 2002; Muller *et al.* 2001; Becker *et al.* 2004).

Glutathione reductase

GR is a flavoenzyme of the pyridine nucleotide-disulfide oxidoreductase family, which forms stable homodimers containing NADPH and GSSG binding sites (Karplus and Schulz 1987). The enzyme has GSSG and NADPH + H^+ as substrates and two molecules of GSH as well as $NADP^+$ as products. Therefore, GR adopts a central role in the glutathione system by maintaining the majority of the intracellular glutathione pool in a reduced state (Jortzik and Becker 2012; Bohme *et al.* 2000). The reaction catalysed by GR comprises a reductive half-reaction and an oxidative half-reaction. The relevance of GR catalysis for the cell has been the subject of a variety of studies. GR from malarial parasites was shown to be essential for oocyst development in the mosquito midgut but not for the blood stage parasites in the vertebrate host (Pastrana-Mena *et al*. 2010; Buchholz *et al.* 2010). GR is dispensable for asexual growth in *P. berghei* blood stages, as the loss of GR function resulted in viable and infectious blood stage parasites *in vivo* (Buchholz *et al*. 2010).

Interestingly, mice exposed to *Anopheles* infected with GR knock out *P. berghei* did not develop malaria (Buchholz *et al*. 2010). However, in contrast to *P. berghei*, *P. falciparum* was shown to require GR for survival during its blood stages in the human host (Patzewitz *et al*. 2012). As human and malarial GR differ significantly concerning their kinetic and redox properties, a variety of strategies to exploit malarial GR as a possible drug target were subject of numerous studies. Therefore, approaches including the irreversible inhibition of the enzyme at the GSSG binding site and the exploitation of the enzyme in order to generate harmful redox cyclers have been made (Farber *et al.* 1998; Buchholz *et al.* 2010; Friebolin *et al.* 2008).

Glutaredoxin

Glutaredoxins (Grxs) are a family of thiol-disulfide oxidoreductases that use glutathione (GSH, GSSG) as cofactor (Stroher *et al*. 2012; Rahlfs *et al.* 2001). The redox-proteins are involved in maintaining the thiol-disulfide redox state within cells. Grxs are associated with a variety of functions. In early studies Grx were mentioned as GSH-dependent hydrogen donors for ribonucleotide reductase and as reductant for methionine sulfoxides and sulfates (Holmgren 1979). *P. falciparum* possesses one dithiol glutaredoxin (*Pf*Grx1) and three monothiol Grx-like proteins (Glp1-3) (Rahlfs *et al.* 2001; Deponte *et al*. 2005). *Pf*Grx-1 has a molecular weight of 12.4 kDa and exhibits the characteristic active site motif CPYC. The protein was shown to be remarkably temperature stable, showing 100% activity at 60 °C and a residual activity of 50 % at 90 °C (Rahlfs *et al.* 2001). The activity of *Pf*Grx-1 has been detected in trophozoites and does not differ between drug-sensitive and drug-resistant parasites (Rahlfs *et al.* 2001). Studies observing the effects of antimalarial drugs on PfGrx-1 revealed an inhibition only up to 20 % of *Pf*Grx-1 activity, suggesting *Pf*Grx-1 unlikely to be a target of antimalarial drugs. One exception was shown to be methylene blue inhibiting *Pf*Grx-1 activity up to 90 % (Rahlfs *et al.* 2001), although this inhibition could be due to the inhibition of GR (Farber *et al.* 1998). Additionally, *Pf*Grx-1 clearly revealed a glutathione dependency showing a non-enzymatic reduction by GSH. Many target proteins of *Pf*Grx-1 overlap with those identified for *Pf*Trx1, indicating similar redox-regulatory features of *Pf*Grx-1 and *Pf*Trx1 (Sturm *et al.* 2009). The glutaredoxin-like proteins *Pf*Glp1 and *Pf*Glp2 are located to the cytosol, whereas *Pf*Glp3 is in the mitochondria and could contribute to the redox network of this organelle (Kehr *et al.* 2010). The exact physiological function of the three

monocysteinic *Pf*Glps could not be elucidated, but the possibility of deglutathionylation of redox-regulated proteins by *Pf*Glp1-3 has been proposed (Jortzik and Becker 2012).

1.3.3 Plasmoredoxin

P. falciparum possesses a large repertoire of small redox-active proteins which have a Trx sequence similarity (Müller 2004) and belong to the group of the thioredoxin superfamily. Beside the above mentioned Grx, Trx and three Grx-like proteins, a 22 kDa protein, Plasmoredoxin (Plrx), has been identified by the Becker group (Becker *et al.* 2003a). On the basis of databank information, Plrx seems to be unique for *Plasmodium* species. Since the inhibition of a *Plasmodium*-specific protein reduces possible side effects in the human host, Plasmoredoxin is a promising approach for antimalarial drug development.

The active site WCKYC-motif of Plrx differs to the WCGPC-motif, which is found in the thioredoxin superfamily. Thioredoxins are a group of small redox-active proteins (12 kDa), which are involved in redox-regulatory processes, antioxidant defence and in the synthesis of desoxyribonukleotids (Rahlfs *et al.* 2002). Thioredoxin and glutaredoxin share structural and functional properties, whereas the identity of Plrx with members of the Trx superfamily is relatively low, with 31.4 % identity with Trx and 27.5 % identity with Grx (Becker *et al*. 2003a). Analogous to Trx and Grx, Plrx is capable of reducing ribonucleotide reductase *in vitro* (Müller 2004; Becker *et al*. 2004; Rahlfs *et al.* 2003). Plasmoredoxin can furthermore be reduced by Trx and Grx (Becker *et al*. 2003a), showing further relations between the thioredoxin and glutathione system in *P. falciparum*. The reduction of Plrx by GSH could also be monitored, which was inefficient and does not seem to be of physiological importance (Becker *et al*.2003a). Interestingly, Plrx cannot be reduced by *Pf*-thioredoxin- and *Pf*-glutathione reductase, leaving the *in vivo* reaction partners to be elucidated. Plasmoredoxin is redox-active in the insulin-reduction assay and reduces glutathione disulfide *in vitro* (Becker *et al*. 2003a). Furthermore, Plrx transfers electrons to *Pf*Prx1a and *Pf*Prx5 (Nickel *et al.* 2005; Becker *et al.* 2003a), whereas the interaction with the latter seems unlikely *in vivo* due to the cellular structure (Becker *et al.* 2003a).

A Plrx knock-out in *P. berghei* was not letal (Buchholz *et al.* 2008). The transcription levels of *Pf*Trx, *Pf*TrxR and *Pf*GR were slightly increased, whereas no changes could

be observed for *Pf*Grx (Buchholz *et al*. 2008). Via pulldown assays 21 interaction partners could be found for Plrx (Sturm *et al*. 2009). Besides numerous proteins which were also found to be target proteins for Trx and Grx, putative partners e.g. co-chaperon GrpE, disulfid isomerases, acyl-carrier proteins and enzymes, which are involved in signal transduction, DNA- synthesis and repair, were identified (Sturm *et al*. 2009). Furthermore, Plrx as well as *Pf*Trx and *Pf*Grx were found to be active in deglutathionylation reactions of modified proteins in *P. falciparum* (Kehr *et al*. 2011).

1.3.4 Peroxiredoxins of *P. falciparum*

In parasitic organisms the Prxs are important for the defence against hydrogen peroxides and peroxynitrite derived by the host´s organism or produced endogenously. Malarial parasites possess five types of Prxs that can be distinguished according to their cellular location (Figure 7), substrate specificity, and active site cysteine motif (Jortzik and Becker 2012; Kehr *et al.* 2010). Interestingly, *Plasmodium* utilizes human Prx2 by importing the enzyme from the human erythrocyte (Koncarevic *et al*. 2009).

Peroxiredoxin 1a

*Pf*Prx1a is a cytosolic peroxiredoxin of *P. falciparum* with a molecular weight of ~ 22 kDa. The 2-Cys Prx1a can be reduced by thioredoxin (Rahlfs and Becker 2001; Akerman and Müller 2003) and plasmoredoxin (Nickel *et al*.2005), and efficiently cleaves hydrogen peroxide *in vitro* which suggests a crucial role as peroxidase (Rahlfs und Becker 2001). Furthermore, pull-down studies using lysate from *P. falciparum* trophozoite blood stages identified 91 proteins which exclusively interacted with Prx1a, 37 of these were located to the cytosol (Brandstaedter *et al*. 2019). The captured proteins were shown to be involved in numerous cellular pathways such as carbohydrate metabolism, protein folding, or signal transduction (Brandstaedter *et al*. 2019).

The catalytic efficiency of *Pf*Prx1a for reducing hydrogen peroxide qualifies the enzyme to be one of the most efficient peroxiredoxins in *P. falciparum.* Recombinant Prx1a showed peroxidase activity when hydrogen peroxide, t-butyl hydroperoxide, and cumene hydroperoxide were available as substrates (Rahlfs and Becker 2001). Prx1a shares 47 % sequence identity with human Prx2 and has been classified as a typical 2-Cys peroxiredoxin (Rahlfs and Becker 2001; Kawazu *et al*. 2001).

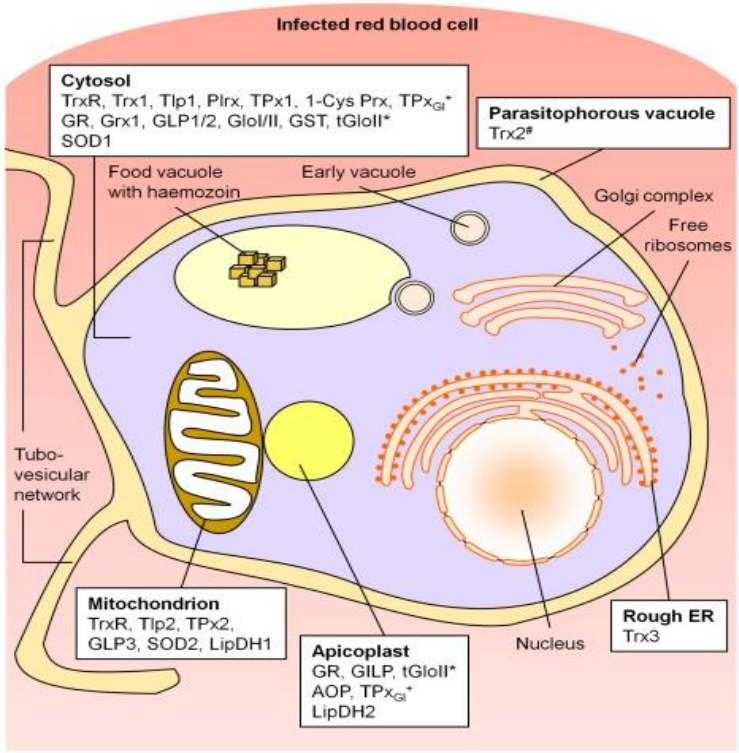

Figure 7: Compartmentation of Prxs and related redox cascade enzymes in malaria parasites. Schematic representation of an intraerythrocytic trophozoite with key parasite intracellular compartments and localization of redox-related enzymes (Kehr *et al.* 2010).

According to structural models, the peroxidatic Cys is in direct proximity to Arg125 and Thr47, the typical active site of 2-Cys Prxs (Wood *et al*. 2003a). In the parasite´s cytoplasm, Prx1a is located and expressed during the parasite intraerythrocytic stage throughout the complete cell cycle (Kehr *et al.* 2010).

In *P. falciparum* a Prx1a knock out line showed slower growth than the parental line when exposed to superoxide and NO, indicating a protective function for the parasite against reactive oxygen and reactive nitrogen species (Komaki-Yasuda *et al.* 2003). Furthermore, *Pf*Prx1a knock out parasites showed hypersensitivity to heat stress. From temperatures up to 41 °C, the Prx1a knock out strains showed a significantly reduced growth rate compared to the parental line (Kimura *et al.* 2013). Under normal conditions, *Pf*Prx1a knock out lines had a similar growth rate and morphology as the parental strain, indicating that Prx1a is not essential for parasitic growth (Komaki-Yasuda *et al.* 2003). A potential connection between the formation of gametocytes and Prx could be possible, since Prx1a knock-out *P. berghei* parasites form 60 % less gametocytes (Yano *et al.* 2006).

Peroxiredoxin 1m

P. falciparum possesses a mitochondrion with a functional electron transport chain. The mitochondrial *Pf*Prx1m is a thioredoxin-dependent peroxidase with a preference for hydrogen peroxide (Rahlfs and Becker 2001), and its structural analysis reveals a typical 2-Cys mechanism with a molecular weight of ~ 25 kDa (Boucher *et al*. 2006). Prx1m is localized to the mitochondria of the asexual erythrocytic stages and is expressed during the trophozoite and schizont stages (Yano *et al*. 2005). The presence of *Pf*Prx1m is of importance for the malarial parasite, as it supports to maintain the function and integrity of the mitochondria, which is exposed to high values of hydrogen peroxide (Boucher *et al*. 2006; Kehr *et al.* 2010). In *in vitro* methods, *Pf*Prx1m prefers *Pf*Trx2 over *Pf*Trx1 (Boucher *et al.* 2006). Since neither of the substrates is present in the mitochondria, the *in vivo* reductants are unclear (Kehr *et al.* 2010). Brandstaedter *et al*. showed 141 proteins interacting with Prx1m, of which one was identified as a putative mitochondrial interaction partner (Brandstaedter *et al*. 2019).

*Pf*Prx1m was formerly referred to as the mitochondrial peroxidase TPx-2 of *P. falciparum*. In studies carried out by Masuda-Suganoma *et al*., TPx-2 knock out strains were generated and compared to TPx-2 wild-type development in blood and insect stage of *Plasmodium berghei*, showing no difference in the morphology of parasite cells between wild-type and knock out. Additionally, no significant difference was found in the development stages of oocysts in wild type and knock out strains, suggesting a non-essential role of TPx-2 in *P. berghei* (Masuda-Suganuma *et al.* 2012). Interestingly, significant differences according to the number of gametocytes in parasite-infected blood were observed. In TPx-2 knock out infected mice, the peak of the number of gametocytes was delayed by one day compared to the peak of Prx wild-type infected mice (Masuda-Suganuma *et al*. 2012). The mitochondria of *Plasmodium* differ morphologically between the asexual and sexual stages. Asexual stage parasites possess one mitochondrion, whereas mature gametocytes have four to six mitochondria and therefore might be more metabolically active compared to the asexual stage (Masuda-Suganuma *et al*. 2012).

Peroxiredoxin 5

*Pf*Prx5, formerly known as antioxidant protein *Pf*AOP (Sarma *et al.* 2005), is localized within the parasitic apicoplast (Kehr *et al.* 2010) and is expressed throughout the erythrocytic blood stage. Based on its crystal structure (Sarma *et al.* 2005), the enzyme is proposed to be a 1-Cys peroxiredoxin with a monothiol mechanism and has a molecular weight of ~21 kDa. Even though the exact physiological role of Prx5 is unknown, Sarma *et al*. showed peroxidase activity *in vitro* on recombinant Prx5 (Sarma *et al*. 2005), with highest relative activities performed with tert-butyl hydroperoxide as substrate (Djuika *et al.* 2013). The peroxide reduction depending on Prx5 was more efficient with a coupled enzymatic assay with the glutathione-system containing NADPH, GR, Grx, and GSH than in assays containing the thioredoxin system (Deponte *et al.* 2007; Nickel *et al*. 2006). Furthermore, Prx5 can also be reduced by Plasmoredoxin (Nickel *et al.* 2006). Whether the apicoplast contains a Grx isoform is unknown (Djuika *et al*. 2013). Interestingly, a *Pf*Prx5 knock out was shown to be dispensible for blood stage parasite survival and did not affect the susceptibility of *P. falciparum* towards artemisinin (Djuika *et al*. 2017).

Peroxiredoxin 6

1-Cys *Pf*Prx6 is located to the cytosol and is expressed during the trophozoite and early schizont stages (Yano *et al.* 2005). Prx6 knock out parasites did not show hypersensitivity towards reactive oxygen or nitrogen species, nor when being exposed to heat stress compared to wild type strains (Kimura *et al.* 2013). *Pf*Prx6 was suggested to compete with GSH for interaction with haem, inhibiting haem degradation by GSH and reducing the amount of haem-derived free iron (Kawazu *et al.* 2005). The IC_{50} value at which chloroquine inhibited haem-polymerization of the *Pf*Prx6 knock out parasite lines was measured, showing no significant difference to chloroquine than the parental strain (Kimura *et al*. 2013). However, a function of *Pf*Prx6 in haem detoxification was proposed to be unlikely (Deponte *et al*. 2007).

Peroxiredoxin Q

The nuclear peroxiredoxin Q (PrxQ) is localized within the parasite´s nucleus (Richard *et al*. 2011). Numerous attempts regarding the recombinant expression of the entire nuclear peroxiredoxin were unsuccessful. Therefore, the N-terminal part of the protein containing 164 amino acids was recombinantly expressed, lacking the

lysine rich C-terminus (Richard *et al*. 2011). Kinetic measurements showed that *Pf*PrxQ prefers Grx over Trx as a reducing substrate and reduces hydrogen peroxide and cumene peroxide equally well (Richard *et al*. 2011). PrxQ is associated strongly with the genome of *Plasmodium*, suggesting that the enzyme has a crucial role in protecting nuclear components such as DNA from oxidative damage or being involved in maintaining chromatin structure, DNA-repair, and in mechanisms that affect transcriptional activities (Richard *et al.* 2011). Apart from acting as an antioxidant, it is suggested that the protein can act as a molecular chaperone to stabilize other DNA-binding factors. Furthermore, *Pf*PrxQ associates with chromatin due to its lysine rich C-terminus, which are unique functions compared to other Prxs (Richard *et al*. 2011).

1.2.4 Peroxiredoxins as drug targets

Prxs seem to be important for life and can therefore be a novel approach for drug development fighting parasitic diseases. However, current drugs tend to target proteins that act in regulating Prxs (Jaeger and Flohé 2006). A possible barrier for developing Prx inhibitors is the strongly conserved FF active site among the Prxs (Hall *et al.* 2011). In several instances, Prxs drug resistances have been observed. Therefore, in *Trypanosoma cruzi* the expression of Prx1a and Prx1m was found to be increased in benznidazole-resistant strains. Moreover, an up regulation of Prx1 of metrodinazole-resistant *Entamoeba histolytica* has been observed (Nogueira *et al*. 2009; Wassmann *et al.* 1999). Perkins *et al*. proposed a possible shift of the FF-LU equilibrium by a small molecule, stabilizing a single conformation. Therefore, the structural changes required for catalytic activity would be inhibited. A stabilization of the LU form would lead to a direct loss of peroxidase activity, whereas stabilizing the FF form would lead to inhibition due to hyperoxidation. As most pathogens such as *P. falciparum* lack sulfiredoxin, Prxs would be permanently inhibited (Perkins *et al.* 2013). Further attempts regarding the inhibition of Prx were made with human Prx2 which is located within erythrocytes (Kehr *et al*. 2010). *P. falciparum* imports hPrx2 from the erythrocyte and exploits the function of the human peroxiredoxin, as it helps maintaining the needed redox balance (Koncarevic *et al*. 2009). Brizuela *et al*. inhibited hPrx2 with Conoidin A and observed an enhanced sensitivity of the parasite towards the antimalarial drug chloroquine (Brizuela *et al.* 2014).

1.4 Redox regulation by post-translational thiol modifications

Redox homeostasis regulates a large number of important cellular processes. Imbalances in pathways that are critical for oxidative and reducing conditions are linked to numerous diseases (Xiong *et al*. 2011). Post-translational modifications (PTMs) are of importance in regulating protein functions and are associated with gene expression, cell signalling, protein trafficking as well as regulating the activity and stability of enzymes (Doerig *et al*. 2015, Xiong *et al.* 2011, Jortzik and Becker 2012). One of the most susceptible targets are thiol groups on cysteines (Grek *et al*. 2013).

1.4.1 *S*-Glutathionylation

S-glutathionylation represents one of the most frequent forms of oxidative thiol modification. The cysteine thiol of glutathione forms a reversibly bound mixed disulfide with a cysteine thiol of a protein, resulting in an *S*-glutathionylated protein. Protein *S*-glutathionylation occurs during oxidative stress, but also under physiological conditions and is of importance for the initiation of functional changes of enzymes and regulates signal transduction (Chen *et al*. 2010, Clavreul *et al*. 2006). Numerous proteins e.g. carboanhydrase III, α-ketoglutarat dehydrogenase, heat shock protein 70, and NF-κB were shown to be reversibly activated or inhibited by *S*-glutathionylation (Dalle-Donne *et al*. 2009; Lillig *et al.* 2008). Furthermore, *S*-glutathionylated thiols are less prone to hyperoxidation under oxidative stress. Besides the possibility of *S*-glutathionylation by glutathione disulfide, proteins can also be glutathionylated in the presence of GSH and oxidants (Xiong *et al*. 2011). Thiols are oxidized by H_2O_2 and ROOH through a two-electron substitution reaction (as explained in chapter 1.2.2), which requires the deprotonation of the thiol to a thiolate anion to assure the needed nucleophilicity (Forman *et al*. 2010). Cysteine sulfenic acids are highly reactive with GSH, which can lead to *S*-glutathionylation (see Figure 8) (Xiong *et al.* 2011). Cysteines of peroxiredoxins form mixed disulfides with GSH which could have a regulatory function, although it remains to be elucidated if these are physiologically relevant. In human Prx1, three cysteines were identified as *S*-glutathionylation targets (Park *et al.* 2009) and glutathionylation shifted the enzymes oligomeric state from decamers to predominantly dimers (Park *et al*. 2011). Furthermore, the glutathionylation of the peroxidatic cysteine of hPrx2 was proposed to protect the enzyme against hyperoxidation to sulfinic acid (Peskin *et al*. 2016).

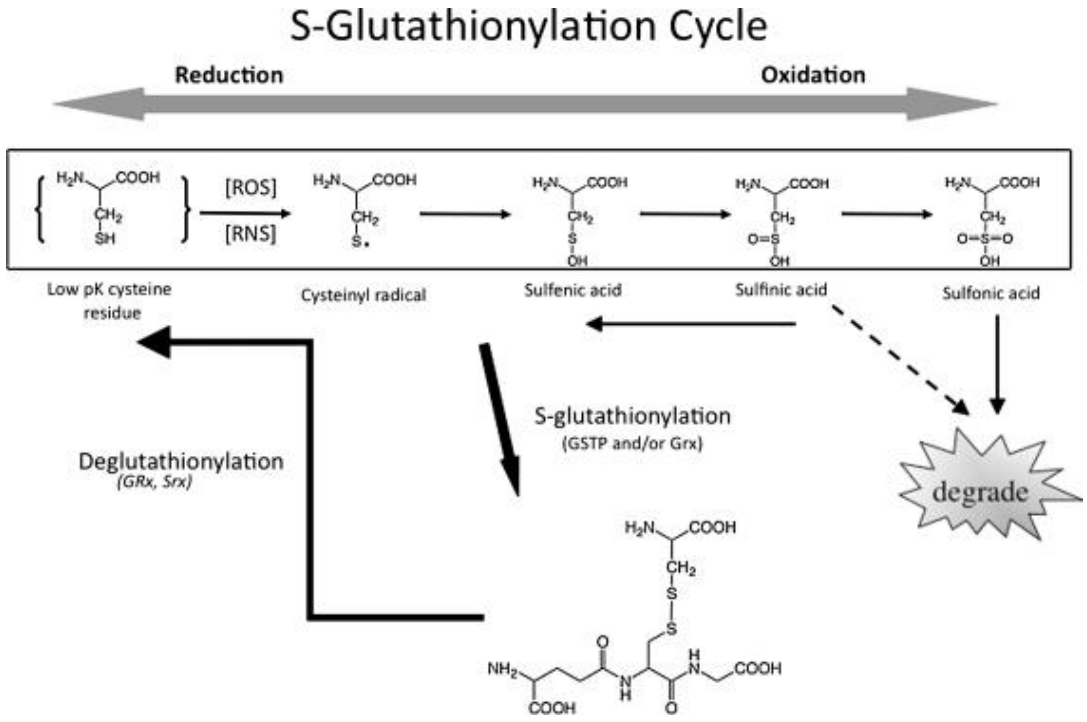

Figure 8: *S*-glutathionylation cycle. *S*-glutathionylation and deglutathionylation by non-enzymatic and enzymatic reactions. For detail see text (Xiong *et al.* 2011).

In a proteomic approach using *P. falciparum* lysate, 493 targets for *S*-glutathionylation were identified (Kehr *et al.* 2011). Interestingly, numerous enzymes, which are components of central metabolic pathways, were shown to be reversibly inhibited by *S*-glutathionylation (Kehr *et al*. 2011). Keeping into account the entire proteome of the parasite, approximately 10 % of the proteins were modified under physiological conditions, which underlines the importance of this post-translational modification.

1.4.2 *S*-Nitrosation

The radical nitrogen monoxide (NO) is a reactive signalling molecule, produced by nitric oxide synthase (NOS) using L-arginine as a substrate (Thomas *et al*. 2001). NO is associated with numerous functions such as controlling pro-inflammatory signalling (Luiking *et al*. 2010) or inducing the production of cGMP (Francis *et al*. 2010). Furthermore, NO binds reversibly to protein cysteines (Hess *et al*. 2005). During this *S*-nitrosation of a protein, NO is reversibly bound to protein thiols, predominantly as a consequence of oxidative stress. The formation of *S*-nitrosothiol can then influence the conformation, stability, activity, and function of the *S*-nitrosated protein (Hara *et al*. 2005; Hess *et al.* 2005; Kim *et al*. 2004), and enable further post-translational

modifications such as phosphorylation, acetylation, and disulfide bond formation (Hess *et al*. 2012; Martinez-Ruiz *et al*. 2004). The *S*-nitrosation level in the cell is regulated by the redox status and by denitrosation reactions. Thus, in an antioxidative cellular milieu, *S*-nitrosation can be prevented, and a decrease in antioxidants increases *S*-nitrosation levels (Clementi *et al.* 1998). Furthermore, non-enzymatic and enzymatic denitrosation reactions regulate the amount of *S*-nitrosated cysteines. These reactions occur spontaneously non- enzymatic by reducing agents, metal ions, or reactive oxygen species, and enzymatically by the TrxR system or S-nitrosoglutathione (GSNO) reductase system (Stomberski *et al*. 2019). GSNO is the most abundant S-nitrosothiol, is the major donor of NO throughout the cell and is generated by the transfer of the nitrosyl group of the haem iron of cytochrome c to glutathione (Benhar *et al*. 2009; Broniowska *et al*. 2012). GSNO can then translocate into the cytosol and organelles, and transnitrosate interacting proteins. During transnitrosation, an *S*-nitrosated protein transfers its nitrosyl moiety to the cysteine thiol of its interacting protein partner (Nakamura and Lipton 2013).

In *Plasmodium*, high amounts of nitrosative stress derive from the human or mosquito host (Ferrari *et al*. 2011). The increasing expression of NOS due to hemozoin production in the erythrocyte can lead to high levels of NO and result in a retarded development of the parasites (Peterson *et al*. 2007b). Interestingly, in the *Plasmodium*-infected human host, expression levels of NOS in macrophages are induced (Ranjan *et al*. 2016).

1.5 Aim of the study

The alarming spread of resistances towards antimalarial drugs has led to an urgent need to identify yet unknown drug targets. Due to the fact that malarial parasites are exposed to high levels of oxidative stress, the parasitic redox metabolism represents a promising approach in drug development. The parasite *P. falciparum* has been shown to develop resistance against antimalarial drugs. As artemisinin induces oxidative stress and is highly effective in eliminating the parasite, new drug targets having a crucial role in maintaining the redox-state are focus of numerous studies.

This thesis focused on the peroxiredoxins from *Plasmodium falciparum*. The thiol-dependent peroxidases are highly abundant and of importance for the parasitic

development. The malarial parasite possesses five Prxs which are distinguished by their subcellular distribution and their number of cysteines involved in catalysis. The following topics were the aim of this thesis:

- Recombinant production, purification and characterization of *Pf*Prx1a wild type enzyme and mutants, especially regarding the impact of site-directed mutagenesis on oligomerization behaviour and enzyme activity
- Characterization of *Pf*Prx1m, *Pf*Prx5 and *Pf*PrxQ regarding their oligomerization behaviour
- Investigation of the subseptability of *Pf*Prx1a, *Pf*Prx1m, *Pf*Prx5, *Pf*PrxQ, and *Pf*Plrx towards two post-translational modifications- *S*-glutathionylation and *S*-nitrosation

2. Material

2.1 Instruments

Instrument	Company
Autoclave	Webeco, Bad Schwartau
Autoclave VX-95	Systec, Wettenberg
Äkta FPLC system (Pump P-920, monitor UPC-900, injection valve INV-907, mixer M-925, Fraction collector Frac-900, column XK 16/60, column material Superdex 200 prep grade)	GE Healthcare, Freiburg
Centrifuge Megafuge 1.0 R	Heraeus Instruments, Hanau
Centrifuge MiniSpin	Eppendorf, Hamburg
Centrifuge Sorvall RC5Plus (rotor SS-34, SLA-3000)	Kendro Laboratory Products, Langenselbold
Centrifuge Sorvall RC 6+ (rotor SS-34, F9S-4x1000y)	Thermo Scientific, Dreieich
Centrifuge 5415R	Eppendorf, Hamburg
ChemoStar	Intas Science Imaging Instruments GmbH, Göttingen
Crystallization robot Honeybee 961	Digilab, Marlborough
Electrophoresis Chamber Mini-PROTEAN 3 cell	BioRad, Munich
Electrophoresis Chamber B1, B1A, B2	Owl Separation System Inc., Portsmouth, USA
Electrophoresis Power Supply EPS 200	Pharmacia Biotec, Dübendorf, Switzerland
GelDoc 2000	BioRad, Munich
Heating block neoBlock II	neoLab, Heidelberg
High-purity water system Astacu	MembraPure, Bodenheim
Icemaker F80C	Icematic Deutschland, Meerbusch
Incubation shaker mytron	Thermo Scientific, Dreieich
Incubation shaker KS 500	Junke & Kunkel, IKA Werke, Staufen
Incubation shaker SM25	Edmund Bühler GmbH, Tübingen

Magnetic stirrer CAT M15	MAGV Laborbedarf, Rabenau-Londorf
Magnetic stirrer color squid	IKA Werke, Staufen
Magnetic stirrer, HI 300N	Hanna instruments, Kehl am Rhein
Magnetic stirrer, RCT basic	IKA Werke, Staufen
PCR cycler Mastercycler	Eppendorf, Hamburg
PCR cycler Mastercycler gradient	Eppendorf, Hamburg
Peleus ball	Deutsch & Neumann, Berlin
pH meter model 350 pH/Temp/mV Meter	Beckman, Krefeld
Pipette Eppendorf Research	Eppendorf, Hamburg
Pipette Gilson Pipetman P10, P20, P100, P200, P1000	Gilson, Middleton, USA
Precision scale ABT 120-5 DM	Kern & Sohn, Balingen
Precision scale AJ100	Mettler-Toledo, Giessen
Precision scale SBC 22	Scaltec Instruments, Göttingen
Scale 474-32	Kern & Sohn, Balingen
Scale Bosch PE626	Bosch & Sohn, Jungingen
Shaker Heidolph Unimax 2010	MAGV GmbH, Rabenau
Spectrophotometer BioPhotometer	Eppendorf, Hamburg
Spectrophotometer NanoDrop ND-1000	Thermo Scientific, Dreieich
Spectrophotometer U-2001	Hitachi, Schwäbisch Gmünd
Stereomicroscope M165 C	Leica Mikrosysteme, Wetzlar
Ultrasound device (GM 2070; UW 2070; SH 706; MS 73)	Bandelin Electronic, Berlin
Ultrasound water bath Sonorex RK100	Bandelin Electronic, Berlin
UV/VIS Spectrophotometer Evolution 300	Thermo Scientific, Dreieich
Vortex mixer MS2 Minishaker	IKA Werke, Staufen
Western Blot Trans-Blot SD Semi-dry transfer cell	BioRad, Munich

2.2 Chemicals

Chemical	Company
Acetic acid	Roth, Karlsruhe
Acrylamide/ Bisacrylamide (Rotiphorese Gel 30 (37.5:1))	Roth, Karlsruhe
Agar-Agar	Roth, Karlsruhe
Agarose (peqGold Universal Agarose)	Roth, Karlsruhe
5-Amino-2,3,-dihydro-1,4,-phthalazinedione	Sigma, Steinheim
6-Aminohexanoic acid	Merck, Hohenbrunn
Ammonium persulfate	Roth, Karlsruhe
Adenosine triphosphate	Boehringer, Mannheim
Bradford reagent (BioRad Protein Assay)	BioRad, Munich
Bromphenol blue	Sigma, Steinheim
Bovine serum albumin	Roth, Karlsruhe
Calcium chloride	Roth, Karlsruhe
Carbenicillin	Roth, Karlsruhe
Coomassie Brilliant Blue R250	Sigma, Steinheim
Cumaric acid	Sigma, Steinheim
Cystatin	Sigma, Steinheim
DMSO (dimethyl sulfoxide)	Roth, Karlsruhe
DNase I	Roth, Karlsruhe
DTT (dithiotreitol)	Roth, Karlsruhe
Ethanol	Roth, Karlsruhe
Glycerol	Roth, Karlsruhe
GSH (glutathione)	Sigma, Steinheim
GSSG (glutathione disulfide)	Sigma, Steinheim
HCl (fuming, 37 %)	Roth, Karlsruhe
HEPES (2-(4-(2-hydroxyethyl)-1-piperazine)-ethanesulfonic acid)	Roth, Karlsruhe
Hydrogen peroxide	Roth, Karlsruhe
Imidazole	Roth, Karlsruhe
IPTG (isoprpypl-β-D-1-thiogalactopyranoside)	Roth, Karlsruhe
Kanamycin sulfate	Roth, Karlsruhe
Methanol	Roth, Karlsruhe

Milk powder	Roth, Karlsruhe
NADPH (Nicotinamid adenine dinucleotide phosphate, reduced)	Biomol GmbH, Hamburg
Ni-NTA Agarose (nickel nitrilotriacetic acid)	Invitrogen, Karlsruhe
PEG (polyethylene glycol)	Sigma, Steinheim
Pepstatin A	Sigma, Steinheim
PMSF (phenylmethanesulfonylfluoride)	Roth, Karlsruhe
Ponceau S	Sigma, Steinheim
Potassium chloride (KCL)	Roth, Karlsruhe
Potassium dihydrogenphosphate (KH_2PO_4)	Roth, Karlsruhe
Di-Potassium hydrogenphosphate (K_2HPO_4)	Roth, Karlsruhe
Potassium hydroxide (KOH)	Roth, Karlsruhe
Select agar	Invitrogen, Karlsruhe
Sodium acetate	Roth, Karlsruhe
Sodium chloride (NaCl)	Roth, Karlsruhe
Sodium citrate	Sigma, Steinheim
Sodium dodecyl sulfate (SDS)	Sigma, Steinheim
Sodium hydroxide (NaOH)	Roth, Karlsruhe
Talon Metal Affinity Resin	Clontech, Takara Bio Europe SAS, Saint-Germain-en-Laye, France
TEMED(N,N,N`,N`-tetramethylethylendiamine)	Sigma, Steinheim
TRIS (tris-(hydroxymethyl)-aminomethane)	Roth, Karlsruhe
Triton X-100	Sigma, Steinheim
Tryptone/ Peptone	Roth, Karlsruhe
TWEEN 20	Sigma, Steinheim
Yeast extract	Oxoid LTD, Basingstoke Hampshire, England

2.3 Consumables

Consumables	**Company**
Crystallization plate, 24 well, VDX plate	Hempton Research, Jena
Cuvettes, polystyrol	Sarstedt, Nümbrecht

Cuvettes, micro, UV	Brand GmbH, Wertheim
Halfmicro cuvettes 10x4x45 mm, polystyrol	Sarstedt, Nümbrecht
Falkon tube 15 mL, 50 mL	Greiner Bio-One, Frickenhausen
Membrane filter ME 25, 0.45 µm	Whatman GmbH, Dassel
Micro pipettes	Brand GmbH, Wertheim
Multiply PCR tube 0.2 mL	Sarstedt, Nümbrecht
Nitrocellulose blotting membrane, 0.45 µm	GE Healthcare, Freiburg
Parafilm `M`laboratory film	Pechiny Plastic Packaging, Menasha, USA
Pasteur pipette 150 mm	Hirschmann laborgeräte, Eberstadt
Petri dish, 15 cm Ø	Sarstedt, Nümbrecht
Pipette tubes and tips, disposable	Eppendorf, Hamburg
Pipette tips Omnitip FastRack 10 µL, 200 µL	Ulplast, Warschau
Plastic Vials	GE Healthcare, Munich
Protein ladder unstained protein MW marker	Fermentas, St. Leon-Rot
PVDF membrane	Roth, Karlsruhe
Rubber Caps	GE Healthcare, Munich
Series S Sensor Chip CM5	GE Healthcare, Munich
Syringe 1 mL Plastipak	Becton Dickson, Madrid, Spain
Syringe 10 mL	B. Braun, Melsungen
Vivaspin 20, 3000 MWCO and 10000 MWCO	Sartorius Stedim Biotech, Göttingen
X-ray film Processore, Optimax	Protec, Oberstenfeld
Zeba^{TM} Desalt Spin Columns	Thermo Scientific, Rockford, USA

2.4 Biological material

2.4.1 Vectors

Vector	**Properties**
pET28a^{+}	Kanamycin resistance, T7 promotor, His_6-tag coding sequence, T7 tag coding sequence, lac I coding sequence, T7 terminator
pQE30	Carbenicillin resistance, T5 promotor, His-tag coding sequence, lac operator

2.4.2 E.coli strains

Strain	Genotype
XL-1 blue	F'::Tn10 proA+B+ lacIq Δ(lacZ)M15/recA1 endA1 gyrA96 (NaIR) thi hdgR17 (rK- mK+) glnV44 relA1 lac
M15	nalS, StrS, rifS, KmR, lac-, ara-, gal-, mtl-, F-, recA+, uvr+

2.4.3 Antibodies

Antibody	Company
Mouse anti-His-tag IgG	Jackson Immuno Research, West Grove, USA
Mouse anti-glutathione IgG	Abcam, Cambridge, UK
Mouse anti-biotin IgG	Santa Cruz, Dallas, TX, USA

2.4.4 Enzymes

Restriction enzymes

Enzyme	Company	Restriction site
DpnI	Thermo Scientific	5´...GA^{-CH3}^TC...3´
EcoRI	Thermo Scientific	5´...G^AATTC...3´

Enzymes for molecular biology

Enzyme	Company
Pfu DNA Polymerase	Promega, Mannheim
RedTaq® Polymerase	Sigma, Steinheim
T4 Ligase	Fermentas, St. Leon-Rot

Recombinant Enzymes and Redoxins

Enzymes	
*Pf*Prx1a	*Pf*Prx5
*Pf*Prx1a$^{C50S/C74A}$	*Pf*Prx5^{C117S}
*Pf*Prx1a$^{C50S/C170S}$	*Pf*Prx5^{C143S}
*Pf*Prx1a$^{C74A/C170S}$	*Pf*Prx5$^{C117S/C143S}$
*Pf*Prx1a$^{C50S/C74A/C170S}$	Truncated *Pf*PrxQ$^{1-164}$
*Pf*Prx1a^{Y42A}	Truncated *Pf*PrxQ$^{1-164/C56S}$

*Pf*Prx1a^{D45A}	Truncated *Pf*PrxQ$^{1-164/C103S}$
*Pf*Prx1a^{D77A}	Truncated *Pf*PrxQ$^{1-164/C56S/C103S}$
*Pf*Prx1a^{H82A}	*Pf*Prx1m
*Pf*Prx1a^{R125A}	*Pf*TrxR
*Pf*Prx1a^{V116D}	
*Pf*Prx1a^{V116T}	
*Pf*Prx1a^{L117W}	
Redoxins	
*Pf*Plrx	*Pf*Trx
*Pf*Plrx^{C3S}	
*Pf*Plrx^{C63S}	
*Pf*Plrx^{C115S}	

2.4.5 Oligonucleotides

Primers for site-directed mutagenesis	**Sequence (5'-3')**
*Pf*Prx1a^{C50S}s	TTTTACGTTTGTATCTCCATCTGAAATC
*Pf*Prx1a^{C50S}as	GATTTCAGATGGAGATACAAACGTAAAA
*Pf*Prx1a^{C170S}s	AACATGGAGATGTTTCCCCAGCAAAC
*Pf*Prx1a^{C170S}as	GTTTGCTGGGGAAACATCTCCATGTT
*Pf*Prx1a^{Y42A}s	GTATTATTATATTTTGCTCCATTAGATTTTACG
*Pf*Prx1a^{Y42A}as	CGTAAAATCTAATGGAGCAAAATATAATAATAC
*Pf*Prx1a^{D45A}s	ATTTTTATCCATTAGCTTTTACGTTTGTATGTC
*Pf*Prx1a^{D45A}as	GACATACAAACGTAAAAGCTAATGGATAAAAAT
*Pf*Prx1a^{D77A}s	GGCTGTAGTGTGGCTAGTAAATATACTCATTT
*Pf*Prx1a^{D77A}as	AAATGAGTATATTTACTAGCCACACTACAGCC
*Pf*Prx1a^{H82A}s	GATAGTAAATATACTGCTTTGGCATGGAAAAAAAC
*Pf*Prx1a^{H82A}as	GTTTTTTTCCATGCCAAAGCAGTATATTTACTATC
*Pf*Prx1a^{W85A}s	ATACTCATTTGGCAGCGAAAAAAACACCATTAAC
*Pf*Prx1a^{W85A}as	GTTAATGGTGTTTTTTTCGCTGCCAAATGAGTAT
*Pf*Prx1a^{R125A}s	TGGTGATAGTGTATCATTAGCAGCATTTGTATTAATC
*Pf*Prx1a^{R125A}as	GATTAATACAAATGCTGCTAATGATACACTATCACCA

*Pf*Prx1a^{V116D}s	TATCAAGAAGTTATAATGATTTGTTTGGTGATAGT
*Pf*Prx1a^{V116D}as	ACTATCACCAAACAAATCATTATAACTTCTTGATA
*Pf*Prx1a^{V116T}s	TATCAAGAAGTTATAATACGTTGTTTGGTGATAGT
*Pf*Prx1a^{V116T}as	ACTATCACCAAACAACGTATTATAACTTCTTGATA
*Pf*Prx1a^{L117W}s	CAAGAAGTTATAATGTGTGGTTTGGTGAT
*Pf*Prx1a^{L117W}as	ATCACCAAACCACACATTATAACTTCTTG
*Pf*Plrx^{C3S}s	GGATCCGCGTCCCAAGTTGATAAC
*Pf*Plrx^{C3S}as	GTTATCAACTTGGGACGCGGATCC
*Pf*Plrx^{C63S}s	GGTGTAAATAC*A*GTGTAACCTTTATAG
*Pf*Plrx^{C63S}as	CTATAAAGGTTACACTGTATTTACACC
*Pf*Plrx^{C115S}s	GATACTTTTTAGATATATATAAATAATTATC
*Pf*Plrx^{C115S}as	GATAATTATTTATATATATCTAAAAAGTATC

2.5 Solutions and buffers

2.5.1 Stock solutions

Stock solution	**Composition**
APS	10% (w/v) in ddH_2O, storage at -20 °C
Carbenicillin	50 mg/mL in 50% (v/v) EtOH, storage at -20 °C
Chloramphenicol	35 mg/mL, 100% EtOH, storage at -20 °C
Cystatin	40 µM in US buffer, storage at -20 °C
DTT	1 M in ddH_2O, storage at -20 °C
IPTG	1 M in ddH_2O, sterile filtration 0.2 µm, storage at -20 °C
Kanamycin	25 mg/mL in ddH_2O, sterile filtration 0.2 µm, storage at -20 °C
Pepstatin	0.3 mg/mL in US buffer, storage at -20 °C
Ponceau S	2% Ponceau S (v/v), 3% TCA (v/v)
PMSF	100 mM in DMSO, storage at -20 °C

2.5.2 Media for cell culture

Medium	**Composition**
Lysogeny broth (LB)	10 g/L tryptone, 5 g/L yeast extract, 10 g/L NaCl Adjusted to 1 L with ddH_2O and autoclaved before use
Terrific broth (TB)	12 g/L tryptone, 24 g/L yeast extract, 9.4 g/L KH_2PO_4, 2.2 g/L K_2HPO_4, 4 mL/L glycerin, pH 7.0 Adjusted to 1 L with dH_2O and autoclaved before use
Agar plates	10 g Tryptone 5 g Yeast extract 10 g Sodium chloride 15 g Agar Adjusted to 1 L with dH_2O and autoclaved before use

2.5.3 Buffers for protein purification

Buffer	**Composition**
Elution buffer *Pf*Prx1a	50 mM Na_2HPO_4 300 mM NaCl, pH 8.0 20, 75, 200 and 500 mM imidazole 0.5 mM DTT
Elution buffer *Pf*Prx1m	50 mM Na_2HPO_4 300 mM NaCl, pH 8.0 20, 50, 100, 200 and 500 mM imidazole 0.5 mM DTT
Elution buffer *Pf*Prx5	50 mM Na_2HPO_4 300 mM NaCl, pH 8.0 30, 100 and 500 mM imidazole 0.5 mM DTT
Elution buffer *Pf*PrxQ$^{1\text{-}164}$	50 mM Na_2HPO_4

	300 mM NaCl, pH 8.0
	10, 30, 50 and 200 mM imidazole
Elution buffer *Pf*Plrx	50 mM Na_2HPO_4
	300 mM NaCl, pH 8.0
	50, 75, 100 and 500 mM imidazole
	0.5 mM DTT

2.5.4 Gels

Gel	**Composition**
15 % separating gel (for 4 gels)	3.6 mL ddH_2O
	3.75 mL separating gel buffer
	7.5 mL acrylamide/bisacrylamid (30% (v/v))
	0.15 mL SDS (10% (w/v))
	75 µL APS (10% (w/v))
	7.5 µL TEMED
12 % separating gel (for 4 gels)	3.6 mL ddH_2O
	3.75 mL separating gel buffer
	7.5 mL acrylamide/bisacrylamid (30% (v/v))
	0.15 mL SDS (10% (w/v))
	75 µL APS (10% (w/v))
	7.5 µL TEMED
4 % stacking gel (for 4 gels)	3.05 mL ddH_2O
	1.25 mL stacking gel buffer
	0.65 mL acrylamide/bisacrylamid (30% (v/v))
	0.05 mL SDS (10% (w/v))
	25 µL APS (10% (w/v))
	5 µL TEMED

2.5.5 Buffers for electrophoresis

Buffer	**Composition**
Stacking gel buffer	0.5 M Tris, pH 6.8
Separating gel buffer	1.5 M Tris, pH 8.8

SDS chamber buffer	192 mM glycine, 25 mM Tris-HCl, pH 8.3 0.1% (w/v) SDS
SDS sample buffer 1x	62.5 mM Tris-HCl pH 6.8, 25% glycerol 20 mL 10% (w/v) SDS 2 mL 0.5% (w/v) bromophenol blue, 50 mM DTT, 40.5 mL H_2O storage at -20°C before usage 5% (v/v) 2-ME were added
SDS sample buffer 4x	3 mL stacking gel buffer, 300 mg DTT 400 mg SDS, 2 mL glycerol tip of a spatula bromophenol blue
Coomassie staining solution	160 mg Coomassie Brilliant Blue R 250, ad 1 L ddH_2O, 2 h stirring, add 3 mL concentrated HCl

2.5.6 Buffers for semi-dry Western blotting

Buffer	**Composition**
Transfer buffer	25 mM Tris 192 mM Glycine 10% (v/v) Ethanol pH 8.3
TBS	10 mM Tris 55 mM NaCl pH 7.4
TBST	10 mM Tris 55 mM NaCl 0.05% (v/v) TWEEN 20 pH 7.4
Ponceau S staining	1% (w/v) Ponceau S 5% (v/v) acetic acid
Ponceau S destaining	1% (v/v) acetic acid
Luminol	1.25 mM luminol 0.0093% (v/v) H_2O_2 0.1 M Tris-HCl

	pH 8.6
ECL reagent	1 mL luminol, 10 µL cumaric acid

2.5.7 Assay buffers

Buffer	**Composition**
Enzyme activity buffer	50 mM sodium phosphate
	300 mM sodium chloride
	pH 8.0
GSNO/ Cys-NO buffer	50 mM Tris
	1 mM EDTA
	0.2 mM Neocuproine
	pH 7.4
Blocking buffer	8 M Urea
	50 mM Tris
	1 mM EDTA
	0.1 mM Neocuproine
	pH 8.0
Labelling buffer	4 M Urea
	50 mM Tris
	1 mM EDTA
	0.01 mM Neocuproine
	pH 8.0

3. Methods

3.1 Molecular biological methods

3.1.1 Plasmid preparation

The plasmid DNA from *E. coli* cells was purified using the Nippon genetics Miniprep Kit or the QIAprep Spin Miniprep Kit (Qiagen, Promega) following the manufacturer's protocol. Briefly, the pellet of 1.5 -3 mL overnight culture containing the plasmid of interest was lysed, neutralized, and centrifuged. The plasmid DNA comprising supernatant was subsequently purified over a silica membrane column.

3.1.2 Determination of DNA concentration

The DNA concentration was determined spectrophotometrically at a wavelength of 260 nm in UV cuvettes using a biospectrophotometer (Eppendorf, Hamburg). The degree of purity was delineated by the ratio of absorbance at 260 nm to 280 nm, with a ratio of ~ 1.8 accepted as "pure", and calculated by the following formula:

$$\text{DNA purity } (A_{260}/A_{280}) = A_{260} \div A_{280}$$

3.1.3 Agarose gel electrophoresis

DNA mixtures were applied to an agarose gel in order to separate various DNA fragments. The DNA sample was mixed 5:1 with DNA-Dye NonTox and loaded on a 0.7% agarose gel. The DNA fragments were separated electrophoretically in 1x TBE running buffer by applying 100 V for approximately 45 min. The 1 kb DNA ladder GeneRuler was used to estimate the size of the DNA bands, and the latter were subsequently visualized with LED light using the gel documentation chamber FAS Digi Gel Imaging System (Nippon Genetics, Düren).

3.1.4 Molecular cloning

The DNA to be cloned and the vector DNA were digested to clone the desired DNA into expression vectors. This was achieved by using restriction endonucleases which create compatible ends at their cleavage sites following the protocols published by the manufacturers. The cleaved vector was linked with the cleaved foreign DNA via ligation with the T4-DNA ligase forming recombinant DNA.

3.1.5 Site-directed mutagenesis for *Pf*Prx1a

Selected amino acid residues of *Pf*Prx1a were mutated with site-directed mutagenesis using the polymerase chain reaction (PCR). *Pf*Prx1a in pQE30 was used as gene template, and oligonucleotide primers containing the respective mutated codons were used to insert the mutation using Pfu polymerase.

Table 1: Reaction mixture used for site-directed mutagenesis of *Pf*Prx1a.

Reaction mixture	
Template DNA	0.5 µL
Forward primer	1 µL
Reverse primer	1 µL
dNTP mix	1 µL
10x Pfu buffer	5 µL
Pfu polymerase (3 U/µL)	1 µL
DMSO	2.5 µL
Sterile H_2O	ad 50 µL

The PCR reaction was performed using the following PCR program:

Table 2: PCR program used for site-directed mutagenesis of *Pf*Prx1a.

PCR program	
Denaturation	90 sec 94 °C
Cycles	24
Denaturation	30 sec 94 °C
Annealing	60 sec 94 °C
Elongation	14 min 68 °C
Final elongation	13 min 68 °C

The PCR products were purified using the QIAquick PCR purification kit according to the manufacturer's protocol. Subsequently, a DpnI digestion was performed at 37 °C for 1h (see Table 3 for used components) and purified.

Table 3: Components for DpnI digestion.

Component	
Nuclease-free water	16 µL
10x buffer Tango	2 µL
DNA	1 µL
DpnI	1 µL

Samples with the respective mutation were sequenced at a sequencing facility at the Justus-Liebig University.

3.1.6 Site-directed mutagenesis for *Pf*Plrx

The cysteine mutants of *Pf*Plrx used in this thesis were prepared in earlier studies in the Becker lab (Sturm *et al*. 2009; Will 2014).

3.2 Microbiological methods

3.2.1 Preparation of competent *E. coli* cells

For molecular cloning or recombinant protein production, competent *E. coli* cells were prepared, which have the ability to take up plasmid DNA from their environment.

A stock sample was streaked onto an agar plate containing the appropriate antibiotics and incubated overnight at 37 °C. One colony was transferred to 10 mL LB medium containing antibiotics, and the cells were grown overnight at 37 °C under constant shaking at 180 rpm. 1 mL of the culture was transferred to 100 mL LB medium containing antibiotics, and the optical density measured at a 600 nm wavelength (OD_{600}) was monitored until 0.7 was reached. The culture was cooled on ice for 5 min, following a centrifugation step at 3,000 rpm and 4 °C for 5 min. The supernatant was discarded, and the cells were resuspended in a total volume of 30 mL cold TFB1 buffer. The cells were incubated on ice for 90 min, followed by a second centrifugation step at 2,000 rpm and 4 °C for 5 min. Subsequently, the supernatant was discarded and the cells were resuspended in 2 mL TFB2 buffer. Aliquots of 125 µL were frozen in liquid nitrogen for 1 min and stored at - 80 °C until transformation.

3.2.2 Transformation

During the process of transformation, plasmids are incorporated by competent *E. coli* cells. Appropriate plasmids and cells were thawed on ice. Approximately 100 ng of plasmid was added to 125 µL of competent *E. coli* cells and incubated for 30 min on ice, so that the plasmids bound to the *E. coli* cell membrane. A heat shock-induced stress for 90 sec at 42 °C resulted in the uptake of the plasmids. Cells were allowed to rest for 1 min on ice and were subsequently incubated with 300 mL of LB medium at 37 °C for 1 h while shaking. 50 - 100 µL of cell suspension was plated out onto agar plates containing the respective antibiotics, incubated over night at 37 °C. The agar plate was sealed with Parafilm 'M, and stored at 4 °C.

3.2.3 Heterologous overexpression in *E. coli* cells

The specific conditions for heterologous overexpression of the genes of interest are given in Table 4. The expression of genes and the production of the proteins of interest were performed in *Escherichia coli* cells. LB medium containing the required concentration of antibiotics was inoculated with one colony. Cell cultures were grown in a 37 °C incubator for 6 hours and were then transferred into 250 mL of the required medium where the cells were incubated over night at 37 °C. Using this culture, 1 litre of LB medium containing the required antibiotics was inoculate, and cells were grown at 37 °C until an optical density OD_{600} of 0.6 - 0.7 was reached. Subsequently, the cells were induced with isopropyl-β-D-1-thiogalactopyranoside (IPTG) and cultures were incubated for 2.5 and 4 hours.

Table 4: Conditions of heterologous overexpression for recombinant proteins.

Shown here are the conditions that resulted in the highest yield of recombinant protein.

	Vector	***E. coli* cells**	**Medium**	**Antibiotics**	**Duration (h)**	**Temperature (°C)**
*Pf*Prx1a and mutants	pQE30	M15	LB	C, K	4	37 °C
*Pf*Prx1m	pQE30	M15	LB	C, K	4	37 °C
*Pf*Prx5 and mutants	pQE30	M15	LB	C, K	4	37 °C

*Pf*PrxQ and mutants	pQE30	M15	LB	C, K	2.5	37 °C
*Pf*Plrx	pQE30	M15	LB	C, K	4	37 °C

C= carbenicillin, K= kanamycin

3.2.4 Cell harvest

The cells were centrifuged at 8.000 rpm for 15 minutes at 4 °C. The pellet was resuspended into the required protein purification buffer, enriched with a protease inhibitor mixture containing cystatin (10 µL/mL resuspended pellet), pepstatin (5 µL/mL resuspended pellet), and PMSF (10 µL/10 mL resuspended pellet) and stored at - 20 °C.

3.3 Protein biochemical methods

3.3.1 Purification by affinity chromatography

The exact conditions for protein purification are listed in Table 5. For the first step of recombinant protein purification, frozen pellets were defrosted at room temperature and resuspended using purification buffer, lysozyme, DTT, and DNase. For cell lysis the mixture was stirred on ice for 30, 45 or 60 min and subsequently treated with ultrasonic waves 3 x 30 seconds. The lysed cells were centrifuged at 18000 rpm for 30 minutes at 4 °C. The clear supernatant was purified by using Ni-NTA or the cobalt-based TALON. Both methods are based on affinity chromatography, using the protein´s hexahistidyl-tag (6x His-tag). The supernatant is applied to and runs slowly through the column, allowing the His-tagged proteins to bind to the nickel ions. The non-binding proteins were removed with protein purification buffer, whereas the binding proteins are eluted with increasing concentrations of imidazole (see Table 5). Here, imidazole displaces the His-tagged proteins and binds to the nickel ions. The eluted fractions were stored at 4 °C, and for verifying purity, the wash and elution fractions were analysed by SDS-PAGE.

Table 5: Conditions for recombinant protein purification.

Shown here are the conditions that resulted in the highest purity of the recombinant proteins.

Protein	DTT	Lysis (in min)	Volume of lysis (in mL)	Column material	Imidazole concentration for elution
*Pf*Prx1a and mutants	0.5 mM	45	30-40	Ni-NTA	200 mM 500 mM
*Pf*Prx1m	0.5 mM	45	30-40	Ni-NTA	100 mM 200 mM 500 mM
*Pf*Prx5 and mutants	0.5 mM	30	30-40	Ni-NTA	100 mM 500 mM
*Pf*PrxQ and mutants	-	60	100	Talon	10 mM, 30 mM
*Pf*Plrx and mutants	0.5 mM	30	30-40	Ni-NTA	100 mM 500 mM

3.3.2 SDS-polyacrylamide gel electrophoresis

In this thesis, sodium dodecyl sulfate polyacrylamide gel electrophoresis (SDS-PAGE) was applied to confirm the purity of the protein samples, and preliminary to protein immunoblotting. SDS denatures and covers the charge of the protein, resulting in an overall negative charge, which is proportional to the protein´s molecular mass. Thus, negatively charged proteins can migrate through an electric field towards the anode, separated by their molecular weight. To break disulfide bonds and denature the proteins, SDS buffer containing DTT was added to the samples (see Tab. 6 for sample preparation) and subsequently boiled for 5 min at 95°C.

Table 6: Protein sample preparation for SDS-PAGE.

Protein sample	SDS sample buffer (1x)	Volume protein sample	Volume applied to gel
Pellet	60 µL	Small amount	5 µL
Cell extract	10 µL	10 µL	5 µL
Flow-through	10 µL	10 µL	5 µL
Washing	10 µL	10 µL	5 µL
Elution fractions	10 µL	10 µL	10 µL

Samples were loaded onto 12 % or 15 % SDS-Gels, and the proteins were able to migrate through the gel, at a steady voltage of 200 V. Gels were then heated for 40 sec in a microwave and washed under constant shaking in ddH_2O for 2 x 10 min. The washed gels were dyed with Coomassie Brilliant Blue G-250 for 15 min after boiling, followed by washing with ddH_2O for 2 x 10 min.

3.3.3 Size-exclusion chromatography

Fast protein liquid chromatography, FPLC, is a method to separate protein mixtures, taking advantage of the difference in affinity of the mixture to the mobile phase and stationary phase. This method is based on the separation of proteins according to their size. Smaller proteins infiltrate the porous matrix of the separation column better than large proteins, resulting in a faster elution of the large proteins. For size fractioning, 1 litre of the running buffer underwent a sterile filtration and degassing for 15 minutes before the solution was applied to the FPLC. In this thesis, a further purification step for the proteins of interest was not needed, since a high degree of purity could be reached by affinity chromatography (> 95 % purity). Here, size-exclusion chromatography was performed to analyse possible multimeric states of wild-type enzymes, and oligomerization shifts in protein mutants. Gel filtration was conducted using a HiLoadTM16/60 SuperdexTM 200 prep grade column attached to an ÄKTA/Unicorn FPLC system (GE Healthcare, Munich). To determine shifts in oligomerization state, proteins were oxidized with 1 mM H_2O_2 or reduced with 0.5 mM DTT, and incubated for 10 minutes on ice. The samples were centrifuged at 13,400 rpm for 10 minutes at 4 °C. Subsequently, a final sample volume of 1 mL was applied to the gel filtration column, which was preliminary equilibrated with 1.5 column

volumes of the buffer of interest. Applied proteins were eluted at a flow rate of 1 mL/min.

3.3.4 Determination of protein concentration

The concentration of the purified protein was determined using the Bradford reagent (Bio-Rad, Munich) which is a spectroscopic analytical assay. The eluted fractions containing the overexpressed protein were pooled into a 10,000 centricon and concentrated via centrifugation. The protein concentration was then determined with Coomassie Brilliant Blue, which binds to proteins and changes from the cationic red form to the anionic blue form and has its absorbance maximum at 590 nm. Before the protein concentrations were determined, a standard curve was carried out by using 0 - 20 µg/mL bovine serum albumin (BSA) as a reference protein. The BSA was solved with H_2O_{dd} and diluted to fit into the concentration of the standard curve. The blank, the protein samples containing BSA, and the protein of interest were mixed with 125 µL Coomassie Brilliant Blue, and the absorbance was measured at 595 nm. The protein concentration was determined according to the following formula:

$$\text{Protein concentration [mg/ml]} = \frac{\Delta A\ 595\ \text{nm}}{Slope\ of\ the\ standard\ curve\ [\text{mg/ml}]} * D$$

ΔA = absorbance; D = dilution

Protein concentrations of protein mixtures and cell extracts are also determined according to Warburg-Christian-Kalkar. This method relies on the absorbance of side changes of the aromatic amino acids tryptophan and tyrosine at 280 nm. As nucleic acids and nucleotides also absorb at 280 nm, their absorbance maximum at 260 nm is subtracted from the measured absorbance of the protein of interest at 280 nm.

$$\text{Protein concentration [mg/ml]} = 1.55\ \Delta A_{280\ nm} - 0.76\ \Delta A_{260\ nm}$$

The concentration of pure enzymes was determined at 280 nm based on their calculated specific extinction coefficient. Some enzymes, like *Pf*GR, contain FAD molecules which also absorb at 280 nm. In this case, 37 $mM^{-1}cm^{-1}$ needs to be added to the extinction coefficient.

The protein concentration was determined according to the following formula:

$$[\text{Protein}] \text{ in mM} = A280\ \varepsilon\ (\text{cm-1mM-1}) * d\ (\text{cm})$$

ε = molar extinction coefficient at λ of 280 nm
d = distance moved by the light in a cuvette (= 1 cm)

3.3.5 Western blotting

Western blot analysis was performed to identify hexahistidyl-tagged proteins or post-translationally modified proteins using specific antibodies listed in Table 7.

Table 7: Antibodies used for Western blot analysis.

	First antibody	**Second antibody**
hexahistidyl-tag	1:1000	1:20,000 (anti-mouse)
***S*-glutathionylated cysteines**	1:750	1:10,000 (anti-mouse)
***S*-nitrosated cysteines**	1:1000	1:10,000 (anti-mouse)

An SDS-PAGE gel with the respective proteins of interest was run and the proteins were transferred to a polyvinylidene difluoride (PVDF) membrane. Prior to usage, the PVDF membrane was activated by soaking in 100 % methanol. For a successful transfer, the SDS gel, the membrane, and twelve filter papers were soaked in Western blot transfer buffer. Six papers were placed at the anodic side of the transfer cassette, directly followed by the membrane, the gel, and another six filter papers. The proteins were transferred from the gel to the membrane by applying 13 V for 30 minutes. To control blotting, the membrane was stained in Ponceau S for 30 seconds and destained with 1 % acetic acid until the bands were visible. Then, the membrane was completely destained by washing it several times in TBST. The membrane was blocked with 5% (w/v) non-fat milk in TBST for 1 h at 22 °C or overnight at 4 °C, to prevent non-specific binding of the antibodies to not occupied protein binding sites. Subsequently, the membrane was washed three times for 10 min in TBST before the first antibody was applied (see Table 7). After incubation with the antibody for 1 h at room temperature, the membrane was washed again in TBST as described above, and the second antibody was applied for 1 h at room temperature, followed by a final washing step in TBST. The membrane was then incubated for 1 minute with the

chemiluminescence mixture, and chemiluminescence was detected with the Intas ECL ChemoStar Imager connected to ChemoStar TS software.

3.3.6 Protein *S*-glutathionylation

To investigate the susceptibility of peroxiredoxins *Pf*Prx1a, *Pf*Prx1m, *Pf*Prx5, and *Pf*PrxQ$^{1-164}$, and *Pf*-plasmoredoxin to *S*-glutathionylation, enzymes (except *Pf*PrxQ$^{1-164}$) were purified under reducing conditions (50 mM sodium phosphate, 300 mM sodium chloride, 0.5 mM DTT, pH 8.0). Afterwards, DTT was removed using Zeba™ spin desalting columns (ThermoFisher Scientific, Waltham, MA, USA) according to the instructions of the manufacturer. 0.8 mg/ml protein was incubated with 0, 0.05, 0.1, 0.2, 0.5, 1, 2, or 5 mM GSSG for 45 min at 37 °C, followed by desalting as described above. Afterwards, the samples were applied to non-reducing SDS-PAGE. Ponceau staining of the membrane after blotting served as a loading control. *S*-glutathionylated protein was detected via semi-dry Western blotting using a monoclonal anti-glutathione antibody (Abcam, Cambridge, UK; diluted 1:750 in 5% nonfat milk with Tris-buffered saline Tween-20 (TBST)) and a horseradish peroxidase-conjugated goat anti-mouse antibody (Dianova, Hamburg, Germany; diluted 1:10,000 in 5% nonfat milk with TBST). Experiments were carried out in triplicate using different batches of enzyme. For glutathionylation analysis of cysteine mutants, proteins were prepared as mentioned above, and 0.8 mg/ml were subsequently incubated with 5 mM GSSG for 10 minutes and desalted. Protein samples were analyzed via Western blotting as described above.

3.3.7 Protein *S*-nitrosation

Potential protein *S*-nitrosation on *Pf*Prx1a, *Pf*Prx1m, *Pf*Prx5, *Pf*PrxQ, and *Pf*Plrx wild type and protein mutants was studied via Western blot analysis and MALDI-TOF MS. The physiologically relevant small molecular weight S-nitrosothiol GSNO and Cys-NO served as an NO donor, which is able to release NO and transnitrosate proteins (Broniowska *et al*., 2013; Hess *et al*., 2005).

For the detection of *S*-nitrosated proteins the biotin-switch assay was performed as described in Wang *et al*. 2014. An antibody for the direct detection of *S*-nitrosation is not available till today. Therefore, the biotin-switch enables the detection of *S*-nitrosated thiol groups via protein immunoblotting using an anti-biotin antibody. Therefore, 0.8 mg/mL prereduced enzyme was incubated with 0 to 1 mM GSNO or Cys-NO in GSNO/ Cys-NO buffer at 22 °C for 1 h in the dark. By adding 100 %

acetone (cold) the reaction was stopped, followed by protein precipitation at -20 °C for 30 minutes. The samples were centrifuged at 8,000 g for 5 minutes, the supernatant was subsequently discarded and the formed pellets were washed (70 % acetone; cold) and centrifuged (1. 8,000 g, followed by 5,000 g for 5 minutes at 4 °C) three times. The pellets were resuspended in blocking buffer containing 200 mM IAA, in order to block residual free cysteine thiols, and incubated in the dark at 50 °C for 45 minutes. By adding 100 % acetone (cold) the reaction stopped, followed by protein precipitation, centrifugation and washing of the pellets using 70 % acetone as described above. In order to change from *S*-nitrosated thiols to biotinylated thiols (biotin-switch), pellets were dissolved in labeling buffer and incubated at 25 °C for 1 h in the dark. As a negative control, samples without sodium ascorbate were prepared. The reaction was stopped by adding 100% acetone (cold), followed by protein precipitation and washing of the pellets as described above. Pellets were resuspended in blocking buffer and applied to SDS-PAGE. The following western blot analysis was performed as described above (see chapter 3.3.5), using the monoclonal anti-biotin antibody (Santa Cruz, Dallas, TX, USA; diluted 1:1,000 in 5% (w/v) non-fat milk in TBST) followed by a horseradish peroxidase-conjugated goat anti-mouse antibody (Dianova, Hamburg; diluted 1:10,000 in 5% (w/v) non-fat milk in TBST).

3.3.8 Mass spectrometric analysis

The following protocol was made available and is published by the working group of Prof. Dr. Linne, Marburg.

For mass spectrometry, enzymes were purified under reducing conditions (50 mM sodium phosphate, 300 mM sodium chloride, 0.5 mM DTT, pH 8.0) and DTT was removed using Zeba™ spin desalting columns (ThermoFisher Scientific, Waltham, MA, USA) according to the instructions of the manufacturer before incubating 0.8 mg/ml protein with 5 mM GSSG for 10 minutes at 37°C. To remove unbound GSSG, the samples were desalted as described above and analyzed via electrospray ionization mass spectrometry. The mass spectrometric analysis of the samples was performed using an Orbitrap Velos Pro mass spectrometer. An Ultimate nanoRSLC-HPLC system, equipped with a custom end-fritted 50cm x 75µm C18 RP column filled with 2.4 µm beads was connected online to the mass spectrometer through a Proxeon nanospray source. The tryptic digest was injected onto a 300 µm ID x 1cm

C18 PepMap pre-concentration column (Thermo Scientific). Automated trapping and desalting of the sample was performed at a flowrate of 6 µL/min using water/0.05% formic acid as solvent. Separation of the tryptic peptides was achieved with the following gradient of water/0.05% formic acid (solvent A) and 80% acetonitrile/0.045% formic acid (solvent B) at a flow rate of 300 nL/min: holding 4% B for five minutes, followed by a linear gradient to 45% B within 30 minutes and linear increase to 95% solvent B in additional 5 minutes. The column was connected to a stainless steel nanoemitter (Proxeon, Denmark) and the eluent was sprayed directly towards the heated capillary of the mass spectrometer using a potential of 2,300 V. A survey scan with a resolution of 60,000 within the Orbitrap mass analyzer was combined with at least three data-dependent MS/MS scans with dynamic exclusion for 30 s either using CID with the linear ion-trap or using HCD combined with orbitrap detection at a resolution of 7500.

Data analysis was performed using Proteome Discoverer 2.2 (Thermo Scientific) with SEQUEST search engine or MaxQuant with Andromeda search engine. Uniprot databases were used (made available by the working group of Prof. Linne, Marburg).

3.4 Structural biology methods

3.4.1 Modelling

Homology modelling (Arnold *et al*. 2006) of *Pf*Prx1a was performed using the crystal structures of Plasmodium vivax Prx1a (2i81) (Artz *et al*. 2006) (2h66) (Vedadi *et al*. 2007) as templates. Structural comparison of the models and the known structures was done with Coot (Emsley *et al*. 2010) and all figures were prepared by using Chimera (Petterson *et al*. 2004). The modelling and the structural models shown in this thesis were prepared by Dr. Karin Fritz-Wolf.

3.5 Determination of kinetic parameters

Enzyme kinetics is determined in order to measure the activity of a catalytically active protein towards its substrate. Therefore, the substrate binds to the enzymes active site. The maximum velocity of the enzymatic reaction is represented by a decrease of substrate and a contemporaneous increase of product over a defined period of time.

The Michaelis-Menten equation shows the dependency of the reaction velocity towards the substrate concentration and can be calculated as follows:

$$V_0 = \frac{Vmax \cdot [S]}{KM + \cdot [S]}$$

v_0: reaction velocity; V_{max}: maximum velocity; [S]: substrate concentration; K_M: Michaelis-Menten constant

V_{max} is the maximum velocity of a reaction and can be reached by high substrate concentrations. The Michaelis-Menten constant K_M is an indicator for the substrate's affinity towards the enzyme and defines the substrate concentration at half maximum velocity. The lower the K_M value, the higher the affinity of the enzyme towards the substrate.

To determine the specific enzyme activity, the change of absorbance of a substrate or product is measured over a defined period of time and can be calculated as follows:

$$VA\ \left(\frac{U}{mL}\right) = \frac{\Delta A \cdot V}{\Delta t \cdot \varepsilon \cdot v \cdot d} \cdot D$$

VA: volume activity; ΔA·Δt-1: alteration of the absorbance over the time; V: total volume; ε: extinction coefficient; v: volume of the enzyme solution; d: thickness of the cuvette; D: dilution factor

$$\text{Specific enzyme activity } \frac{U}{mg} = \frac{VA}{[E]}$$

VA: volume activity; [E]: enzyme concentration in $mg \cdot mL^{-1}$

The activity of an enzyme is given in units (U), and one unit is defined as the conversion of 1 µmol substrate per minute.

The peroxidase activity of *Pf*Prx1a and mutants was determined at 25°C in 50 mM sodium phosphate, 300 mM sodium chloride, pH 8.0 using a thioredoxin-based reducing system containing *Pf*TrxR, *Pf*Trx1, NADPH, and hydrogen peroxide. 200 µmol/min*mg *Pf*TrxR, 20 µM *Pf*Trx1 and 100 µM NADPH were preincubated for 5 minutes. 100 µM H_2O_2 was added and the slight change in absorbance at 340 nm was monitored as background. Depending on the specific activity of the Prx (Wt and mutants), 50-200 nM Prx was added to start the reaction. The decrease in NADPH

concentration was monitored at 340 nm and the specific activity was calculated as described above (Rahlfs and Becker, 2001).

Statistical analyses.

Values are mean values ± SEM of at least three independent experiments. A student`s unpaired, two-tailed t-test with a 95% confidence interval level was performed with Graph Pad Prism 6.0 in order to compare means.
* $p < 0.05$; ** $p < 0.01$; *** $p < 0.001$

4. Results

4.1 Peroxiredoxins in *P. falciparum*

In this chapter the in-depth characterization of *Pf*Prxs wild type and especially of *Pf*Prx1a mutants, with respect to their catalytic activity and oligomerizational state, is described.

4.1.1 Site-directed mutagenesis of *Pf*Prxs

For in-depth characterization of amino acid residues, which are in direct proximity to the enzymes´ active site or at the A-type and B-type interfaces, site-directed mutagenesis was performed. Within this thesis, mutants of *Pf*Prx1a (*Pf*Prx1a^{Y42A}, *Pf*Prx1a^{H82A}, *Pf*Prx1a^{W85A}, *Pf*Prx1a^{R125A}, *Pf*Prx1a^{D77A}, *Pf*Prx1a^{V116D}, *Pf*Prx1a^{V116T}, *Pf*Prx1a^{L117W}) were constructed. Site-directed mutagenesis of *Pf*Prxs cysteine mutants of *Pf*Prx1a (*Pf*Prx1a^{C50S}, *Pf*Prx1a^{C74A}, *Pf*Prx1a^{C170S}, *Pf*Prx1a$^{C50S/C74A}$, *Pf*Prx1a$^{C50S/C170S}$, *Pf*Prx1a$^{C74A/C170S}$, *Pf*Prx1a$^{C50S/C74A/C170S}$), *Pf*Prx5 (*Pf*Prx5^{C117S}, *Pf*Prx5^{C143S}) and *Pf*PrxQ (*Pf*PrxQ^{C56S}, *Pf*PrxQ^{C103S}) were created in earlier studies in the Becker lab and published (Brandstaedter *et al*. 2019; Brandstaedter 2017).

4.1.2 Heterologous overexpression and purification of *Pf*Prxs

The heterologous overexpression and purification of *Pf*Prxs Wt were performed using the protocols described in Chapter 3.2.3. The purification of the *Pf*Prxs wild types are visualized in Fig. 9, using Coomassie stained gels after Ni-NTA or TALON affinity chromatography. The respective mutants of *Pf*Prxs were purified according to the above-mentioned protocols, which had been prepared for the purification of *Pf*Prxs wild type enzymes. *Pf*Prx1a, *Pf*Prx1m, and *Pf*Prx5 were purified under reducing conditions using 0.5 mM DTT to prevent hyperoxidation and to maintain a fully reduced enzyme for studies on post-translational modifications, which under specific conditions require a fully reduced protein. *Pf*PrxQ$^{1-164}$ was lysed and purified without reducing agents. The purified proteins were stored at 4°C or at -20 °C with 1 mM TCEP.

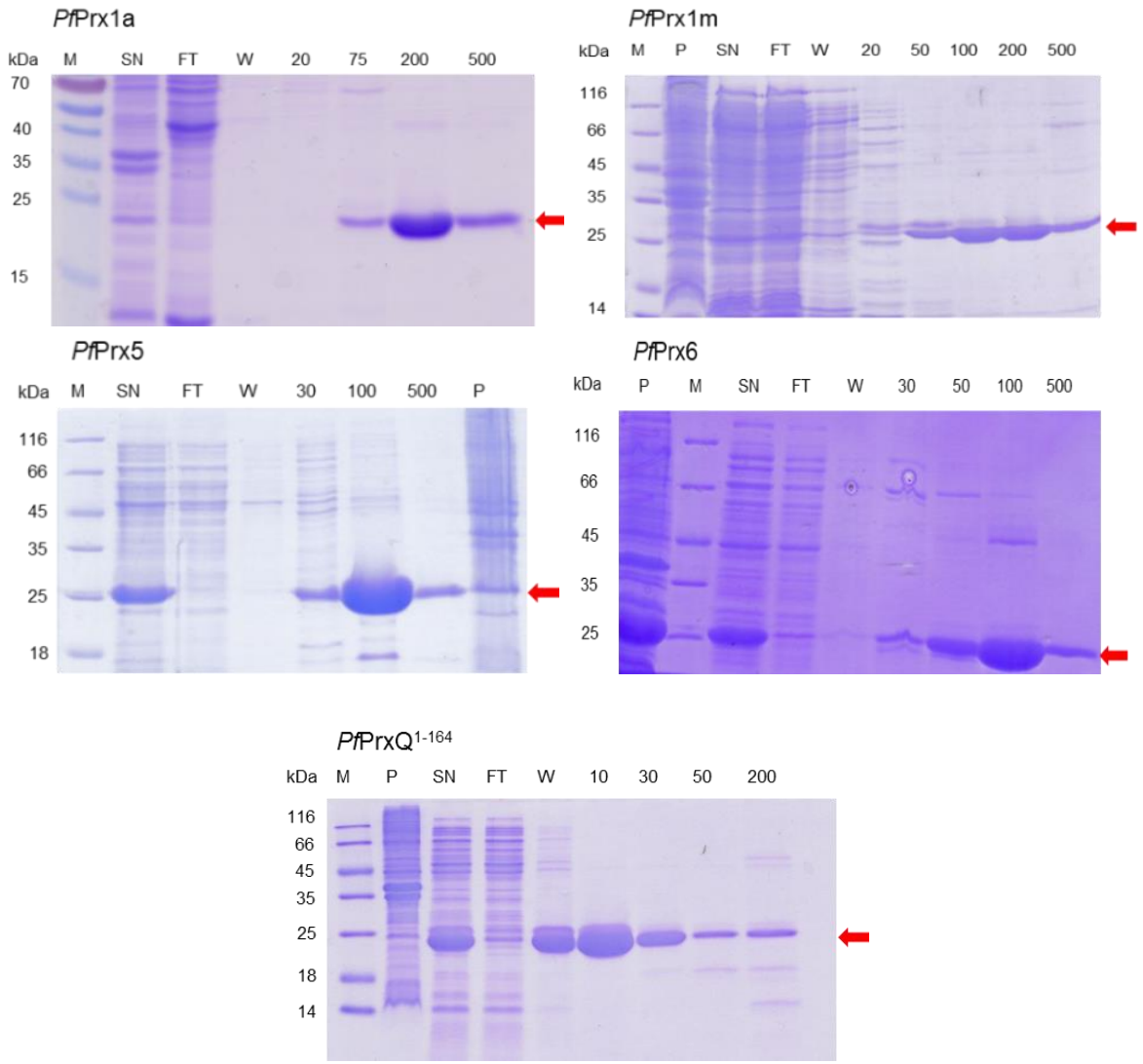

Figure 9: Protein purification of *Pf*Prxs wild type enzymes using affinity chromatography. *Pf*Prx1a, *Pf*Prx1m, and *Pf*Prx5 were purified via Ni-NTA affinity chromatography resin, *Pf*PrxQ with TALON resin. M: Marker (protein ladder), P: Pellet, Sn: supernatant, FT: flow through, W: wash, numbers: imidazole concentrations in mM used for protein elution. Red arrows show the respective protein.

4.1.3 Oligomerization behavior of *Pf*Prxs

In order to study the effects of reduction and oxidation on the oligomerization of *Pf*Prxs wild type proteins, gel filtration experiments were carried out. Therefore, samples were prepared and treated with 5 mM DTT or 10 mM H_2O_2, and incubated for 10 minutes at 4 °C. The samples were desalted using Zeba Spin Desalting columns and subsequently applied to an ÄKTA FPLC System for analysis.

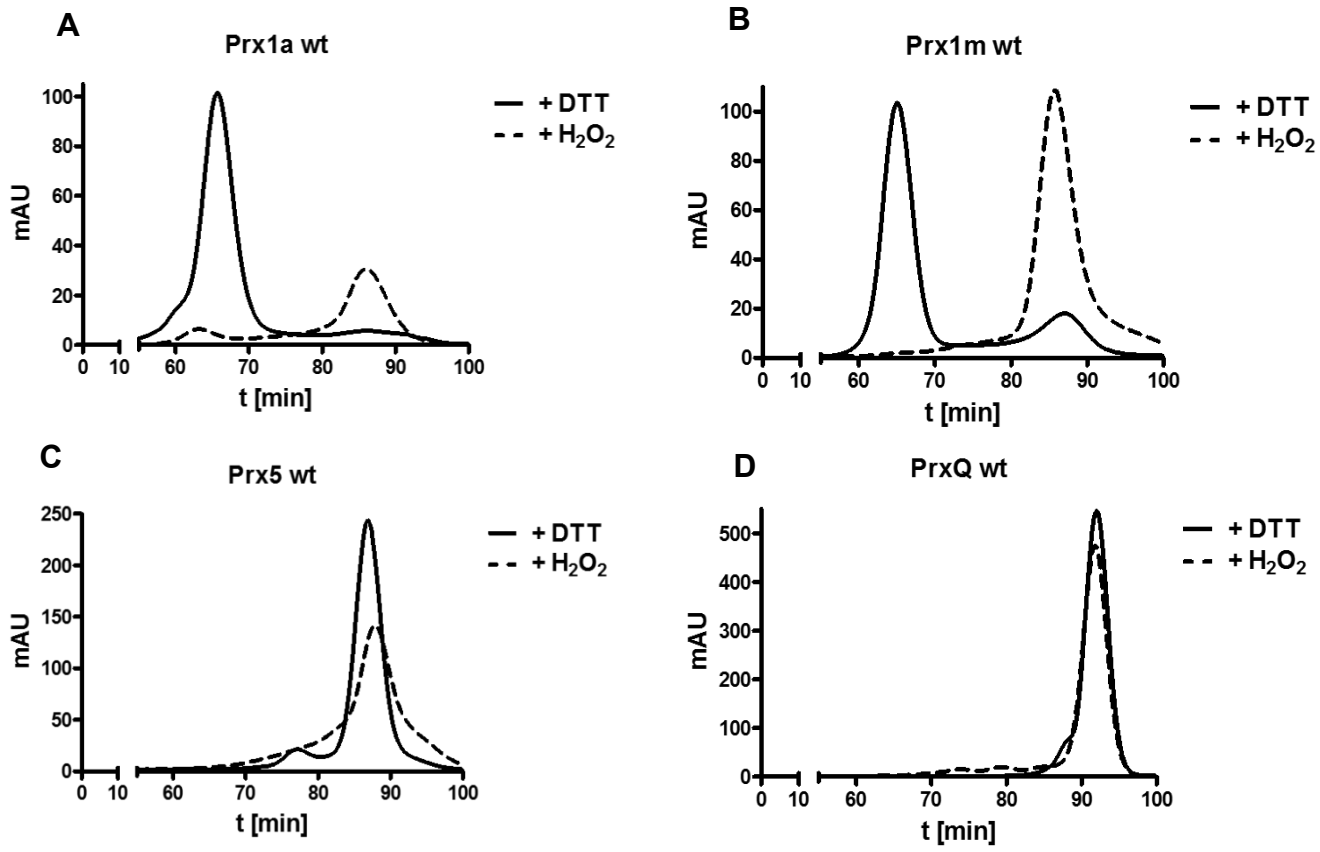

Figure 10: Size-exclusion chromatography of *Pf*Prx wild types under reducing (0.5 mM DTT) and oxidizing (1 mM H_2O_2) conditions. Oligomerization behaviour of *Pf*Prx1a, *Pf*Prx1m, *Pf*Prx5, and *Pf*PrxQ wild type proteins. Solid: decamer (~230 kDa), Dashed: dimer (~46 kDa).

As shown in Figure 10, 2-Cys peroxiredoxins *Pf*Prx1a and *Pf*Prx1m undergo a change in oligomerization, from a decameric (solid line, ~230 kDa) to a dimeric (dashed line, ~ 46 kDa) oligomerisation state, when reduced with DTT or oxidized with H_2O_2, respectively (Fig.10, A and B). *Pf*Prx5 and *Pf*PrxQ do not show changes in the proteins molecular mass depending on the redox state, with *Pf*Prx5 being in a dimeric and *Pf*PrxQ in a monomeric state (Fig 10, C and D).

As basis for further studies, a structural comparison of the amino acid residues potentially contributing to peroxidase activity and oligomerization in *P. falciparum* peroxiredoxins was carried out, based on sequence alignments and three-dimensional structural models (Fig. 12) and is listed in Table 8.

Table 8: Comparison of analogous amino acids of *Plasmodium falciparum* peroxiredoxins. The amino acid residues potentially contributing to the peroxidase activity in the different peroxiredoxins are indicated. The *Pf*Prx1a model used to support primary structures is based on *P. vivax* Prx1a (2i81) [35], (2h66) [36], sequence identity ~ 0.86. The *Pf*PrxQ model is based on *Xanthomonas campestris* Prx (5iiz) [39], sequence similarity = 0.31.

***Pf*Prx1a**	Y42	C50	C74	D77	H82	W85	V116	L117	R125	C170
***Pf*Prx1m**	Y59	C67	I91	D94	H99	W102	V133	L134	R142	C187
***Pf*Prx5**	L51	C59	I86	N89	L94	W97	M122	L123	R137	
***Pf*PrxQ**	Y59	C56	L91	D94	Q99	W102	L126	T127	R135	

All of the above mentioned peroxiredoxins possess the typical peroxidatic cysteine and active site proximal tryptophan and arginine residues (W85 and R125 for *Pf*Prx1a). With an exception for *Pf*Prx5, the peroxiredoxins *Pf*Prx1a, *Pf*Prm1m and *Pf*PrxQ possess a tyrosine and aspartic acid residue (see Table 8), which can potentially contribute to the enzymes peroxidase activity and oligomerization (Y42 and D77 for *Pf*Prx1a). To experimentally dissect the amino acid interaction and contribution to the enzymes activity and oligomerization behavior, the further studies are focused on the typical 2-Cys peroxiredoxin *Pf*Prx1a of *P. falciparum*.

4.2 In-depth characterization of *Pf*Prx1a and mutants

4.2.1 Heterologous overexpression and purification of *Pf*Prx1a mutants

The heterologous overexpression and purification of *Pf*Prx1a mutants were performed using the protocols mentioned in Chapter 3.2.3. The purification of the *Pf*Prx1a mutants are visualized exemplarily in Fig. 11, using Coomassie stained gels after Ni-NTA affinity chromatography. *Pf*Prx1a mutants were purified under reducing conditions using 0.5 mM DTT to prevent hyperoxidation.

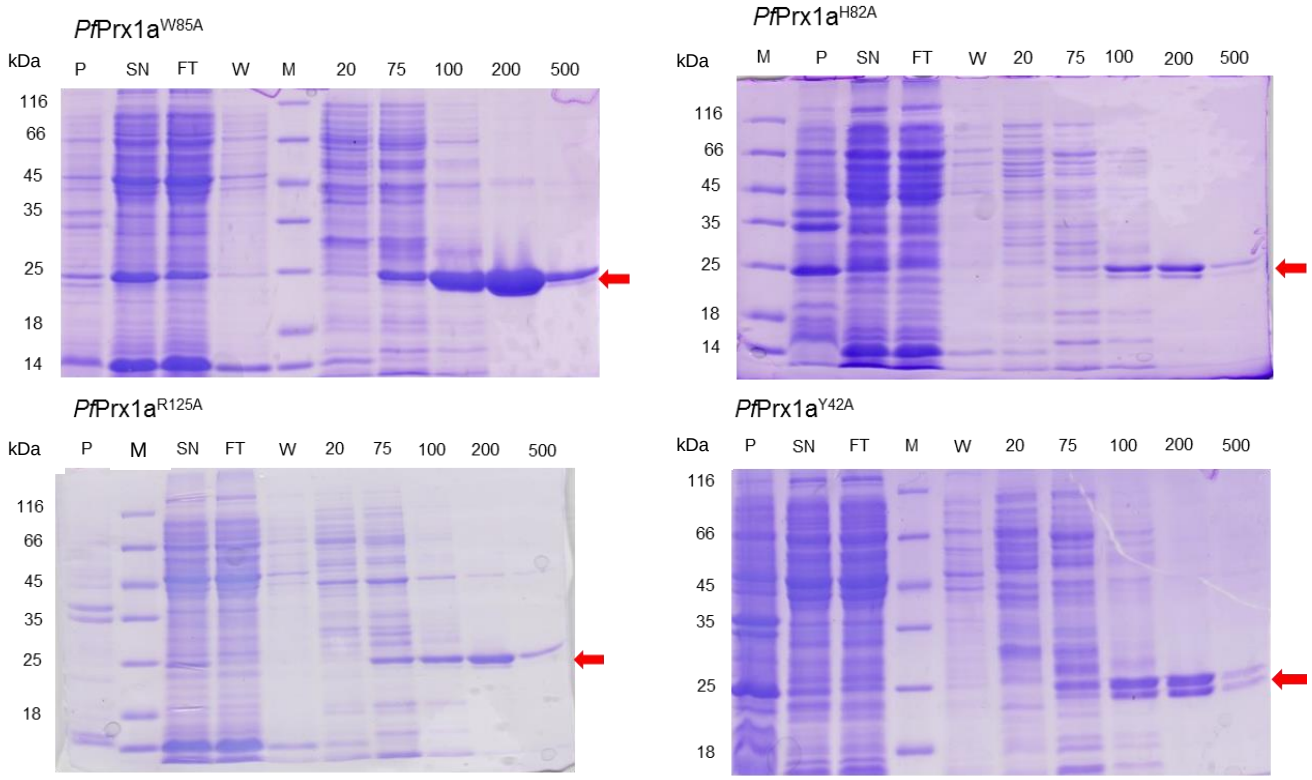

Figure 11: Protein purification of *Pf*Prx1a mutants using affinity chromatography. Coomassie-stained SDS gels of *Pf*Prx1a^{W85A}, *Pf*Prx1a^{H82A}, *Pf*Prx1a^{R125A}, and *Pf*Prx1a^{Y42A} are shown exemplarily for the purification of mutants and were purified with Ni-NTA affinity resin. M: Marker (protein ladder), P: Pellet, SN: supernatant, FT: flow through, W: wash, numbers: imidazole concentrations in mM used for protein elution. Red arrows show the respective protein.

4.2.2 Structural dissection of *Pf*Prx1a

*Pf*Prx1a shares the typical characterics of cytosolic 2-Cys peroxiredoxins, including the conformational changes of the peroxidase catalysis active site and the changes in oligomerisation from (do)decamer to dimer. In Figure 12 the structural model of *Pf*Prx1a decamer shows the five dimers, with a lighter and a darker color representing the two monomers. The monomers are built to dimers via the monomer/monomer interface and the decamer via the dimer/dimer interface (in Fig. 12 referred to as mon/mon and dim/dim). The dimer/dimer and monomer/monomer interfaces are shown with grey lines. The peroxidatic active site with C50 and C170 is marked in purple in every monomer.

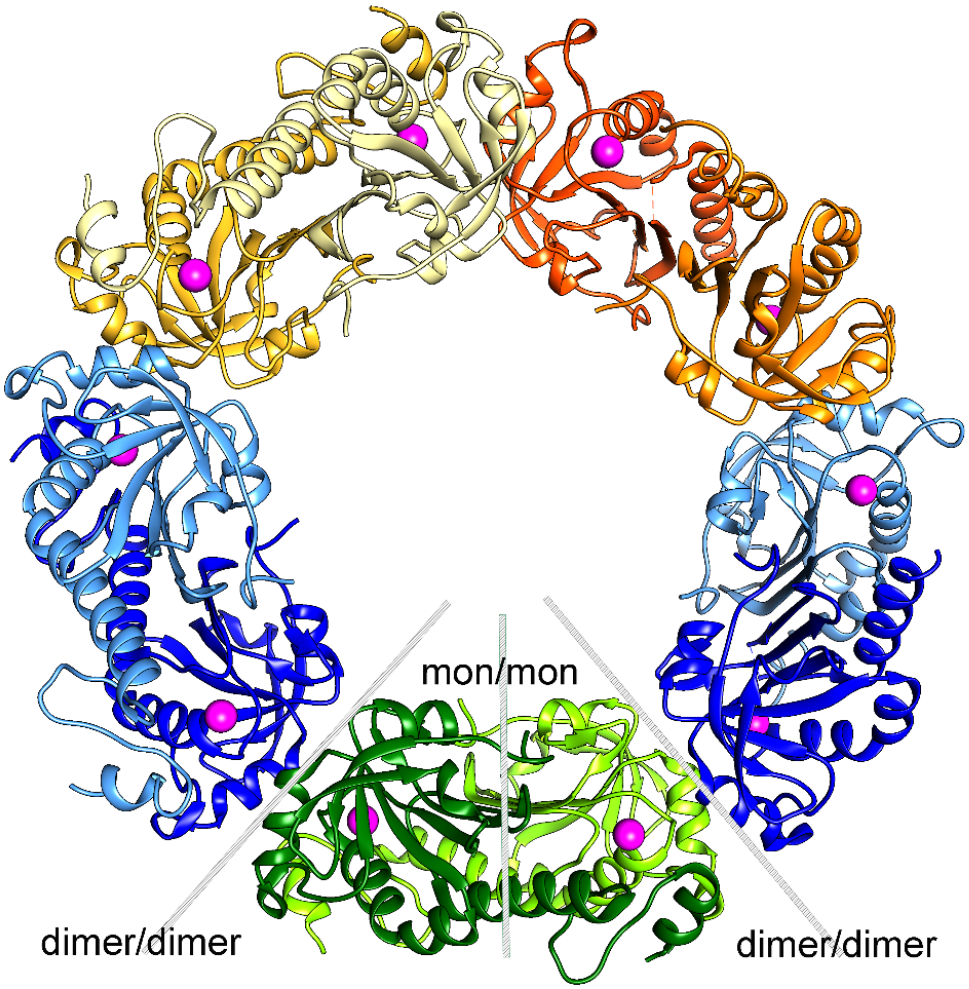

Figure 12: Structural model of the *Pf*Prx1a – decamer. The five dimers are represented in orange, yellow, blue or green, with a lighter and a darker color distinguishing the two subunits (monomer) of one dimer. The peroxidase active sites of each subunit are visualized in purple and grey lines show the dimer/dimer and the monomer/monomer interfaces. The model is based on the crystal structure of *P. vivax* Prx1a in its reduced form (2i81) (Artz *et al*. 2006). Molecular graphics images are produced by Dr. Karin Fritz-Wolf using the UCSF Chimera (Pettersen *et al*. 2004). The figure was prepared by Dr. Karin Fritz-Wolf.

For in-depth dissection of peroxiredoxin catalysis, numerous mutants were analyzed regarding their impact on conformational and oligomerization change, as well as on the enzymes catalytic activity. All mutations performed were chosen because the amino acids of interest are interfacial residues at the monomer/monomer interface (V116D, V116T, L117W), at the dimer/dimer interface (D77A), interact with interfacial residues, or are involved in stabilizing the active site loop (Y42, H82, W85).

The active site loop, which includes the peroxidatic cysteine C50, is especially stabilized by amino acid residues H82, Y42 and D45, and undergoes a rotation upon oxidation especially in the region D45 to S52 (see Fig. 13). In the reduced form of

the enzyme (Fig. 13, A, Fig 14, B), the fully folded C-term of the second subunit and the hydrogen bond between C50 and R125 are visible. Residue H82 and the loop residue D45 are hydrogen bonded, and Y42 stabilizes the loop via Van der Waals interactions. Furthermore, in reduced *Pf*Prx1a, dimer/dimer interface residue D77 of the adjacent dimer forms a hydrogen bond to the main chain of D45 (Fig. 13, A).

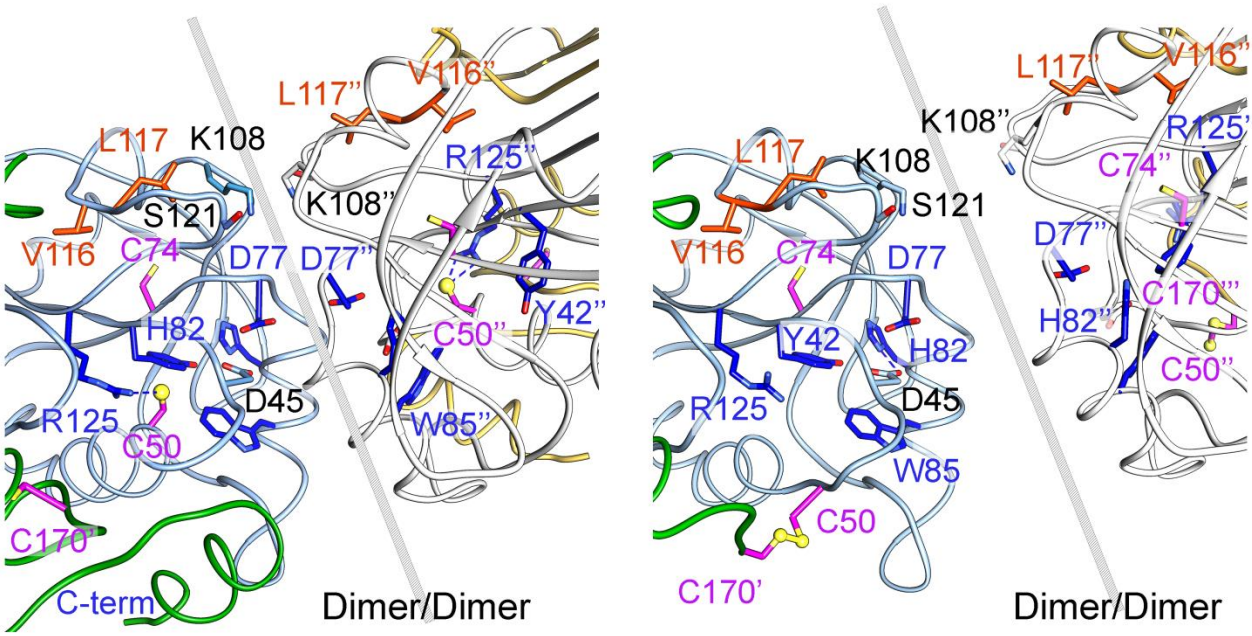

Figure 13: Close up of the dimer/dimer interface and the peroxidase–active site in its reduced (A) and its oxidized form (B). The two subunits of the dimers are colored green and light blue or white and yellow. Cysteine residues are shown in purple, mutated residues lining the peroxidase active site or the dimer/dimer interface are shown in blue and the monomer/monomer interface residues V116 and L117 are shown in orange. Amino acids interacting with mutated residues are colored according to their subunits. The models are based on the crystal structures of *P. vivax* Prx1a in its reduced and in its oxidized form (2h66 (Vedadi *et al*. 2007), 2i81 (Arzt *et al*.2006). (A) Reduced form. The fully folded C-term of the second subunit and the hydrogen bond between C50 and R125 are visible. (B) Oxidized form. The C-term is partially unfolded and a disulfide bond between C50 and C170' is formed. The figure was prepared by Dr. Karin Fritz-Wolf.

In the oxidized form, the C-term is partially unfolded and a disulfide bond between C50 and C170' is formed. The dimer/dimer interface (Fig.13, B) undergoes a change in oligomerization from decamer to dimer. Numerous residues (40 – 50) of a helix, which are close to the peroxidase active site, rearrange to a more stretched conformation (see Fig. 14, A). These sterical changes make C50 no longer able to interact with R125 and instead lead to the formation of a disulfide to C170' of the neighbouring subunit (Fig. 14A).

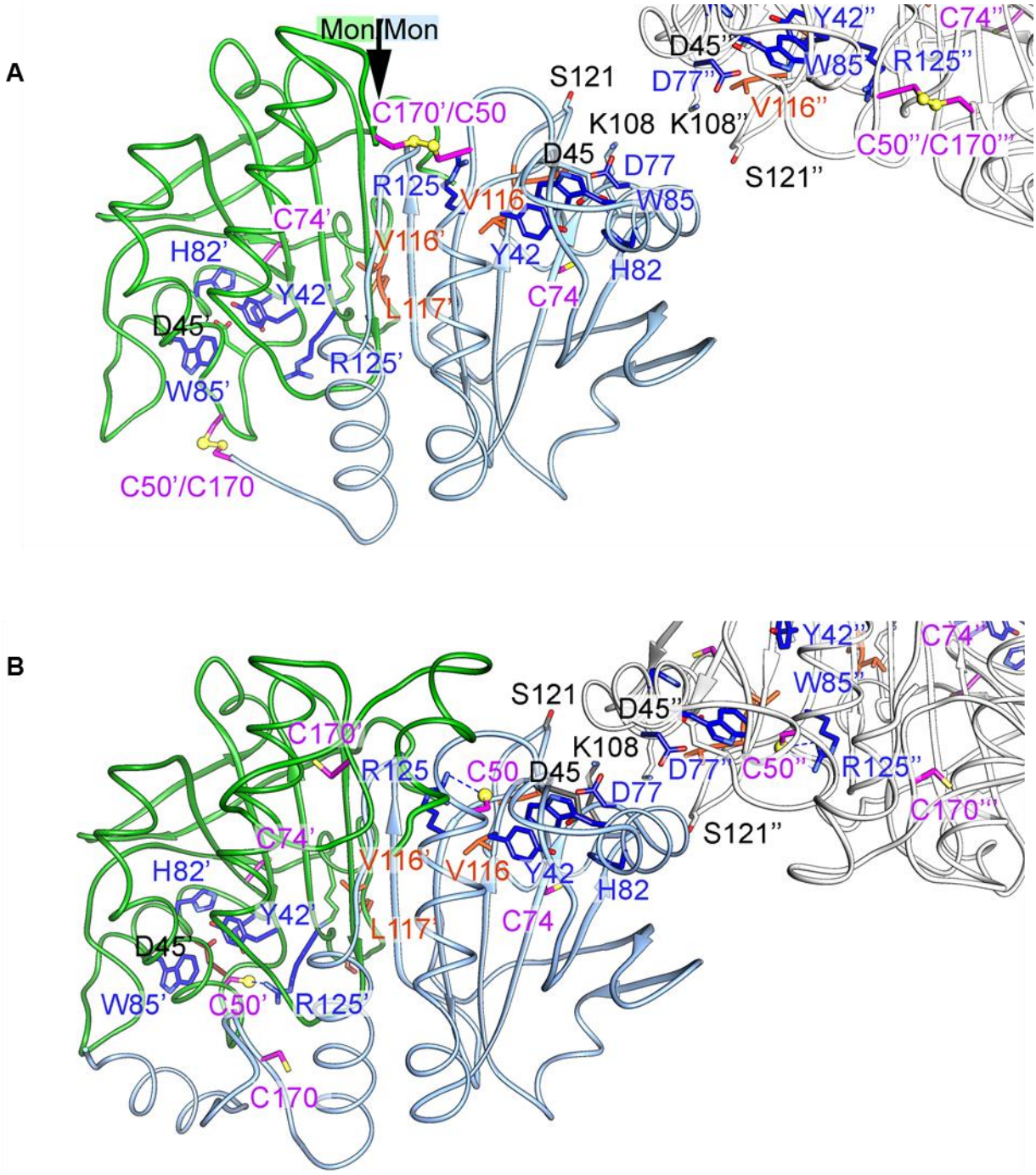

Figure 14: Close up of the monomer/monomer interface in its oxidized (A) and reduced (B) state. The models are prepared as described in Figure 13. The figure was prepared by Dr. Karin Fritz-Wolf.

Figure 14 illustrates the monomer/monomer interface more clearly and shows the changes in oxidized (A) and reduced (B) state from a different perspective.

4.2.3 Oligomerization behavior of *Pf*Prx1a mutants

Analysis of the *Pf*Prx1a mutants via size exclusion chromatography revealed changes in oligomerisation, which often depended on the redox state (see Fig.15 -

18). All cysteines present in the protein were mutated to serine or alanine (C50S, C74A, C170S). In the reduced form of the Wt enzyme, the active site loop is stabilized through decamer interactions. Peroxidatic cysteine C50, included in the loop, interacts with Arg125. The C-terminus, including resolving cysteine C170, is ordered in a fully folded decameric state. In the oxidized enzyme, the C-terminus is partially unfolded, and a disulfide between C50 and C170' is formed, accompanied by the transition from decamer to dimer.

As expected for a typical 2-Cys peroxiredoxin, reduced *Pf*Prx1a Wt was predominantly decameric, whereas oxidized protein was present as a dimer (see Fig. 10). The mutant of the peroxidatic cysteine C50S appeared solely as a (do)decamer, independent of the redox-state, whereas the resolving cysteine mutant C170S eluted as a mixture of decamers and dimers (Fig. 15). All samples had a protein concentration of ~ 3.5 mg/mL. The differences in the height of the respective peaks can be due to a potentially instable protein, caused by incubation with oxidizing or reducing agents and protein loses due to desalting.

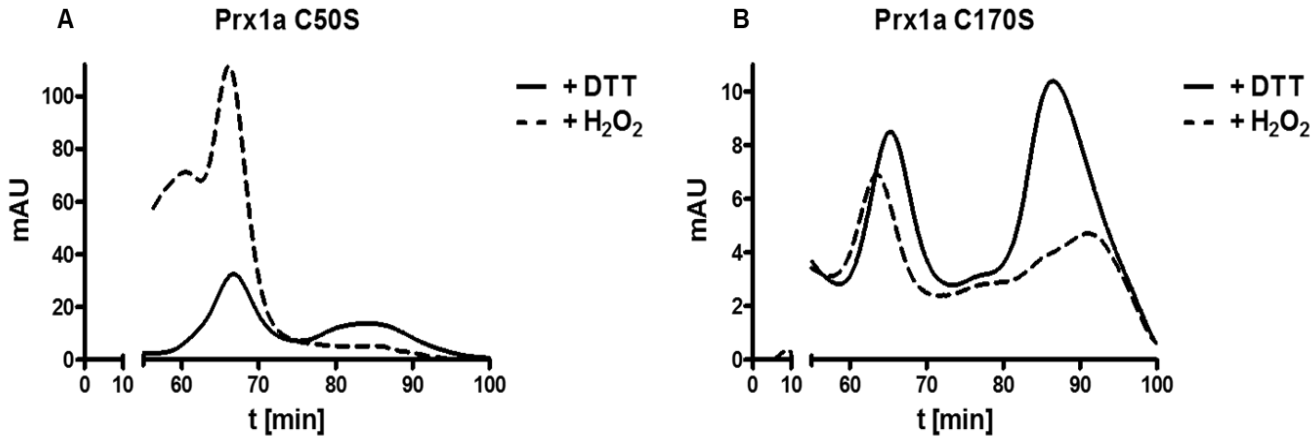

Figure 9: Size-exclusion chromatography of *Pf*Prx1a^{C50S} and *Pf*Prx1a^{C170S} under reducing (0.5 mM DTT) and oxidizing (1 mM H_2O_2) conditions. Oligomerization behavior of *Pf*Prx1a Cysteine mutants C50S (A) and C170S (B). . Elution profiles of reduced proteins are portrayed with solid line, oxidized proteins with dashed lines.

Mutant *Pf*Prx1a^{R125A} showed oligomerization states comparable to the wild type enzyme, illustrating a reduced decamer and an oxidized dimer (Fig. 16, A). The oligomerization behavior of mutants *Pf*Prx1a^{Y42A} and *Pf*Prx1a^{H82A} were independent of the redox state and eluted solely as dimers (Fig. 16, B and C). Mutant

*Pf*Prx1a^{W85A} was decameric in reduced state and the oxidized protein mutant did not dissociate into dimers but eluted as $(\alpha_2)_3$ oligomers (~140 kDa) (Fig. 16, D).

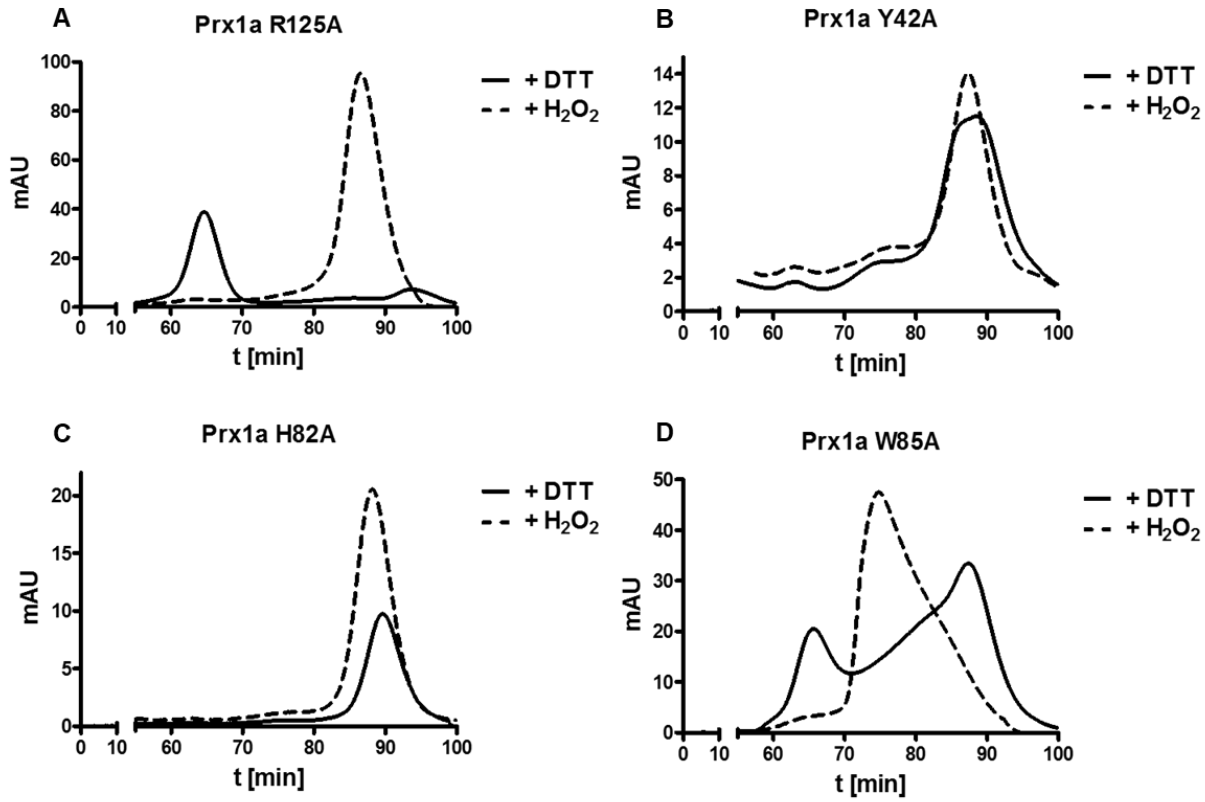

Figure 10: Oligomerisation behavior of *Pf*Prx1a mutants in reduced and oxidized state. A. *Pf*Prx1a^{R125A}. B. *Pf*Prx1a^{Y42A}. C. *Pf*Prx1a^{H82A}. D. *Pf*Prx1a^{W85A}. Elution profiles of reduced proteins are portrayed with solid line, oxidized proteins with dashed lines.

The dimer/dimer interface mutant *Pf*Prx1a^{D77A} eluted solely as dimer in oxidized and reduced state, whereas a slight drift in size could be observed for the reduced protein mutants (Fig. 17).

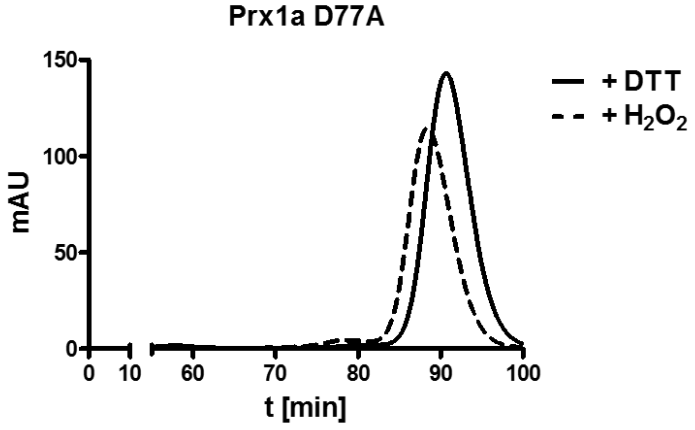

Figure 11: Oligomerisation behavior of *Pf*Prx1a^{D77A} in reduced and oxidized state. Elution profiles of reduced proteins are portrayed with solid line, oxidized proteins with dashed lines.

The oligomerization of *Pf*Prx1a with a mutation at position V116 depended on the substituted amino acid. A mutation to threonine did not affect the oligomerization behavior, showing a reduced decamer and an oxidized dimer (Fig. 18, B). For *Pf*Prx1a^{V116D}, the mutant eluted solely as dimer, independent of its redox status (Fig. 18, A). The second monomer/monomer interface mutant, *Pf*Prx1a^{L117W}, was in a dimeric oligomerization state as oxidized protein, and eluted as mixtures of dimers and monomers when reduced (Fig. 18, C) (see Table 9).

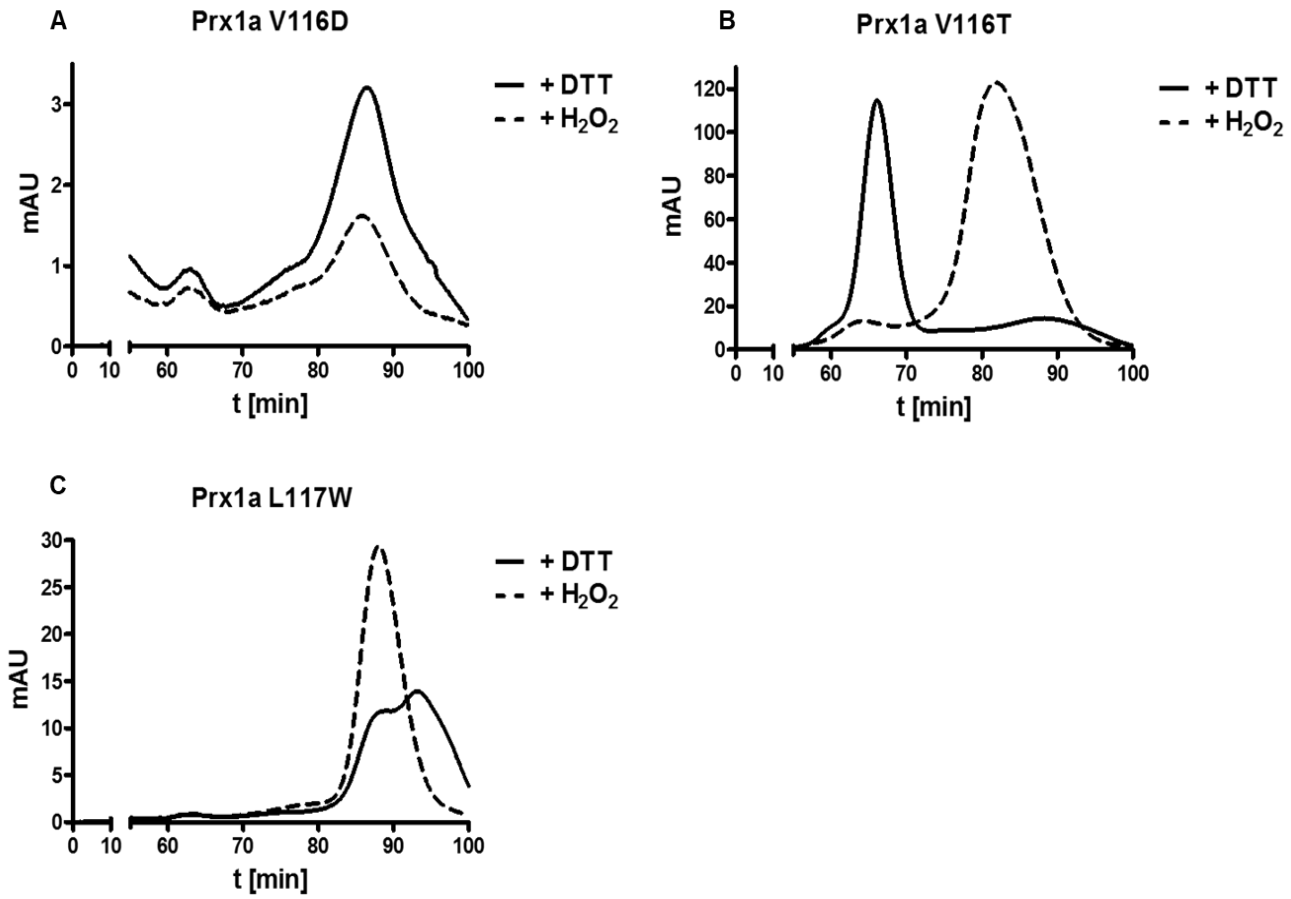

Figure 12: Oligomerisation behavior of *Pf*Prx1a mutants in reduced and oxidized state. A. *Pf*Prx1a^{V116D}. B. *Pf*Prx1a^{V116T}. C. *Pf*Prx1a^{L117W}.

4.2.4 Enzyme activity of *Pf*Prx1a mutants/ Kinetic alterations in mutants

As listed in Table 9, the specific activity of *Pf*Prx1a wild type and mutants were measured using the peroxidase activity assay with thioredoxin and thioredoxin reductase as backup system. For a better overview of the impact of amino acid

substitution, the changes in oligomerization in reduced and oxidized state are given for means of comparison.

Table 9: Oligomerization state and peroxidase activity of *Pf*Prx1a wild type and mutants. Oligomerization states under reducing and oxidizing conditions are provided. Substrate (H_2O_2) turnover per enzyme molecule and min is shown [min^{-1}]. Peroxidase activity was determined at 25°C and in the presence of 100 µM H_2O_2. Values represent mean values ± SEM obtained in at least three independent experiments. For determining statistical significance, the student`s t-test was performed. * p <0.05; ** p < 0.01; *** p < 0.001.

***Pf*Prx1a**	**Oligomerization state**		**Peroxidase activity**	
	+ DTT	+ H_2O_2	Substrate turnover [min^{-1}]	Spec. activity [µmol/min*mg]
Wt	decamer	dimer	56.1 ± 6.7	2.41 ± 0.29
C50S	(do)-decamer	(do)-decamer	< 0.02	< 0.02
C170S	decamer/ dimer	decamer/ dimer	< 0.02	< 0.02
R125A	decamer	dimer	6.39 ± 0.3*	0.27 ± 0.01***
Y42A	dimer	dimer	< 0.02	< 0.02
D77A	dimer	dimer	12.2 ± 0.95*	0.53 ± 0.04**
H82A	dimer	dimer	14.5 ± 0.7**	0.62 ± 0.03***
W85A	decamer/ dimer	oligomer $(\alpha_2)_3$	89.9 ± 2.7*	24 ± 9.7*
V116T	decamer	dimer	74.8 ± 5.08	3.22 ± 0.22
V116D	dimer	dimer	< 0.02	< 0.02
L117W	monomer/ dimer	dimer	< 0.02	< 0.02

The wild type enzyme had a substrate turnover of 56.1 ± 6.7 [min^{-1}] and revealed a specific activity of 2.41 ± 0.29 [µmol/min*mg]. Cysteine mutants *Pf*Prx1a^{C50S} and *Pf*Prx1a^{C170S} had a not measurable activity below 0.02. Furthermore, *Pf*Prx1a^{R125} is a known important active site residue, and interestingly peroxidase activity of the R125A mutant dropped to 10% compared to wild type enzyme. The mutants, which eluted solely as dimers independent of the redox status, had a significant decrease in peroxidase activity. The interfacial mutant *Pf*Prx1a^{D77A} and also *Pf*Prx1a^{H82A} showed a significant loss of specific activity with 0.53 ± 0.04 [µmol/min*mg] and 0.62 ± 0.03 [µmol/min*mg], respectively. Interestingly, the overall dimeric mutant *Pf*Prx1a^{Y42A} had a not measurable activity below 0.02. The peroxidase activity of interfacial mutants *Pf*Prx1a^{V116D} and *Pf*Prx1a^{L117W} was also not measurable, since the activity was below base line. Interestingly, the interfacial mutant *Pf*Prx1a^{V116T} showed a slight increase in activity compared to *Pf*Prx1a wild type, with a substrate turnover of 74.8 ± 5.08 [min^{-1}] and showed a specific activity of 3.22 ± 0.22 [µmol/min*mg].

4.3 Post-translational modifications of *Pf*Prxs and their cysteine mutants

Post-translational modifications (PTMs) are of importance in regulating protein functions and are associated with gene expression, cell signalling, protein trafficking as well as regulating the activity and stability of enzymes (Doerig *et al*. 2015, Xiong *et al.* 2011, Jortzik and Becker 2012). One of the most susceptible targets are thiol groups on cysteines (Grek *et al*. 2013).

4.3.1 Protein *S*-glutathionylation in *P. falciparum* peroxiredoxins

To gain insight into the susceptibility of *Plasmodium* peroxiredoxins to post-translational modifications and potential regulation, the accessibility of *Pf*Prxs to *S*-glutathionylation was systematically studied within this study. First, oxidized Prxs were incubated with reduced glutathione (5 mM GSH; 10 min, 37°C), which did not result in signals in anti-glutathione Western Blots. However, when incubating reduced Prxs with oxidized glutathione (5 mM GSSG; 10 min, 37°C) *Pf*Prx1a, *Pf*Prx5, *Pf*PrxQ clearly showed bands of glutathionylated proteins. When the incubation time with GSSG was prolonged, also glutathionylation of *Pf*Prx1m became visible. Therefore, 45 minutes of incubation time were chosen to test the effects of different GSSG concentrations (0-5 mM). Under these conditions, all Prx wild types (*Pf*Prx1a dimer and monomer, *Pf*Prx1m monomer, *Pf*Prx5 monomer, and *Pf*PrxQ monomer) showed

increasingly prominent bands of glutathionylated proteins at increasing GSSG concentrations (Fig. 19).

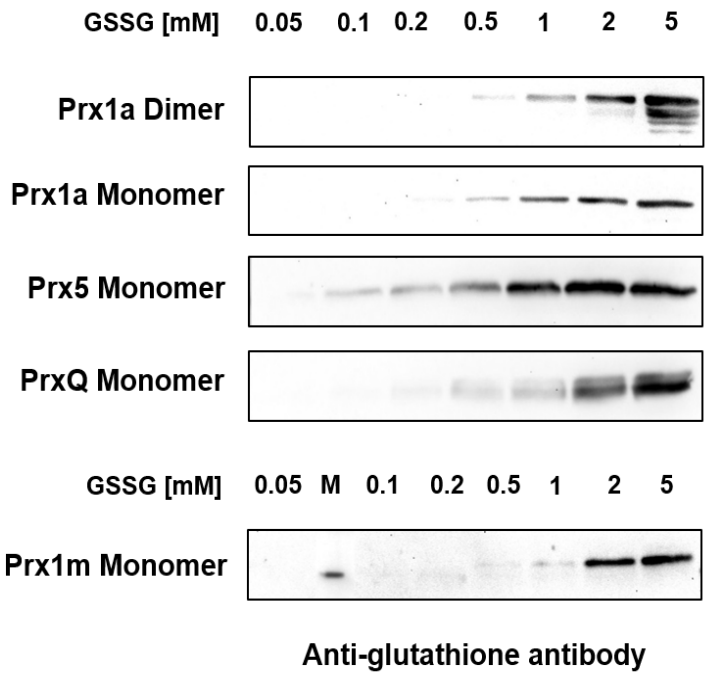

Figure 13: Concentration dependency of glutathionylation of *Pf*Prxs. *Pf*Prx1a dimer and monomer, *Pf*Prx5 monomer, *Pf*PrxQ monomer, and *Pf*Prx1m monomer are shown glutathionylated in anti-glutathione antibody Western Blots. Glutathionylation was induced by incubation with 0.05 mM to 5 mM GSSG at 37°C for 45 minutes. M = Marker. Blots were prepared with the support of Dr. Julia Hahn.

For further in-depth analysis of the susceptible cysteine residues, cysteine mutants of *Pf*Prx1a (C50S/C74A, C74A/C170S, C50S/C170S, C50S/C74A/C170S), *Pf*Prx5 (C117S, C143S, C117S/C143S), and *Pf*PrxQ (C56S, C103S, C56S/C103S) were glutathionylated using 5 mM GSSG and were subsequently desalted. For *Pf*Prx1a, all cysteines were found to be glutathionylated with particular susceptibility of Cys74 and Cys50 (Fig. 20, A). Both cysteines of *Pf*Prx5 were glutathionylated, with a slight preference for Cys117 (C_P of Prx5) over Cys143 (Fig. 20, B). For *Pf*PrxQ, solely the peroxidatic cysteine Cys56 was found to bind glutathione (Fig. 20, C).

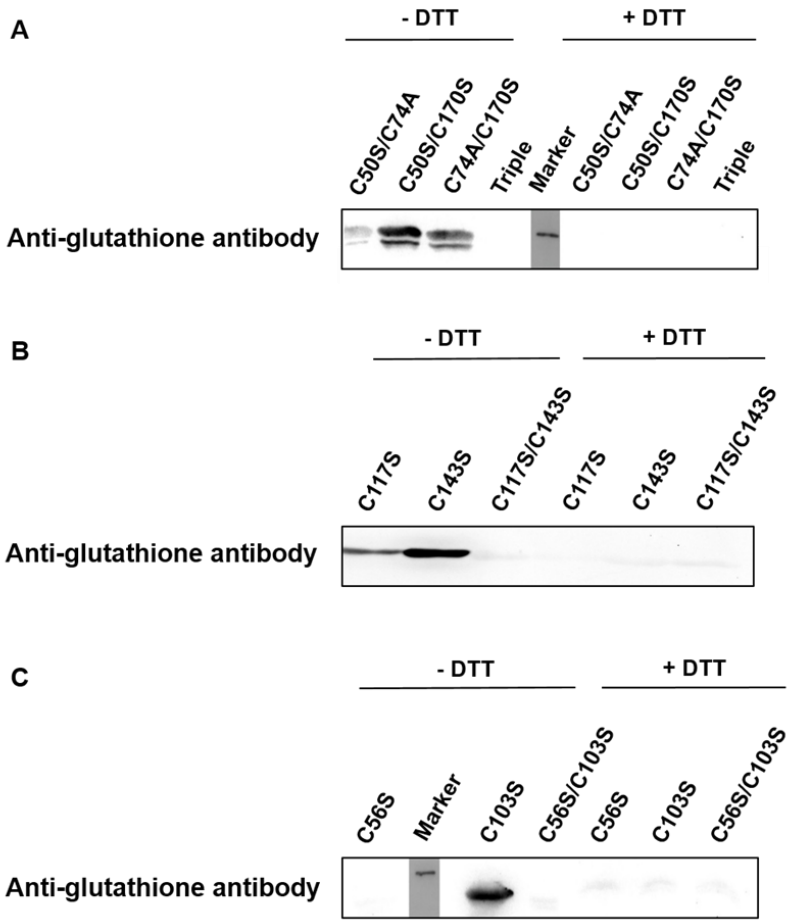

Figure 14: Glutathionylation of *Pf*Prxs cysteine mutants. (A). *Pf*Prx1a cysteine mutants C50S/C74A, C74A/C170S, C50S/C170S, and C50S/C74A/C170S (Triple) were glutathionylated with 5 mM GSSG for 10 minutes at 37°C, (B). *Pf*Prx5 cysteine mutants C117S, C143S, and C117S/C143S, (C). *Pf*PrxQ cysteine mutants C56S, C103S, and C56S/C103S. Blots were prepared with the support of Dr. Julia Hahn.

Due to the presence of six cysteines per monomer, cysteine mutants of *Pf*Prx1m were not systematically studied. However, all wild type Prxs were analyzed for their glutathionylation sites via mass spectrometry. This method confirmed glutathionylation of all three cysteines in *Pf*Prx1a, and both cysteines in *Pf*Prx5. Although Western Blot analysis had indicated only Cys56 of *Pf*PrxQ as target of glutathionylation, mass spectrometry (MS) showed that also the resolving cysteine Cys103 might be accessible. For *Pf*Prx1m, MS indicated C152 and the resolving cysteine (C187) as glutathionylation sites (Table 10).

Table 10: Mass spectrometry data of glutathionylated *Pf*Prxs. Mass spectrometry analysis was carried out in triplicates for *Pf*Prxs wild type enzymes.

Protein	MW [kDa]	Score Sequest	Modifications (Glutathione)
*Pf*Prx1a	21,8	799,67	[C50; C74; C170]
*Pf*Prx1a	21,8	1281,68	[C50; C74; C170]
*Pf*Prx1a	21,8	1359,32	[C74; C170]
*Pf*Prx1m	24,7	816,95	[C152; C187]
*Pf*Prx1m	24,7	250,58	[C152; C187]
*Pf*Prx1m	24,7	816,94	[C152; C187]
*Pf*Prx5	28,1	361,86	[C117]
*Pf*Prx5	28,1	92,61	[C117]
*Pf*Prx5	28,1	295,92	[C117; C143]
*Pf*PrxQ	18,5	697,7	[C103]
*Pf*PrxQ	18,5	1004,53	[C56; C103]
*Pf*PrxQ	18,5	1045,9	[C56; C103]

4.3.2 Oligomerisation state of glutathionylated *Pf*Prx1a wild type

To assess the contributions of post-translational modifications on the oligomerization behavior of *Pf*Prx1a wild type, the pre-reduced enzyme was incubated with 5 mM GSSG according to the protocol mentioned in chapter 3.3.6. The protein was desalted and subsequently applied to an ÄKTA FPLC System (see Fig. 21).

The protein with glutathionylated cysteines was found to elute as a decamer, which cannot be distinguished by gel filtration from the reduced enzyme with open disulfide bridges.

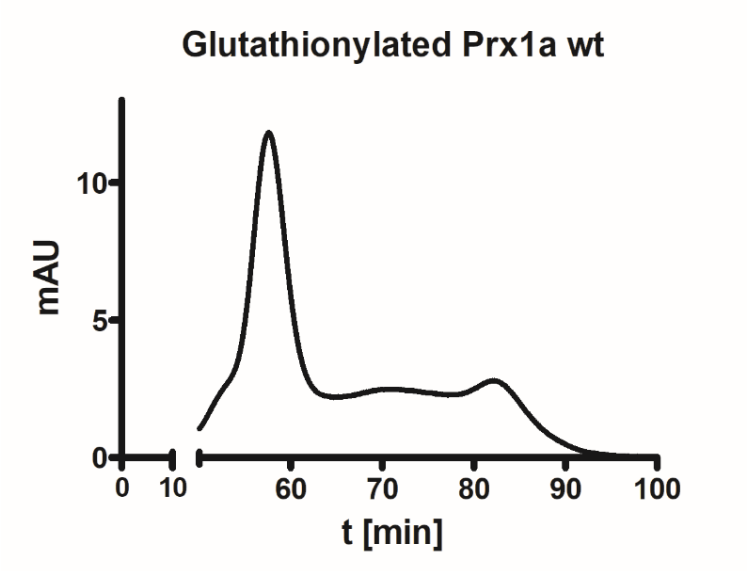

Figure 15: Oligomerization behavior of glutathionylated *Pf*Prx1a wild type. Glutathionylated *Pf*Prx1a wild type with predominantly decameric oligomerisation state and a small dimeric peak. The prereduced sample was incubated with 5 mM GSSG, desalted and subsequently applied to an ÄKTA FPLC System.

4.3.3 Protein *S*-nitrosation in *P. falciparum* peroxiredoxins

To study the susceptibility of *Pf*Prx1a, *Pf*Prx1m, *Pf*Prx5, and *Pf*PrxQ to *S*-nitrosation, pre-reduced enzymes were incubated with 1 mM GSNO and analyzed via the biotin-switch assay (described in chapter 3.3.7) followed by Western Blot analysis using an anti-biotin antibody. Samples without GSNO and/or without sodium ascorbate were prepared in parallel as controls. As shown in Figure 22, samples treated with 1 mM GSNO and sodium ascorbate resulted in a prominent signal for all of the four enzymes, indicating that they are *S*-nitrosation targets.

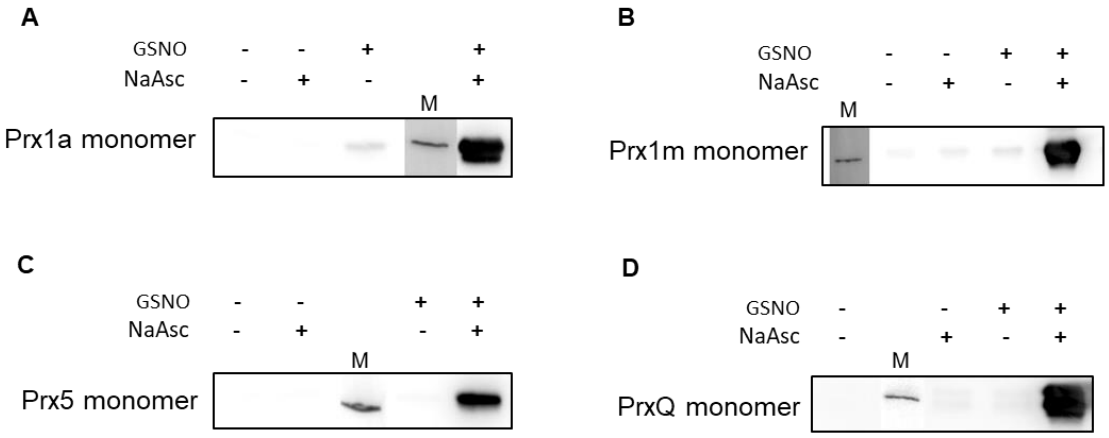

Figure 16: *S*-Nitrosation of *Pf*Prxs wild type. (- -): without GSNO and sodium ascorbate (NaAsc); (- +): without GNSO, with NaAsc; (+ -): with GNSO, without NaAsc; (+ +): with GSNO and NaAsc; M: marker. A. *Pf*Prx1a. B. *Pf*Prx1m. C. *Pf*Prx5. D. *Pf*PrxQ. Reduced enzymes were incubated with 1 mM GSNO for 1 h at 22 °C in the dark and analyzed via the biotin- switch assay. Controls without sodium ascorbate and/or GSNO were prepared in parallel. *S*-nitrosated proteins were detected indirectly with Western Blot analysis using an anti-biotin antibody. Coomassie staining of the samples served as a loading control, data not shown. Representative blots from at least three independent experiments are shown. Blots were prepared with the support of Norma Schulz.

To further assess the nitrosation sites in peroxiredoxins, the cysteine residues in 2-Cys peroxiredoxin *Pf*Prx1a were mutated, resulting in double and triple *Pf*Prx1a cysteine mutants. The *S*-nitrosation experiments were repeated according to the above mentioned protocol. As shown in figure 23, two of the cysteine mutants (*Pf*Prx1a$^{C50S/C74A}$ and *Pf*Prx1a$^{C74A/C170S}$) have a very prominent signal after western blotting, whereas for cysteine mutants *Pf*Prx1a$^{C50S/C170S}$ and *Pf*Prx1a$^{C50S/C74A/C170S}$ only shadow bands are visible. These slightly visible signals, which also occur within the controls, do not show positive signals. The positive signals for the above mentioned mutants implement the peroxidatic cysteine C50 and the resolving cysteine C170 of *Pf*Prx1a being targets for *S*-nitrosation.

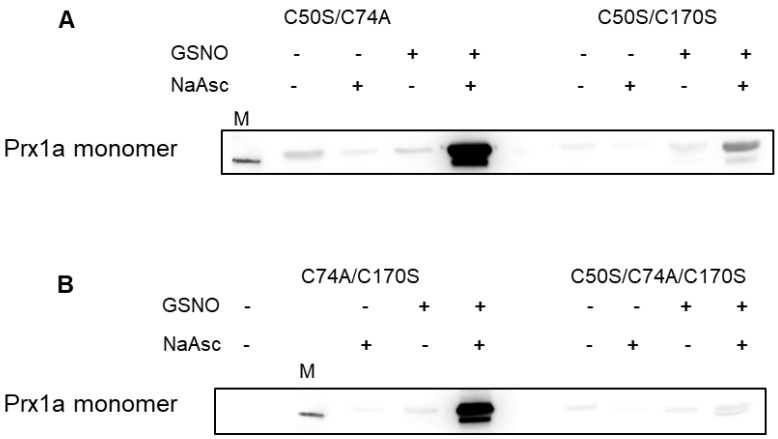

Figure 17: *S*-Nitrosation of *Pf*Prx1a cysteine mutants. (- -): without GSNO and NaAsc; (- +): without GSNO, with NaAsc; (+ -): with GSNO, without NaAsc; (+ +): with GSNO and NaAsc; M: marker. A. *Pf*Prx1a$^{C50S/C74A}$ and *Pf*Prx1a$^{C50S/C170S}$. B. *Pf*Prx1a$^{C74A/C170S}$ and *Pf*Prx1a$^{C50S/C74A/C170S}$. Reduced enzymes were incubated with 1 mM GSNO for 1 h at 22 °C in the dark and analyzed via the biotin- switch assay. Controls without sodium ascorbate and/or GSNO were prepared in parallel. *S*-nitrosated proteins were detected indirectly with Western blot analysis using an anti-biotin antibody. Coomassie staining of the samples served as a loading control, data not shown. Representative blots from at least three independent experiments are shown. Blots were prepared with the support of Norma Schulz.

4.4 Plasmoredoxin in *P. falciparum*

In this chapter, the oligomerisation state of *Pf*-plasmoredoxin is shown. Furthermore, post-translational modification studies of *Pf*Plrx wild type and cysteine mutants were performed by western blotting and mass spectrometric analysis within this thesis.

4.4.1 Mutagenesis, heterologous overexpression and purification of *Pf*Plrx and mutants

The cysteine mutants of *Pf*Plrx used in this thesis were prepared in earlier studies in the Becker lab (Becker *et al*. 2003a; Will 2014). Heterologous overexpression and protein purification of *Pf*Plrx wild type and cysteine mutants were performed according to the protocol mentioned in chapter 3.3.1. The purification of *Pf*Plrx wild type is exemplarily shown in Fig. 24 using a Coomassie stained gel after Ni-NTA affinity chromatography.

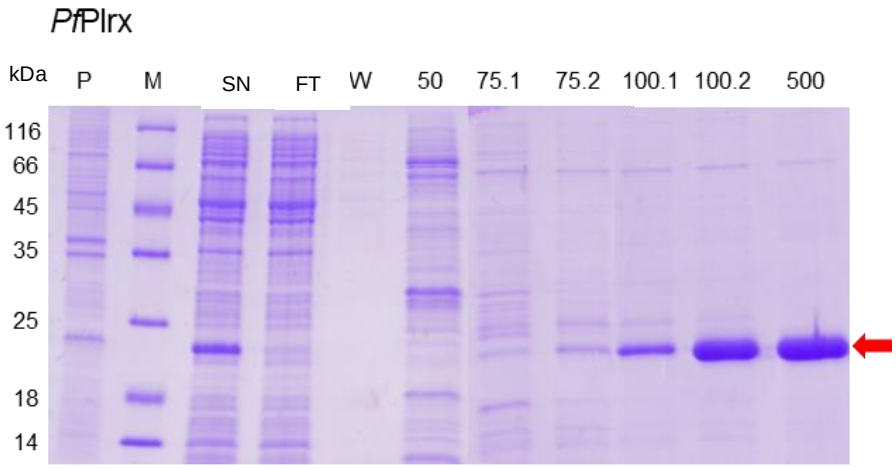

Figure 18: Protein purification using Ni-NTA affinity chromatography. Purification of *Pf*Plrx with Ni-NTA resin. P: pellet, M: Marker (protein ladder), SN: supernatant, FT: flow through, W: wash, numbers: imidazole concentrations in mM used for protein elution. Red arrows show the respective protein.

The cysteine mutants of *Pf*Plrx were purified according to the same protocol. *Pf*Plrx and mutants were purified under reducing conditions using 0.5 mM DTT to assure a fully reduced enzyme for post-translational modification studies. The purified proteins were stored with 1 mM TCEP and were stable for up to one week.

4.4.2 Size-exclusion chromatography of *Pf*Plrx

In order to assess the oligomerisation state of *Pf*Plrx wild type enzyme after purification under reducing conditions, preparative gel filtration experiments were carried out. The samples were desalted using Zeba Spin Desalting columns and subsequently applied to an ÄKTA FPLC System for analysis.

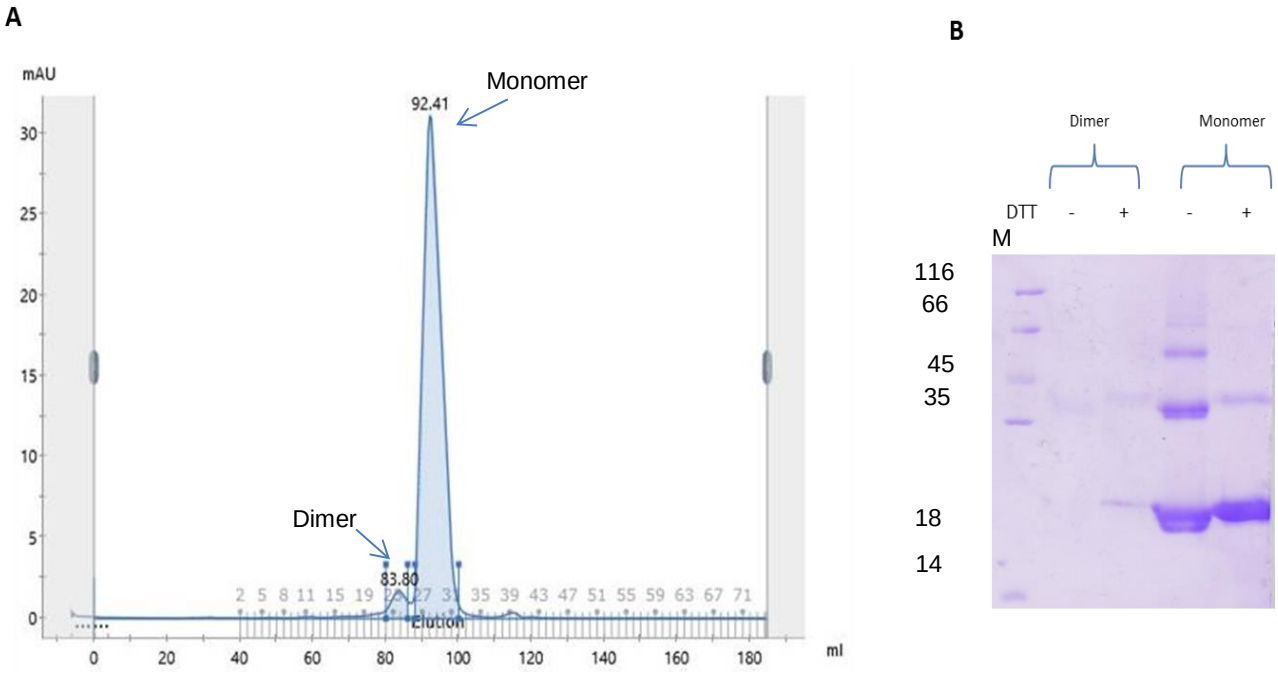

Figure 19: Size-exclusion chromatography of *Pf*Plrx wild type under reducing (0.5 mM DTT) conditions. A. Oligomerization state of *Pf*Plrx under reducing conditions showing a large monomer peak (92.41 ml) and a small dimer peak (83.80 ml). B. Coomassie-stained SDS gel with non-reducing and reducing conditions of the dimer and monomer peak of *Pf*Plrx, respectively. Representative graphs and blots from at least two independent experiments are shown. M= marker.

Under reducing conditions, *Pf*Plrx eluted predominantly as monomer and only showed a slight peak as a dimer (Fig. 25, A). Fractions were collected separately and applied to a SDS gel with and without the addition of DTT (Fig. 25, B). By adding DTT to the dimer fraction which was collected after size-exclusion chromatography, a weak signal at ~ 22 kDa is visible. Furthermore, under non-reducing conditions the monomer fraction shows numerous signals varying from ~ 22 kDa to ~ 60 kDa, whereas by adding DTT to the sample, only the monomer and a weak signal at ~ 40 kDa are visible. Taken together, *Pf*Plrx is a monomeric protein under reducing conditions.

4.4.3 Post-translational modification of *Pf*Prx

To gain insight into the susceptibility of *Plasmodium* plasmoredoxin to post-translational modifications, the accessibility of *Pf*Prx to *S*-glutathionylation and *S*-nitrosation was studied within this thesis.

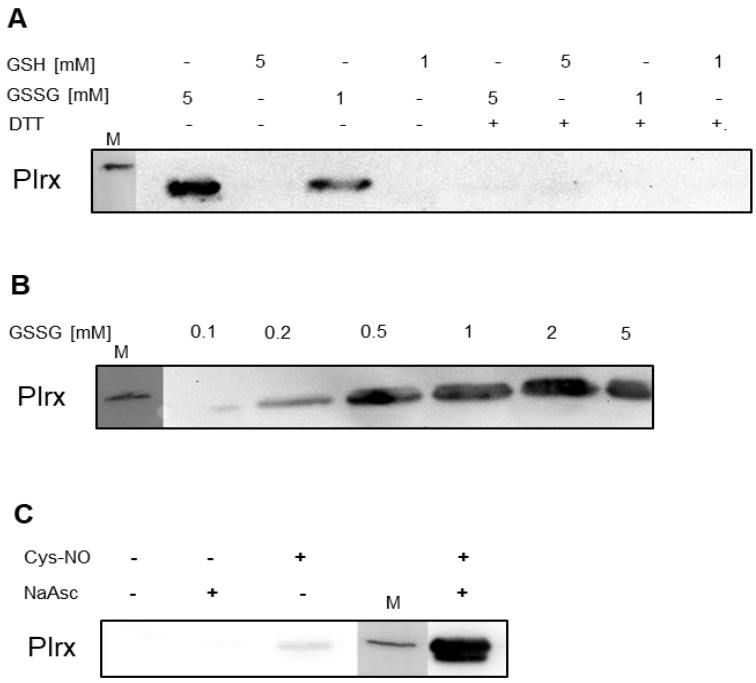

Figure 26: Post-translational modifications of *Pf*Prx. A. Glutathionylation of *Pf*Prx using 1 mM and 5 mM of reduced glutathione (GSH) or glutathione disulfide (GSSG), without (-) and with (+) addition of DTT. B. Concentration dependency of glutathionylated *Pf*Prx using GSSG concentrations from 0.1 - 5 mM. C. Nitrosation of *Pf*Prx. The reduced enzyme was incubated with 1 mM Cys-NO for 1 h at 22 °C in the dark and analyzed via the biotin- switch assay. Controls without sodium ascorbate and/or GSNO were prepared in parallel. *S*-nitrosated proteins were detected indirectly with Western Blot analysis using an anti-biotin antibody. Coomassie- staining of the samples served as a loading control, data not shown. Representative blots from at least three independent experiments are shown.

For *S*-glutathionylation, oxidized *Pf*Prx was incubated with reduced glutathione (1 mM and 5 mM GSH; 10 min, 37°C), which did not result in signals in anti-glutathione Western Blots. However, when incubating reduced Prxs with oxidized glutathione (1 mM and 5 mM GSSG; 10 minutes, 37°C) *Pf*Prx clearly showed bands of glutathionylated protein (Fig. 26, A). Since prominent signals were visible after 10 minutes of incubation, the same duration was chosen to test the effects of different GSSG concentrations (0-5 mM). Under these conditions, *Pf*Prx showed increasingly prominent bands of glutathionylated proteins at increasing GSSG concentrations, beginning at 0.1 mM GSSG (Fig. 26, B).

To study the susceptibility of *Pf*Plrx to *S*-nitrosation, pre-reduced enzyme was incubated with 1 mM Cys-No and analyzed via the biotin-switch assay (described in chapter 3.3.7) followed by Western Blot analysis using an anti-biotin antibody. Control samples without Cys-NO and/or without sodium ascorbate were prepared in parallel. As shown in Figure 26 C, the sample treated with 1 mM Cys-NO and sodium ascorbate resulted in a prominent signal for *Pf*Plrx, which indicates plasmoredoxin also being a target for *S*-nitrosation.

For further in-depth analysis of the *S*-glutathionylation sites, *Pf*Plrx wild type enzyme and cysteine mutants *Pf*Plrx^{C3S}, *Pf*Plrx^{C63S}, and *Pf*Plrx^{C115S} were analyzed for their glutathionylation sites via mass spectrometry according to the protocol mentioned in chapter 3.3.8 (see Table 11). This method confirmed the *S*-glutathionylation of the two active site cysteines C60 and C63. According to MS data, cysteines C3 and C115 are not modified post-transcriptionally by nitrogen species.

Table 11: Mass spectrometry data of glutathionylated *Pf*Plrx wild type, *Pf*Plrx^{C3S}, *Pf*Plrx^{C63S}, and *Pf*Plrx^{C115S}. Representative data from at least three independent experiments are shown.

Protein	MW [kDa]	Score Sequest	Modifications (Glutathione)
*Pf*Plrx Wt	21.7	499.25	[C60; C63]
*Pf*Plrx^{C3S}	21.7	546	[C60; C63]
*Pf*Plrx^{C63S}	21.7	594.43	[C60]
*Pf*Plrx^{C115S}	21.7	791.34	[C60; C63]

5. Discussion

In the following chapter, changes in oligomerization of *Pf*Prxs wild type enzymes and alterations in enzymatic activities of *Pf*Prx1a mutants will be discussed.

The second part of this discussion focuses on *Pf*-plasmoredoxin. Furthermore, a potential impact of post-translational modifications of cysteines in peroxiredoxins and plasmoredoxin will be addressed.

5.1 Peroxiredoxins in *Plasmodium falciparum*

5.1.1 Oligomerization behavior of wild type peroxiredoxins in *P. falciparum*

One part of this work was dedicated to the differences in the redox-related oligomerization states of 1-Cys and 2-Cys peroxiredoxins of the pathogen *P. falciparum*. The oligomerization behavior differs in 1-Cys and 2-Cys peroxiredoxins of malaria parasites. In this thesis, 1-Cys peroxiredoxins *Pf*Prx5 and *Pf*PrxQ were dimeric and monomeric, respectively, independent of their redox state. 2-Cys peroxiredoxins *Pf*Prx1a and *Pf*Prx1m exhibited a dynamic change in oligomerization which was accompanied by conformational changes from a fully folded to a locally unfolded conformation. With this in mind, it is important to take a closer look at the structural conditions within the protein. Numerous aromatic residues are present at the active site or at the decamer building interface (Loberg *et al*. 2019). These are especially amino acids D77, Y42 and H82 in *Pf*Prx1a. During evolution, peroxiredoxins oriented their active sites around the dimer/dimer interfaces differently. While the typical peroxiredoxin forms decamers at the A-type interface, the atypical class uses it as dimerization interface (Karplus and Hall 2007). Interestingly, some members of the peroxiredoxin Q class have hydrophilic residues in place of the above-mentioned conserved aromatic residues (Loberg *et al*. 2019, Reeves *et al*. 2011). The oligomerization behavior of the truncated *Pf*PrxQ analyzed via size-exclusion chromatography showed an overall monomeric enzyme, which strongly supports this statement.

According to Gretes *et al*. (2012), *Pf*Prx1a has two different conformations. Two monomers form a dimer which can unite to build a decamer. The results of the performed size-exclusion chromatography via an FPLC system underline this

statement. Under oxidizing conditions, *Pf*Prx1a had a size of ~46 kDa corresponding to a dimer. Exposing the peroxiredoxin to a reducing environment caused a shift of size towards approximately ~235 kDa. This size corresponds to the size of a decamer of *Pf*Prx1a. The execution of a reducing vs. non-reducing gel delivers an additional proof for this statement. Adding DTT to the sample buffer and cooking the sample for five minutes caused the occurrence of a band at ~25 kDa. Here, *Pf*Prx1a was split up into its monomers through the reducing environment. Due to the use of a 15 % SDS gel, which is suitable for small protein sizes, the decameric form was not visible in the same SDS-PAGE (data not shown).

Wood *et al*. (2002) support the hypothesis that the oligomerization of 2-Cys Prxs is redox-dependent. The mentioned study focused on the conformational change of *Salmonella typhimurium* AhpC. It showed that the oxidized enzyme favored the dimeric formation, which is consistent with the results in this thesis. Due to the structural analogy of 2-Cys Prxs it can be assumed that all 2-Cys Prxs perform an equally redox-sensitive oligomerization (Wood *et al*. 2002). Interestingly, Tairum *et al.* hypothesized that 2-Cys Prxs appear preferably as decamers or even higher molecular weight complexes (Tairum *et al*. 2016). Kawazu *et al*. (2001) also showed that the recombinant *Pf*Prx1 in its native form was a dimer. In contrast to the results in this thesis, Kawazu *et al*. observed that the application of DTT caused the dissociation into monomers (Kawazu *et al*. 2001). Other factors influencing the oligomerization of *Pf*Prxs are discussed, for instance slight changes of pH (Morais *et al.* 2015) and protein concentration (Matsumura *et al*. 2008, Nelson *et al*. 2016). To further investigate these differences, it would be important to compare the A-type interfaces, i.e. the decamer-building interface of the peroxiredoxins of these species. Furthermore, further features would have to be considered. These include, above all, the pH sensitivity already mentioned above, which can lead to changes in the oligomerization state of the protein resulting from changes in the pH value alone. Additionally, the protein concentration should be investigated as a factor influencing oligomerization. However, since peroxiredoxins are present in high concentrations within the cell, the concentrations can be set quite narrowly. These factors should be taken into account in further analyses.

5.1.2 Kinetics and oligomerization behavior of *Pf*Prx1a mutants

Another important part of this thesis was the in-depth investigation of specific amino acids of *Pf*Prx1a using a structural model. In particular, potentially important regions that may be responsible for the structural constitution and changes within the protein were analyzed in detail.

The reversible transition between decamers and dimers is a well-characterized feature of 2-Cys Prxs (Angelucci *et al*. 2016, Hall *et al*. 2011, Perkins *et al*. 2013). Based on the results in this thesis, it is to be assumed that residues proximal to the peroxidase active site are highly associated with the catalytic activity of the enzyme, the transition from decamer to dimer, and the conformational change from a fully folded to a locally unfolded form.

Perkins *et al*. demonstrated that the *St*AhpC mutant, equivalent to C50S in *Pf*Prx1a, is always fully folded (Perkins *et al*. 2013). In this study, the oxidized C50S mutant of *Pf*Prx1a eluted as mixture of dodecamers and decamers. It can be assumed, that the enzyme is "stuck" in a fully folded state. This can be based on the fact, that the hydrogen bond between the serine side chain and R125 is stronger than the interaction between C50 and R125 in the wild type enzyme. Furthermore, AhpC active site proximal mutations lowered the enzymes catalytic efficiency, and increased the pK_a values of the peroxidatic cysteine (Nelson *et al*. 2018). It could therefore be assumed, that the C_P mutant of *Pf*Prx1a mimicked an overoxidized protein, thus showing higher oligomers when oxidized. To further support the statement of Nelson *et al*., the pK_a values of *Pf*Prx1a C_P mutant would be of importance to understand the intramolecular interactions within the peroxiredoxin.

To continue, a study by Nakamura *et al*. showed the crystal structure of a peroxiredoxin from *Aeropyrum pernix* K1 with its substrate hydrogen peroxide (Nakamura *et al*. 2010). Interestingly, in a mutant lacking the peroxidatic cysteine the substrate was capable of binding to the active site, which shows that the C_P is not essential for hydrogen peroxide binding (Nakamura *et. al*. 2010). However, in the performed peroxidase activity assay, *Pf*Prx1a mutant C50S had a dramatic loss of function. It can be concluded that the binding pocket for the substrate is still intact in *Pf*Prx1a^{C50S}, but the nucleophilic attack by the C_P cannot take place and therefore there is no detectable activity in the assay.

To continue the discussion regarding the amino acid impact on the oligomerization and activity of peroxiredoxins, in wild type *Ap*K1, the conformational change forces

an active site proximal Arg residue to turn to the molecule´s interior. These structural changes resulted in a neutralized former positive surface potential (Nakamura *et al*. 2010). Furthermore, in *Xanthomonas campestris*, the distal Arg123 amino group is oriented at an intermediary position, presumably stabilizing the transition of the peroxide oxygen to the Cys S. Due to rotation of the sulfonate oxygen, the Arg residue flips outward, which promotes local unfolding, and could also reduce the rate of hyperoxidation by suppressing substrate binding and activation by the Arg residue (Perkins *et al*. 2016). This shift could not be seen in sensitive Prx enzymes, such as human Prx2, indicating a possible favoring of hyperoxidation of the enzyme over local unfolding. Another published study on *St*AhpC showed a significant loss in catalytic activity in the R119A mutant (Nelson *et al*. 2018). These findings are consistent with the results achieved in this thesis, with *Pf*Prx1a^{R125A} showing a dramatic loss in function, even though the active-site cysteines were present. This loss in enzymatic activity of the R125A mutant can be explained due to the lack of substrate binding possibility and its activation. Interestingly, the enzymes´ transition from decamer to dimer was not affected. As formerly argued by Nelson *et al*., the recent study supports the hypothesis, that even though the Prx's active site cysteines are present, the enzyme does not have its key catalytic residues correctly positioned (Nelson *et al*. 2018, Nakamura *et al*. 2010, Perkins *et al*. 2013). The results on this mutation show the importance of the interaction of amino acids at the active site. *Pf*Prx1a^{R125A} does not seem to interact with the A- and B-type interfaces, since the oligomerization was not affected, but it seems to have an immense influence on the arrangement of the active site loop. Although the active-site cysteines were fully present in the protein, only a residual activity of 10% was observed.

To continue, the results in this thesis show that all substitutions which led to a solely dimeric enzyme, independent of the redox state, resulted in enzymes with a drastic decreased peroxidase activity. Especially of importance are mutants *Pf*Prx1a^{Y42A}, *Pf*Prx1a^{D77A}, *Pf*Prx1a^{H82A}, *Pf*Prx1a^{V116D}, and *Pf*Prx1a^{L117W}. The most drastic effect on catalytic activity was observed in *Pf*Prx1a^{Y42}. Amino acid residue Y42 is not an interfacial residue, but located in direct proximity to the enzymes´ active site. The substitution from tyrosine to alanine seems to have disrupted the reduced decameric structure and additionally, showed an undetectable activity in the thioredoxin-coupled assay. As mentioned earlier, Y42 is of importance for stabilizing the active site loop, which includes the catalytic residue C50. Furthermore, the structural modell of

*Pf*Prx1a shows that the loop can stabilize the decamer and is also in contact with the A-type interface. In absence or replaced by Ala, it can be assumed that the side chain of *Pf*Prx1a^{Y42A} can no longer stabilize the loop. This could again result in an overall displacement of important active site residues and to the impossibility of decamer formation. The results on this mutant are of particular importance. 2-Cys peroxiredoxins are highly conserved enzymes that occur in a large number of organisms. As mentioned above, the malaria parasite uses human Prx2 to support its own defense against oxidative stress. A potential drug to inhibit the peroxiredoxins that occupy the active site of the enzyme would inevitably also inhibit the enzymes of the host. By mutating Tyr42 to Ala, a possible inhibition of this amino acid has been shown. The FPLC data showed that the protein is present as a dimer regardless of the redox state and that no aggregations due to steric changes occurred. Furthermore, it showed no detectable activity in the thioredoxin coupled assay. These data on this important amino acid in close proximity to the active site of the protein provide important information on the overall catalysis and the interaction of reduction and oxidation in different oligomerization states. It would be particularly important to make sequence and structure comparisons with other peroxiredoxins of other species in the future and thus to broaden our knowledge in this regard.

Interesting findings were also obtained for further mutants. *Pf*Prx1a^{H82A} had a significantly reduced activity and with the help of size-exclusion chromatography it is to be assumed that the A-type interface of this mutant is disrupted. Since H82 and D45 are hydrogen bonded and both act in stabilizing the loop, a substitution from His to Ala seems to alter and misalign the above mentioned interactions. The stabilization of the active site loop is missing. Due to these steric hindrances, it is to be assumed, that the catalytic activity of the enzyme is modified.

The substitution of the interfacial residue D77 to Ala led to the incapability of decamer formation and presumably led to the destruction of the A-type interface. With a structural comparison of reduced *P. vivax* Prx1a (2i81) and oxidized *Pf*Prx1m (2cod) a rearrangement of analogous regions of D45 to D77 (nomenclature for *Pf*Prx1a) upon oxidation is visible, leading to an enlargement of the distance between D45 and D77 (Information provided by Dr. Karin Fritz-Wolf, data not shown). Due to the substitution of D77 to Ala, the dimer/dimer interface was disrupted, resulting in a dimeric protein with a significant loss in activity. Residue D77 of the adjacent dimer in reduced *Pf*Prx1a forms a hydrogen bond to the main chain of D45. Former studies on

S. typhimurium peroxiredoxin mutant T77I did not only disrupt the decamer interface, but also allosterically altered the loop on which the peroxidatic active site is located (Nirudodhi *et al*. 2011). Taken together, the results for *S. typhimurium* indicated that the mutation of these conserved residues at the decamer building interface (A-type interface), weaken or directly disrupt decamer formation under reducing conditions. These findings are consistent with the results in this study.

Furthermore, Loberg *et al*. showed altered enzyme activity when substituting aromatic residues to Ala or Leu. The mutant *Pf*Prx1a^{D77A} had a significant loss in peroxidase activity, which strongly supports this statement. The results presented here indicate that specific amino acid residues contribute directly to the enzyme´s quaternary structure and also to the enzyme´s catalytic activity. A putative reason for this correlation is that the formation of decamers can prepare the peroxidatic cysteine for catalysis by maintaining a fully folded active site architecture and allowing the pK_a of the thiol to be depressed (Loberg *et al*. 2019, Parsonage *et al*. 2005, Kamariah *et al.* 2018, Wood *et al.* 2002).

To continue, amino acid residues V116 and L117 of *Pf*Prx1a are located to the monomer/monomer interface (or B-type interface). The peroxidase activities of mutants V116D and L117W were not detectable whereas only minor changes were found for mutant V116T. Interestingly, also the oligomerization of amino acid V116 was strongly dependent on the substituted amino acid. Mutation to threonine was not critical, showing a decamer/dimer transition comparable to *Pf*Prx1a wild type enzyme. The substitution to the polar residue aspartic acid resulted in a dimeric enzyme, which was independent of the redox state. It can be assumed, that the mutation V116D disturbs the alignment of β-strands in the protein.

The tryptophan substitution of L117 influences A- and B-type interfaces. The exchange from leucine to the large tryptophan side chain leads to the fact that important amino acid residues, especially K108 and S121 (Information provided by Dr. Karin Fritz-Wolf) are not optimally aligned. This in turn can lead to the fact, that the important contact of the amino acids K108/K108’ and S121/S121’ of the neighboring monomer is not present and thus the decamer buidling interface is not positioned properly. Moreover, the backbone of residue 117 interacts with the N-terminus of the other subunit of the dimer. Interestingly, the mutated enzyme in reduced form eluted as a mixture of dimers and monomers, whereas the oxidized enzyme was present solely as monomer.

This data provide a profound understanding of the diverse interactions of amino acid residues and their impact on the composition and overall structure of 2-Cys Prxs in *P. falciparum*. Since Prx catalysis relies on a very dynamic shift from a fully folded to a locally unfolded conformation in decameric and dimeric state, molecules trapping the enzyme in any oligomeric state will show inhibitory effects (Nelson *et al*. 2018, Tairum *et al*. 2016, Nakamura *et al*. 2010, Perkins *et al*. 2013)**.** Potential differences in conformational states between pathogens and humans could function as basis to target pathogen Prxs.

These findings suggest that residues in direct proximity to the active site or located at the interfaces, are of interest as targets for potential inhibitors.

5.1.2 Post-translational cysteine modifications in peroxiredoxins

Protein *S*-glutathionylation

Protein *S*-glutathionylation may occur in cells under oxidative stress and is involved in the regulation of protein structure, function, and interaction as well as in redox signaling (Jortzik *et al*. 2012). Also in malaria parasites, glutathionylation seems to play a major role as indicated by a large-scale proteomic approach (Kehr *et al*. 2011).

Protein *S*-glutathionylation of peroxiredoxins

Based on the data obtained in the present study, all *Pf*Prx wild type proteins are accessible to glutathionylation. However, they differ in susceptibility and concentration dependency. As *Pf*Prx1a is located in the cytoplasm, *Pf*Prx1m in mitochondria, *Pf*Prx5 in the apicoplast, and *Pf*PrxQ in the nucleus (Kehr *et al*. 2010), compartmentation might have an influence on this susceptibility. Furthermore, the individual Prx cysteine residues modified by glutathione could be identified by a combination of Western blotting and mass spectrometry. Based on this, in all wild type *Pf*Prxs the peroxidatic cysteine can be glutathionylated by GSSG, which - depending on the availability of reducing agents - is likely to have an impact on peroxidase activity *in vivo*. Deglutathionylation in mammalian cells is mainly catalysed by glutaredoxin or thioredoxin (Chrestensen *et al*. 2000). Also in *P. falciparum*, e.g. Prx1a and pyruvate kinase can be efficiently deglutathionylated by *Pf*Trx, *Pf*Grx, and *Pf*Plrx (Kehr *et al*. 2011). As the *in vitro* peroxidase activity assay depends on a reducing backup system comprising Trx and TrxR, the activity of

glutathionylated Prx cannot be measured as glutathione would be removed immediately by the thioredoxin-system.

However, to learn more about the functional consequences of glutathionylation, the oligomerization state of glutathionylated *Pf*Prx1a was analyzed in this present study. As delineated above, in principle all cysteine residues of the protein are accessible to glutathionylation. Furthermore, size-exclusion chromatography revealed a glutathionylated protein in decameric state. This indicates that the overall structure of the protein is intact, which, in addition to the direct impact on activity, might lead to conformational changes with potential regulatory or signaling effects (Jortzik *et al.* 2012, Greetham *et al*. 2010).

Protein *S*-nitrosation

The radical nitrogen monoxide ($NO^{\cdot}$) is a reactive signalling molecule, produced by nitric oxide synthase (NOS) using L-arginine as a substrate (Thomas *et al*. 2001). NO is associated with numerous functions such as controlling pro-inflammatory signalling (Luiking *et al*. 2010) or inducing the production of cGMP (Francis *et al*. 2010).

In *Plasmodium*, high amounts of nitrosative stress derive from the human or mosquito host (Ferrari *et al*. 2011). The increasing expression of NOS due to hemozoin production in the erythrocyte can lead to high levels of NO and result in a retarded development of the parasites (Peterson *et al*. 2007). A large scale proteomic approach identified 319 putative target proteins for *S*-nitrosation.

The potential *S*-nitrosation of a protein was analyzed by incubating reduced enzymes with the naturally occurring *S*-nitrosoglutathione (GSNO), followed by indirect detection of the modification using the biotin-switch assay as described earlier (Broniowska *et al*. 2013, Forrester *et al.* 2009a). Reactions between reduced glutathione and nitrous acid can synthesize GSNO, which is able to transfer its nitroso group to thiols of other proteins, which results in *S*-nitrosation. Interestingly, GSNO is in addition able to react with thiols by forming a disulfide bridge, resulting in *S*-glutathionylation rather than *S*-nitrosation (Broniowska *et al*. 2013). The indirect detection using the biotin-switch assay is based on replacement of the modification by biotin. It has been reported before that ascorbate, used to transform SNOs to free thiols, does not reduce *S*-glutathionylated cysteines (Forrester *et al*. 2009a). Therefore, *S*-glutathionylation caused by GSNO should not result in a signal when applying the biotin-switch assay. Experiments could be repeated using *S*-nitrosocysteine instead of GSNO as an agent for *S*-nitrosation (Grossi and

Montevecchi, 2002, *Peterson et al.* 2007), in order to completely exclude false negative detection of *S*-nitrosation.

Protein *S*-nitrosation of peroxiredoxins

Within this thesis, four peroxiredoxins (*Pf*Prx1a, *Pf*Prx1m, *Pf*Prx5, and *Pf*PrxQ) of *P. falciparum* were identified as *S*-nitrosation targets. Since the peroxidase activity assay is based on the thioredoxin/thioredoxin reductase recycling system, an impact of *S*-nitrosation on the enzymatic activity could not be detected. Interestingly, in yeast Prx1 nitrosation successfully inhibited the peroxiredoxin-thioredoxin system (Engelman *et al*. 2012). Here, the peroxidase activity assay was coupled with Fox reagent, and the absorbance of 560 nm was read and compared with an H_2O_2 standard curve. Under these assay conditions, *Ec*Prx1 was efficiently inhibited with low doses of Cys-NO (5 µM led to 50 % inhibition) (Engelman *et al*. 2012). Taking this into account, it would be highly interesting to conduct future experiments regarding the peroxidase activity assay coupled with Fox reagent. Since *P. falciparum* is highly depending on a successful detoxification capacity, a putative inhibition of peroxiredoxins by *S*-nitrosation emphasizes the importance of post-translational cysteine modifications.

To continue, cysteine mutants of *Pf*Prx1a were *S*-nitrosated and only the two active site cysteines were identified as *S*-nitrosation targets. This underlines the above mentioned statement, that the activity of peroxiredoxins is inhibited by *S*-nitrosation, presumably by inhibiting the enzymes` active site.

5.2 Plasmoredoxin in *Plasmodium falciparum*

Plasmoredoxin is a redox-active protein centrally positioned in the redox metabolism of *Plasmodium* with versatile interactions within the antioxidative network. In addition to its biochemically interesting properties, it is of particular importance, since a homologous protein is missing in the human host cell. Plasmoredoxin seems to occur only in *Plasmodium* species.

Plasmoredoxin of *P. falciparum* shares sequence identities with *Plasmodium yoelii* plasmoredoxin (72.6 %), *Plasmodium berghei* plasmoredoxin (66.9 %), *Plasmodium vivax* plasmoredoxin (67.4 %), and *Plasmodium knowlesi* plasmoredoxin (67.2 %) (Becker *et al*. 2003a). Within the thioredoxin family, *P. falciparum* plasmoredoxin has

the highest identity with *P. falciparum* thioredoxin (31.4%). Phylogenetic analyses further show that *Plasmodium* plasmoredoxin represents a new family of redox-active proteins within the thioredoxin superfamily. Interestingly, it has been shown that Plrx does not appear to play an essential role in the life cycle of the malaria parasite *Plasmodium berghei* (Buchholz *et al*. 2008). In addition to plasmoredoxin, *Plasmodium* has a number of small redox proteins with sequence similarities to thioredoxin. This family includes thioredoxins, peroxiredoxins, glutaredoxins, tryparedoxin of the trypanosomes and protein disulfide isomerases.

In this thesis the oligomerization state of Plrx was investigated as well as the possible susceptibility of cysteines to post-translational modifications. *Pf*Plrx showed a monomeric structure by size-exclusion chromatography under reducing conditions. Interestingly, several oligomerization states of the protein could be determined on a non-reducing SDS gel. The changes of the oligomerization state mentioned here are also important characteristics of 2-Cys peroxiredoxins, which could also be shown in this thesis. In the case of peroxiredoxins, the transition from decamer to dimer and vice versa serves the peroxidase activity of the enzyme. In the experiments shown in this thesis, changes in important amino acid residues led to the enzyme losing some or all of its peroxidase activity and the ability to change oligomerization states. The reduction and interaction partners of *P. falciparum* plasmoredoxin are still unknown. In the future it would be interesting to determine a possible physiological relevance of oligomerization on the activity and function of the enzyme by means of the appropriate reduction partners.

P. falciparum plasmoredoxin has four cysteines at positions 3, 115, 60 and 63, the latter being the active-site cysteines of the protein. In this present thesis it was shown by Western blot analysis that *Pf*Plrx is glutathionylated and nitrosylated post-translationally. With regard to the glutathionylization of the enzyme, it was also shown by MS that only the active-site cysteines C60 and C63 are accessible for post-translational modifications by glutathione.

Protein *S*-glutathionylation in plasmoredoxin

As mentioned above, Plrx possesses four cysteines which could be potentially targeted by glutathione. In Western blot analysis and mass spectrometry, only the two active site cysteines were glutathionylated. This is particular interesting, since C115 is potentially accessible for modification. The cytosol of *Plasmodium* is highly reducing, with a redox potential of -314 mV (Kasozi *et al*. 2013). The level of total glutathione in unstressed *Plasmodium* parasites is approximately 2 mM, with the majority being present as GSH (Becker *et al*. 2003a). As mentioned earlier, the direct reaction partner of Plrx is still unknown, meaning that a potential impact of glutathionylation on the activity of Plrx could not be addressed. Becker *et al*. showed that Plrx could be reduced by dithiols such as *Pf*Grx, *Pf*Trx, and trypanothione. Furthermore, Plrx was active in the insulin-reduction assay (Becker *et al*. 2003a), with Plrx receiving the needed electrons from the reducing agent dithiothreitol (DTT) (Becker *et al*. 2003a). Since DTT reduced disulfide-bonds of cysteines, it would not have been possible to detect a putative impact of post-translational cysteine modification in this assay.

Taken together, it remains to be elucidated if glutathionylated active site cysteines in Plrx have an impact on the redox activity within the parasite.

To continue, for *Pf*Plrx it has been shown that the protein was able to deglutathionylate and thus activate glutathionylized *Pf*GAPDH. Similar results could be shown for other redoxins (Kehr *et al*. 2011). *Pf*Plrx, *Pf*Trx and *Pf*Grx are also involved in the redox regulation of a large number of other proteins. *Pf*Plrx target proteins for deglutathionylation were especially active in protein folding and signal transduction but also in DNA synthesis and repair (Sturm *et al*. 2009).

This shows that Plrx seems to play an important role not only in redox regulation but also in other important processes within the organism. Interestingly, no essential role in the life cycle of the parasite *P. berghei* could be attributed to Plrx (Buchholz *et al*. 2008). One explanation for this dispensability could be redundancy in the functions of members of the thioredoxin family. A similar situation is found in different organisms. As one example, the yeast *Saccharomyces Cerevisiae* contains two thioredoxins and two glutaredoxins. Only the quadruple mutant is not viable. Each individual thioredoxin and glutaredoxin has the ability to compensate for the tasks of the missing redoxins (Draculic *et al*. 2000).

Protein *S*-nitrosation of plasmoredoxin

*Pf*Plrx was identified as target for *S*-nitrosation. As mentioned earlier, since the direct reaction partner of *Pf*Plrx is still unknown, the activity of this redoxin cannot be directly measured.

Due to the highest sequence similarity to thioredoxin, a comparison with thioredoxin is important at this point. So far, five thioredoxin-related proteins have been identified in *P. falciparum* in addition to plasmoredoxin (Nickel *et al*. 2006). The cytoplasmic Trx1 is the main substrate for thioredoxin reductase and is itself capable of reducing thioredoxin-dependent peroxidases. In addition, Trx1 is able to react directly with peroxides, dehydroascorbate, lipoic acid, GSSG and lipoamide. A mitochondrial localization has been demonstrated for Trx2 (Kehr *et al*. 2010). It also shows a general activity of disulfide reduction and serves as an electron donor for peroxiredoxins and glutathione disulfide. Trx3 has a potential apicoplast targeting sequence and can be reduced by *P. falciparum* thioredoxin reductase. Two other thioredoxin-like proteins have also been identified that are believed to have similar functions to classical thioredoxins.

Numerous studies have dealt with the influence of nitrosylated thioredoxin (Li *et al.* 2012, Wang *et al*. 2014). It has been shown that thioredoxin can transnitrosylate other proteins and also denitrosylate them. In addition to the active-site cysteines C32 and C35, human thioredoxin1 has three other cysteines outside the active-site sequence: C62, C69, and C73. Interestingly, C73 is responsible for transnitrosylation and the free active-site cysteine C32 in Trx1 is responsible for denitrosylation activities. *S*-nitrosylation of Trx1 shows an influence on the inhibition of cellular apoptosis, with Trx-1 mediated regulation of apoptosis via caspase-3 serving as example (Haendeler *et al*. 2002, Hashemy and Holmgren 2008, Wu *et al*. 2010). In a large study, Wang *et al.* identified 319 potential target proteins for *S*-nitrosylation in *Plasmodium falciparum*. Similar to human Trx1, *Pf*Trx1 has a third cysteine at position 43 in addition to the active-site cysteines. C43 of *Pf*Trx1 appears to be essential for S-nitrosylation of the protein. Furthermore, Wang *et al.* could show that *Pf*Trx1 acts as a general denitrosylase and also has a transnitrosylation activity that occurs via Cys43 (Wang *et al*. 2014).

As shown above, *Pf*Plrx has a large number of potential interaction proteins and thus an important status in the redox regulation of the malaria parasite *Plasmodium*

falciparum. In this thesis it could be shown that the active-site cysteines C60 and C63 of *Pf*Plrx are glutathionylated. In addition, Western blot analyses have shown that Plrx is nitrosylated. Since *Plasmodium* possesses a large number of thioredoxins and thioredoxin-like proteins, it can be assumed that Plrx can also be nitrosylated by Trx. Whether and how this post-translational modification alters or impairs the functions of *Pf*Plrx is an exciting question that should be addressed in the future.

References

Akerman, Susan E; Müller, Sylke (2003): 2-Cys peroxiredoxin *Pf*Trx-Px1 is involved in the antioxidant defence of *Plasmodium falciparum*. *Mol Biochem Parasitol* 130 (2), 75-81.

Andrews, Katherine T.; Lanzer, Michael (2002): Maternal malaria: *Plasmodium falciparum* sequestration in the placenta. *Parasitol Res* 88 (8), 715–723.

Andricopulo, A. D.; Akoachere, M. B.; Krogh, R.; Nickel, C.; McLeish, M. J.; Kenyon, G. L. *et al.* (2006): Specific inhibitors of *Plasmodium falciparum* thioredoxin reductase as potential antimalarial agents. *Bioorg Med Chem Lett* 16 (8), 2283–2292.

Angelucci, F. *et. al*. (2016): Typical 2-Cys peroxiredoxins in human parasites: Several physiological roles for a potential chemotherapy target. *Mol Biochem Parasitol* 206, 2-12.

Aravind, L.; Iyer, Lakshminarayan M.; Wellems, Thomas E.; Miller, Louis H. (2003): *Plasmodium* Biology. *Cell* 115 (7), 771–785.

Arnold, K., Bordoli, L., Kopp, J. & Schwede, T. (2006):The SWISS-MODEL workspace: a web-based environment for protein structure homology modelling. *Bioinformatics* 22, 195-201.

Artz, J. D. *et. al.* (2006): DOI: 10.2210/pdb2i81/pdb.

Atamna, Hani; Pascarmona, Gianpiero; Ginsburg, Hagai (1994): Hexose-monophosphate shunt activity in intact *Plasmodium falciparum*-infected erythrocytes and in free parasites. *Mol Biochem Parasitol* 67 (1), 79–89.

Ballou, W. R.; Rothbard, J.; Wirtz, R. A.; Gordon, D. M.; Williams, J. S.; Gore, R. W. *et al.* (1985): Immunogenicity of synthetic peptides from circumsporozoite protein of *Plasmodium falciparum*. *Science* 228 (4702), 996–999.

Banmeyer, Ingrid; Marchand, Cécile; Clippe, André; Knoops, Bernard (2005): Human mitochondrial peroxiredoxin 5 protects from mitochondrial DNA damages induced by hydrogen peroxide. *FEBS Lett* 579 (11), 2327–2333.

Becker, K.; Gromer, S.; Schirmer, R. H.; Müller, S. (2000): Thioredoxin reductase as a pathophysiological factor and drug target. *Eur J Biochem* 267 (20), 6118–6125.

Becker, Katja; Kanzok, Stefan M.; Iozef, Rimma; Fischer, Marina; Schirmer, R. Heiner; Rahlfs, Stefan (2003a): Plasmoredoxin, a novel redox-active protein unique for malarial parasites. *Eur J Biochem* 270 (6), 1057–1064.

Becker, Katja; Koncarevic, Sasa; Hunt, Nicholas H. (2005): Oxidative Stress and Antioxidant Defense in Malarial Parasites. *Sherman: Molecular Approaches to Malaria: ASM*, 365–383.

Becker, Katja; Rahlfs, Stefan; Nickel, Christine; Schirmer, R. Heiner (2003b): Glutathione--functions and metabolism in the malarial parasite *Plasmodium falciparum*. *Biol Chem* 384 (4), 551–566.

Becker, Katja; Tilley, Leann; Vennerstrom, Jonathan L.; Roberts, David; Rogerson, Stephen; Ginsburg, Hagai (2004): Oxidative stress in malaria parasite-infected erythrocytes: host-parasite interactions. *Int J Parasitol* 34 (2), 163–189.

Beeson, James G.; Amin, Nishal; Kanjala, Maxwell; Rogerson, Stephen J. (2002): Selective accumulation of mature asexual stages of *Plasmodium falciparum*-infected erythrocytes in the placenta. *Infect Immun* 70 (10), 5412–5415.

Benhar, Moran; Forrester, Michael T.; Stamler, Jonathan S. (2009): Protein denitrosylation: enzymatic mechanisms and cellular functions. *Nat Rev Mol Cell Biol* 10 (10), 721-732.

Berndt, Carsten; Lillig, Christopher Horst; Holmgren, Arne (2008): Thioredoxins and glutaredoxins as facilitators of protein folding. *Biochim Biophys Acta* 1783 (4), 641-650.

Bohme, C. C.; Arscott, L. D.; Becker, K.; Schirmer, R. H.; Williams, C. H. (2000): Kinetic characterization of glutathione reductase from the malarial parasite *Plasmodium falciparum*. Comparison with the human enzyme. *J Biol Chem* 275 (48), 37317–37323.

Boucher, Ian W.; McMillan, Paul J.; Gabrielsen, Mads; Akerman, Susan E.; Brannigan, James A.; Schnick, Claudia et al. (2006): Structural and biochemical characterization of a mitochondrial peroxiredoxin from *Plasmodium falciparum*. *Mol Microbiol* 61 (4), 948–959.

Brandstaedter, Christina (2017): Disulfide-dithiol exchange in thioredoxin-dependent reactions of *Plasmodium falciparum* and its human host cells. *Dissertation*.

Brandstaedter, Christina; Delahunty, Claire; Schipper, Susanne; Rahlfs, Stefan; Yates, John R.; Becker, Katja (2019): The interactome of 2-Cys peroxiredoxins in *Plasmodium falciparum*. *Sci Rep* 9 (1), 13542.

Brizuela, Mariana; Huang, Hong Ming; Smith, Clare; Burgio, Gaetan; Foote, Simon J.; McMorran, Brendan J. (2014): Treatment of erythrocytes with the 2-cys peroxiredoxin inhibitor, Conoidin A, prevents the growth of *Plasmodium falciparum* and enhances parasite sensitivity to chloroquine. *PloS One* 9 (4), e92411.

Broniowska, Katarzyna A.; Hogg, Neil (2012): The Chemical Biology of *S*-Nitrosothiols. *Antioxid Redox Signal* 17 (7), 969-980.

Buchholz, Kathrin; Putrianti, Elyzana D.; Rahlfs, Stefan; Schirmer, R. Heiner; Becker, Katja; Matuschewski, Kai (2010): Molecular genetics evidence for the in vivo roles of the two major NADPH-dependent disulfide reductases in the malaria parasite. *J Biol Chem* 285 (48), 37388–37395.

Buchholz, Kathrin; Rahlfs, Stefan; Schirmer, R. Heiner; Becker, Katja; Matuschewski, Kai (2008): Depletion of *Plasmodium berghei* plasmoredoxin reveals a non-essential role for life cycle progression of the malaria parasite. *PloS one* 3 (6), e2474.

Budde, Heike; Flohé, Leopold (2003): Enzymes of the thiol-dependent hydroperoxide metabolism in pathogens as potential drug targets. *Biofactors* 17 (1-4), 83–92.

Chae, H. Z.; Chung, S. J.; Rhee, S. G. (1994): Thioredoxin-dependent peroxide reductase from yeast. *J Biol Chem* 269 (44), 27670–27678.

Chae, H. Z.; Kang, S. W.; Rhee, S. G. (1999): Isoforms of mammalian peroxiredoxin that reduce peroxides in presence of thioredoxin. *Methods Enzymol* 300, 219–226.

Chang, J. W.; Jeon, H. B.; Lee, J. H.; Yoo, J. S.; Chun, J. S.; Kim, J. H.; Yoo, Y. J. (2001): Augmented expression of peroxiredoxin I in lung cancer. *Biochem Biophys Res Commun* 289 (2), 507–512.

Chang, Tong-Shin; Jeong, Woojin; Woo, Hyun Ae; Lee, Sun Mi; Park, Sunjoo; Rhee, Sue Goo (2004): Characterization of mammalian sulfiredoxin and its reactivation of hyperoxidized peroxiredoxin through reduction of cysteine sulfinic acid in the active site to cysteine. *J Biol Chem* 279 (49), 50994–51001.

Chen, Chun-An; Wang, Tse-Yao; Varadharaj, Saradhadevi; Reyes, Levy A.; Hemann, Craig; Hassan Talukder, M. A.; Chen, Yeong-Renn; Druhan, Lawrence J.; Zweier, Jay L. (2010): *S*-glutathionylation uncouples eNOS and regulates its cellular and vascular function. *Nature* 468 (7327), 1115-1118.

Chen, Wen; Ji, Jianguo; Xu, Xiaoman; He, Sizhi; Ru, Binggen (2003): Proteomic comparison between human young and old brains by two-dimensional gel electrophoresis and identification of proteins. *Int J Dev Neurosci* 21 (4), 209–216.

Chrestensen, C. A.; Starke, D. W.; Mieyal, J. J. (2000): Acute cadmium exposure inactivates thioltransferase (Glutaredoxin), inhibits intracellular reduction of protein-glutathionyl-mixed disulfides, and initiates apoptosis. *J Biol Chem* 275 (34), 26556-26565.

Clarebout, G.; Slomianny, C.; Delcourt, P.; Leu, B.; Masset, A.; Camus, D.; Dive, D. (1998): Status of *Plasmodium falciparum* towards catalase. *Br J Haematol* 103 (1), 52–59.

Clarke, Geraldine M. *et al.*(2017): Characterisation of the opposing effects of G6PD deficiency on cerebral malaria and severe malarial anaemia. *eLife* 6.

Clavreul, Nicolas; Adachi, Takeshi; Pimental, David R.; Ido, Yasuo; Schöneich, Christian; Cohen, Richard A. (2006): *S*-glutathiolation by peroxynitrite of p21ras at cysteine-118 mediates its direct activation and downstream signaling in endothelial cells. *FASEB J* 20 (3), 518-520.

Clementi, E.; Brown, G. C.; Feelisch, M.; Moncada, S. (1998): Persistent inhibition of cell respiration by nitric oxide: crucial role of S-nitrosylation of mitochondrial complex I and protective action of glutathione. *Proc Natl Sci USA* 95 (13), 7631-7636.

Copley, Shelley D.; Novak, Walter R. P.; Babbitt, Patricia C. (2004): Divergence of function in the thioredoxin fold suprafamily: evidence for evolution of peroxiredoxins from a thioredoxin-like ancestor. *Biochem* 43 (44), 13981-13995.

Cox-Singh, Janet; Davis, Timothy M. E.; Lee, Kim-Sung; Shamsul, Sunita S. G.; Matusop, Asmad; Ratnam, Shanmuga *et al*. (2008): *Plasmodium knowlesi* malaria in humans is widely distributed and potentially life threatening. *Clin Infect Dis* 46 (2), 165–171.

Dalle-Donne, Isabella; Rossi, Ranieri; Colombo, Graziano; Giustarini, Daniela; Milzani, Aldo (2009): Protein *S*-glutathionylation: a regulatory device from bacteria to humans. *Trends Biochem Sci* 34 (2), 85-96.

Deponte, Marcel; Becker, Katja; Rahlfs, Stefan (2005): *Plasmodium falciparum* glutaredoxin-like proteins. *Biol Chem* 386 (1), 33–40.

Deponte, Marcel; Rahlfs, Stefan; Becker, Katja (2007): Peroxiredoxin systems of protozoal parasites. *Subcell Biochem* 44, 219–229.

Djuika, Carine F.; Fiedler, Sabine; Schnölzer, Martina; Sanchez, Cecilia; Lanzer, Michael; Deponte, Marcel (2013): *Plasmodium falciparum* antioxidant protein as a model enzyme for a special class of glutaredoxin/glutathione-dependent peroxiredoxins. *Biochim Biophys Acta* 1830 (8), 4073–4090.

Djuika, Carine F.; Staudacher, Verena; Sanchez, Cecilia P.; Lanzer, Michael; Deponte, Marcel (2017): Knockout of the peroxiredoxin 5 homologue *PF*AOP does not affect the artemisinin susceptibility of *Plasmodium falciparum*. *Sci Rep* 7 (1), 4410.

Doerig, Christian; Rayner, Julian C.; Scherf, Artur; Tobin, Andrew B. (2015): Post-translational protein modifications in malaria parasites. *Nat Rev Microbiol* 13 (3), 160-172.

Draculic, T.; Dawes, I.W.; Grant, C.M. (2000): A single glutaredoxin or thioredoxin gene is essential for viability in the yeast *Saccharomyces cerevisiae*. *Mol Microbiol* 36 (5), 1167-1174.

Eckman, J. R.; Eaton, J. W. (1979): Dependence of plasmodial glutathione metabolism on the host cell. *Nature* 278 (5706), 754–756.

Emsley, P., Lohkamp, B., Scott, W. G. & Cowtan, K. (2010): Features and development of Coot. *Acta Crystallogr D Biol Crystallogr* 66, 486-501.

Engelman, Rotem; Weisman-Shomer, Pnina; Ziv, Tamar; Xu, Jianqiang; Arnér, Elias S. J.; Benhar, Moran (2013): Multilevel Regulation of 2-Cys Peroxiredoxin Reaction Cycle by S-Nitrosylation. *J Biol Chem* 288 (16), 11312-11324.

Farber, P. M.; Arscott, L. D.; Williams, C. H., JR; Becker, K.; Schirmer, R. H. (1998): Recombinant *Plasmodium falciparum* glutathione reductase is inhibited by the antimalarial dye methylene blue. *FEBS Lett* 422 (3), 311–314.

Feld, Kristina; Geissel, Fabian; Liedgens, Linda; Schumann, Robin; Specht, Sandra; Deponte, Marcel (2019): Tyrosine substitution of a conserved active-site histidine residue activates *Plasmodium falciparum* peroxiredoxin 6. *Protein Sci* 28 (1), 100–110.

Ferrari, Carlos K. B.; Souto, Paula C. S.; França, Eduardo L.; Honorio-França, Adenilda C. (2011): Oxidative and nitrosative stress on phagocytes' function: from effective defense to immunity evasion mechanisms. *Arch Immunol Ther Ex* 59 (6), 441-448.

Flohé, Leopold; Budde, Heike; Bruns, Karsten; Castro, Helena; Clos, Joachim; Hofmann, Birgit *et al*. (2002): Tryparedoxin peroxidase of *Leishmania donovani*: molecular cloning, heterologous expression, specificity, and catalytic mechanism. *Arch Biochem Biophys* 397 (2), 324–335.

Forman, Henry Jay; Maiorino, Matilde; Ursini, Fulvio (2010): Signaling Functions of Reactive Oxygen Species. *Biochemistry* 49 (5), 835-842.

Forrester, Michael T.; Foster, Matthew W.; Benhar, Moran; Stamler, Jonathan S. (2008): Detection of Protein *S*-Nitrosylation with the Biotin Switch Technique. *Free radical Bio Med* 46 (2), 119-126.

Francis, Sharron H.; Busch, Jennifer L.; Corbin, Jackie D.; Sibley, David (2010): cGMP-dependent protein kinases and cGMP phosphodiesterases in nitric oxide and cGMP action. *Pharmacol Rev* 62 (3), 525-563.

Friebolin, Wolfgang; Jannack, Beate; Wenzel, Nicole; Furrer, Julien; Oeser, Thomas; Sanchez, Cecilia P. *et al*. (2008): Antimalarial dual drugs based on potent inhibitors of glutathione reductase from *Plasmodium falciparum*. *J Med Chem* 51 (5), 1260–1277.

Goldberg, D. E.; Slater, A.F.G. (1992): The pathway of hemoglobin degradation in malaria parasites. *Parasitol Today* 8 (8), 280–283.

Greetham, D., Vickerstaff, J., Shenton, D., Perrone, G.G., Dawes, I.W., Grant, C.M. (2010): Thioredoxins function as deglutathionylase enzymes in the yeast *Saccharomyces cerevisiae*. *BMC Biochem* 11 (3).

Grek, Christina L.; Zhang, Jie; Manevich, Yefim; Townsend, Danyelle M.; Tew, Kenneth D. (2013): Causes and Consequences of Cysteine *S*-Glutathionylation. *J Biol Chem* 288 (37), 26497-26504.

Gretes, Michael C.; Poole, Leslie B.; Karplus, P. Andrew (2012): Peroxiredoxins in parasites. *Antioxid Redox Sign* 17 (4), 608–633.

Grossi, Loris; Montevecchi, Pier Carlo (2002): *S*-nitrosocysteine and cystine from reaction of cysteine with nitrous acid. A kinetic investigation. *J Org Chem* 67 (24), 8625-8630.

Haendler, J.; Hoffmann, J.; Tischler, V.;Berk, B.C.; Zeiher, A.M.; Dimmeler, S. (2002): Redox regulatory and anti-apoptotic functions of thioredoxin depend on S-nitrosylation at cysteine 69. Nat Cell Biol 4, 743-749.

Hall, Andrea; Nelson, Kimberly; Poole, Leslie B.; Karplus, P. Andrew (2011): Structure-based insights into the catalytic power and conformational dexterity of peroxiredoxins. *Antioxid Redox Sign* 15 (3), 795–815.

Hanschmann, Eva-Maria; Godoy, José Rodrigo; Berndt, Carsten; Hudemann, Christoph; Lillig, Christopher Horst (2013): Thioredoxins, glutaredoxins, and peroxiredoxins--molecular mechanisms and health significance: from cofactors to antioxidants to redox signaling. *Antioxid Redox Sign* 19 (13), 1539–1605.

Hara, Makoto R.; Agrawal, Nishant; Kim, Sangwon F.; Cascio, Matthew B.; Fujimuro, Masahiro; Ozeki, Yuji; Takahashi, Masaaki; Cheah, Jaime H.; Tankou, Stephanie K.; Hester, Lynda D.; Ferris, Christopher D.; Hayward, S. Diane; Snyder, Solomon H.; Sawa, Akira (2005): *S*-nitrosylated GAPDH initiates apoptotic cell death by nuclear translocation following Siah1 binding. *Nat Cell Biol* 7 (7), 665-674.

Harding, J. J.; Blakytny, R.; Ganea, E. (1996): Glutathione in disease. *Biochem Soc Trans* 24 (3), 881-884.

Hashemy, S.I.; Holmgren, A. (2008): Regulation of the catalytic activity and structure of human thioredoxin 1 via oxidation and S-nitrosylation of cysteine residues. *J Biol Chem* 283, 21890-21898.

Hess, Douglas T.; Matsumoto, Akio; Kim, Sung-Oog; Marshall, Harvey E.; Stamler, Jonathan S. (2005): Protein *S*-nitrosylation: purview and parameters. *Nat Rev Mol Cell Biol* 6 (2), 150-166.

Hess, Douglas T.; Stamler, Jonathan S. (2012): Regulation by *S*-nitrosylation of protein post-translational modification. *J Biol Chem* 287 (7), 4411-4418.

Holmgren, A. (1978): Glutathione-dependent enzyme reactions of the phage T4 ribonucleotide reductase system. *J Biol Chem* 253 (20), 7424–7430.

Holmgren, A. (1979): Glutathione-dependent synthesis of deoxyribonucleotides. Purification and characterization of glutaredoxin from *Escherichia coli*. *J Biol Chem* 254 (9), 3664–3671.

Holmgren, A.; Bjornstedt, M. (1995): Thioredoxin and thioredoxin reductase. *Methods Enzymol* 252, 199–208.

Huh, Joo Young; Kim, Yunghee; Jeong, Jaeho; Park, Jehyun; Kim, Inok; Huh, Kyu Ha; Kim, Yu Seun; Woo, Hyun Ae; Rhee, Sue Goo; Lee, Kong-Joo; Ha, Hunjoo (2012): Peroxiredoxin 3 is a key molecule regulating adipocyte oxidative stress, mitochondrial biogenesis, and adipokine expression. *Antioxid Redox Sign* 16 (3), 229-243.

Hunt, N. H.; Stocker, R. (1990): Oxidative stress and the redox status of malaria-infected erythrocytes. *Blood cells* 16 (2-3), 499.

Idro, Richard; Marsh, Kevin; John, Chandy C.; Newton, Charles R. J. (2010): Cerebral malaria: mechanisms of brain injury and strategies for improved neurocognitive outcome. *Pediatr Res* 68 (4), 267–274.

Jaeger, Timo; Flohé, Leopold (2006): The thiol-based redox networks of pathogens: unexploited targets in the search for new drugs. *Biofactors* 27 (1-4), 109–120.

Jortzik, Esther; Becker, Katja (2012): Thioredoxin and glutathione systems in *Plasmodium falciparum*. *Int J Med Microbiol Suppl* 302 (4-5), 187–194.

Kamariah, N., Sek, M. F., Eisenhaber, B., Eisenhaber, F. & Gruber, G. (2016): Transition steps in peroxide reduction and a molecular switch for peroxide robustness of prokaryotic peroxiredoxins. *Sci Rep.* 6, 37610.

Kanzok, S. M.; Schirmer, R. H.; Turbachova, I.; Iozef, R.; Becker, K. (2000): The thioredoxin system of the malaria parasite *Plasmodium falciparum*. Glutathione reduction revisited. *J Biol Chem* 275 (51), 40180–40186.

Karplus, P. A.; Schulz, G. E. (1987): Refined structure of glutathione reductase at 1.54 A resolution. *J Mol Biol* 195 (3), 701–729.

Karplus, P. Andrew; Hall, Andrea (2007): Structural survey of the peroxiredoxins. *Subcell biochem* 44, 41–60.

Kasozi, Denis; Mohring, Franziska; Rahlfs, Stefan; Meyer, Andreas J.; Becker, Katja (2013): Real-time imaging of the intracellular glutathione redox potential in the malaria parasite *Plasmodium falciparum*. *PLoS Pathog* 9 (12), e1003782.

Kawazu, Shin-ichiro; Komaki, Kanako; Tsuji, Naotoshi; Kawai, Satoru; Ikenoue, Nozomu; Hatabu, Toshimitsu; Ishikawa, Hiroyuki; Matsumoto, Yoshitsugu; Himeno, Kunisuke; Kano, Shigeyuki (2001): Molecular characterization of a 2-Cys peroxiredoxin from the human malaria parasite *Plasmodium falciparum*. *Mol Biochem Parasitol* 116(1), 73-79.

Kawazu, Shin-ichiro; Ikenoue, Nozomu; Takemae, Hitoshi; Komaki-Yasuda, Kanako; Kano, Shigeyuki (2005): Roles of 1-Cys peroxiredoxin in haem detoxification in the human malaria parasite *Plasmodium falciparum*. *FEBS J* 272 (7), 1784–1791.

Kehr, Sebastian; Jortzik, Esther; Delahunty, Claire; Yates, John R.; Rahlfs, Stefan; Becker, Katja (2011): Protein *S*-glutathionylation in malaria parasites. *Antioxid Redox Sign* 15 (11), 2855–2865.

Kehr, Sebastian; Sturm, Nicole; Rahlfs, Stefan; Przyborski, Jude M.; Becker, Katja (2010): Compartmentation of redox metabolism in malaria parasites. *PLoS Pathog* 6 (12),. e1001242.

Kim, S. H.; Fountoulakis, M.; Cairns, N.; Lubec, G. (2001): Protein levels of human peroxiredoxin subtypes in brains of patients with Alzheimer's disease and Down syndrome. *J Neural Transm-Supp* (61), 223–235.

Kim, Sangwon; Wing, Simon S.; Ponka, Prem (2004): *S*-nitrosylation of IRP2 regulates its stability via the ubiquitin-proteasome pathway. *Mol Cell Biol* 24 (1), 330-337.

Kimura, Risa; Komaki-Yasuda, Kanako; Kawazu, Shin-ichiro; Kano, Shigeyuki (2013): 2-Cys peroxiredoxin of *Plasmodium falciparum* is involved in resistance to heat stress of the parasite. *Parasitol Int* 62 (2), 137–143.

Klotz, F. W.; Hadley, T. J.; Aikawa, M.; Leech, J.; Howard, R. J.; Miller, L. H. (1989): A 60-kDa *Plasmodium falciparum* protein at the moving junction formed between merozoite and erythrocyte during invasion. *Mol Biochem Parasitol* 36 (2), 177–185.

Komaki-Yasuda, Kanako; Kawazu, Shin-ichiro; Kano, Shigeyuki (2003): Disruption of the *Plasmodium falciparum* 2-Cys peroxiredoxin gene renders parasites hypersensitive to reactive oxygen and nitrogen species. *FEBS Lett* 547 (1-3), 140–144.

Koncarevic, Sasa; Rohrbach, Petra; Deponte, Marcel; Krohne, Georg; Prieto, Judith Helena; Yates, John *et al.* (2009): The malarial parasite *Plasmodium falciparum* imports the human protein peroxiredoxin 2 for peroxide detoxification. *Proc Natl Acad Sci USA* 106 (32), 13323–13328.

König, Janine; Lotte, Kirsten; Plessow, Regina; Brockhinke, Andreas; Baier, Margarete; Dietz, Karl-Josef (2003): Reaction mechanism of plant 2-Cys peroxiredoxin. Role of the C terminus and the quaternary structure. *J Biol Chem* 278 (27), 24409–24420.

Krapfenbauer, Kurt; Engidawork, Ephrem; Cairns, Nigel; Fountoulakis, Michael; Lubec, Gert (2003): Aberrant expression of peroxiredoxin subtypes in neurodegenerative disorders. *Brain Res* 967 (1-2), 152–160.

Krauth-Siegel, R. Luise; Bauer, Holger; Schirmer, R. Heiner (2005): Dithiol proteins as guardians of the intracellular redox milieu in parasites: old and new drug targets in *trypanosomes* and malaria-causing *plasmodia*. *Angewandte Chemie* 44 (5), 690–715.

Krnajski, Zita; Gilberger, Tim-Wolf; Walter, Rolf D.; Cowman, Alan F.; Müller, Sylke (2002): Thioredoxin reductase is essential for the survival of *Plasmodium falciparum* erythrocytic stages. *J Biol Chem* 277 (29), 25970–25975.

Li, Huili; Wan, Ajun; Xu, Guoqiang; Ye, Dequan (2013): Small changes huge impact: the role of thioredoxin 1 in the regulation of apoptosis by *S*-nitrosylation. *Acta Biochim Biophys Sin* 45, 153-161.

Lillig, Christopher Horst; Berndt, Carsten; Holmgren, Arne (2008): Glutaredoxin systems. *Biochim Biophys Acta* 1780 (11), 1304-1317.

Loberg, Matthew A.; Hurtig, Jennifer E.; Graff, Aaron H.; Allan, Kristin M.; Buchan, John A.; Spencer, Matthew K. *et al*. (2019): Aromatic Residues at the Dimer-Dimer Interface in the Peroxiredoxin Tsa1 Facilitate Decamer Formation and Biological Function. *Chem Res Toxicol* 32 (3), 474–483.

Low, Felicia M.; Hampton, Mark B.; Winterbourn, Christine C. (2008): Peroxiredoxin 2 and peroxide metabolism in the erythrocyte. *Antioxid Redox Sign* 10 (9), 1621–1630.

Lucantoni, Leonardo; Duffy, Sandra; Adjalley, Sophie H.; Fidock, David A.; Avery, Vicky M. (2013): Identification of MMV malaria box inhibitors of *Plasmodium falciparum* early-stage gametocytes using a luciferase-based high-throughput assay. *Antimicrob Agents Chemother* 57 (12), 6050–6062.

Luiking, Yvette C.; Engelen, Mariëlle P. K. J.; Deutz, Nicolaas E. P. (2010): Regulation of nitric oxide production in health and disease. *Curr Opin Clin Nutr* 13 (1), 97-104.

Martínez-Ruiz, Antonio; Lamas, Santiago (2004): *S*-nitrosylation: a potential new paradigm in signal transduction. *Cardiovasc Res* 62 (1), 43-52.

Masuda-Suganuma, Hirono; Usui, Miho; Fukumoto, Shinya; Inoue, Noboru; Kawazu, Shin-ichiro (2012): Mitochondrial peroxidase TPx-2 is not essential in the blood and insect stages of *Plasmodium berghei*. *Parasite vector* 5, 252.

Matsumura, Tomohiro; Okamoto, Ken; Iwahara, Shin-ichiro; Hori, Hiroyuki; Takahashi, Yuriko; Nishino, Takeshi; Abe, Yasuko (2008): Dimer-oligomer interconversion of wild-type and mutant rat 2-Cys peroxiredoxin: disulfide formation at dimer-dimer interfaces is not essential for decamerization. *J Biol Chem* 283 (1), 284-293.

Meierjohann, Svenja; Walter, Rolf D.; Müller, Sylke (2002): Glutathione synthetase from *Plasmodium falciparum*. *Biochem J* 363 (Pt 3), 833–838.

Metzger, Wolfram Gottfried; Sulyok, Zita; Theurer, Antje; Köhler, Carsten (2020): Entwicklung von Impfstoffen gegen Malaria – aktueller Stand. *Bundesgesundheitsblatt, Gesundheitsforschung, Gesundheitsschutz* 63 (1), 45–55.

Montemartini, M.; Kalisz, H. M.; Hecht, H. J.; Steinert, P.; Flohé, L. (1999): Activation of active-site cysteine residues in the peroxiredoxin-type tryparedoxin peroxidase of *Crithidia fasciculata*. *Eur J Biochem* 264 (2), 516–524.

Moore, R. B.; Mankad, M. V.; Shriver, S. K.; Mankad, V. N.; Plishker, G. A. (1991): Reconstitution of Ca(2+)-dependent K+ transport in erythrocyte membrane vesicles requires a cytoplasmic protein. *J Biol Chem* 266 (28), 18964–18968.

Morais, Mariana A. B.; Giuseppe, Priscila O.; Souza, Tatiana A. C. B.; Alegria, Thiago G. P.; Oliveira, Marcos A.; Netto, Luis E. S.; Murakami, Mario T. (2015): How pH modulates the dimer-decamer interconversion of 2-Cys peroxiredoxins from the Prx1 subfamily. *J Biol Chem* 290 (13), 8582-8590.

Muller, S.; Gilberger, T. W.; Krnajski, Z.; Luersen, K.; Meierjohann, S.; Walter, R. D. (2001): Thioredoxin and glutathione system of malaria parasite *Plasmodium falciparum*. *Protoplasma* 217 (1-3), 43–49.

Müller, Sylke (2004): Redox and antioxidant systems of the malaria parasite *Plasmodium falciparum*. *Mol Microbiol* 53 (5), 1291–1305.

Nakamura, Tomohiro; Lipton, Stuart A. (2013): Emerging role of protein-protein transnitrosylation in cell signaling pathways. *Antioxid Redox Sign* 18 (3), 239-249.

Nakamura, T. *et. al*. (2010): Crystal structure of peroxiredoxin from *Aeropyrum pernix* K1 complexed with its substrate, hydrogen peroxide. *J Biochem* 147, 109-115.

Nakaso, Kazuhiro; Kitayama, Michio; Mizuta, Einosuke; Fukuda, Hiroki; Ishii, Tetsuro; Nakashima, Kenji; Yamada, Kazuo (2000): Co-induction of heme oxygenase-1 and peroxiredoxin I in astrocytes and microglia around hemorrhagic region in the rat brain. *Neurosci Lett* 293 (1), 49–52.

Nakaso, Kazuhiro; Yano, Hidetaka; Fukuhara, Yoko; Takeshima, Takao; Wada-Isoe, Kenji; Nakashima, Kenji (2003): PI3K is a key molecule in the Nrf2-mediated regulation of antioxidative proteins by hemin in human neuroblastoma cells. *FEBS Lett* 546 (2-3), 181–184.

Nelson, Kimberly J.; Perkins, Arden; Van Swearingen, Amanda E D; Hartman, Steven; Brereton, Andrew E.; Parsonage, Derek *et al.* (2018): Experimentally Dissecting the Origins of Peroxiredoxin Catalysis. *Antioxid Redox Sign* 28 (7), 21–536.

Neumann, Carola A.; Krause, Daniela S.; Carman, Christopher V.; Das, Shampa; Dubey, Devendra P.; Abraham, Jennifer L. *et al.* (2003): Essential role for the peroxiredoxin Prdx1 in erythrocyte antioxidant defence and tumour suppression. *Nature* 424 (6948), 561–565.

Nguetse, Christian N.; Meyer, Christian G.; Adegnika, Ayola Akim; Agbenyega, Tsiri; Ogutu, Bernhards R.; Kremsner, Peter G.; Velavan, Thirumalaisamy P. (2016): Glucose-6-phosphate dehydrogenase deficiency and reduced haemoglobin levels in African children with severe malaria. *Malar J* 15 (1), 346.

Nickel, Christine; Rahlfs, Stefan; Deponte, Marcel; Koncarevic, Sasa; Becker, Katja (2006): Thioredoxin networks in the malarial parasite *Plasmodium falciparum*. *Antioxid Redox Sign* 8 (7-8), 1227–1239.

Nickel, Christine; Trujillo, Madia; Rahlfs, Stefan; Deponte, Marcel; Radi, Rafael; Becker, Katja (2005): *Plasmodium falciparum* 2-Cys peroxiredoxin reacts with plasmoredoxin and peroxynitrite. *Biol Chem* 386 (11), 1129–1136.

Nirudodhi, Sasidhar; Parsonage, Derek; Karplus, P. Andrew; Poole, Leslie B.; Maier, Claudia S. (2011): Conformational studies of the robust 2-Cys peroxiredoxin *Salmonella typhimurium* AhpC by solution phase hydrogen/deuterium (H/D) exchange monitored by electrospray ionization mass spectrometry. *Int J Mass Spectrom* 302 (1-3), 93-100.

Nogueira, Fernanda B.; Ruiz, Jerônimo C.; Robello, Carlos; Romanha, Alvaro J.; Murta, Silvane M. F. (2009): Molecular characterization of cytosolic and mitochondrial tryparedoxin peroxidase in *Trypanosoma cruzi* populations susceptible and resistant to benznidazole. *Parasitol Res* 104 (4), 835–844.

Park, Ji Won; Mieyal, John J.; Rhee, Sue Goo; Chock, P. Boon (2009): Deglutathionylation of 2-Cys peroxiredoxin is specifically catalyzed by sulfiredoxin. *J Biol Chem* 284 (35), 23364-23374

Park, Ji Won; Piszczek, Grzegorz; Rhee, Sue Goo; Chock, P. Boon (2011): Glutathionylation of peroxiredoxin I induces decamer to dimers dissociation with concomitant loss of chaperone activity. *Biochemistry* 50 (15), 3204-3210.

Park, Mi Hee; Jo, MiRan; Kim, Yu Ri; Lee, Chong-Kil; Hong, Jin Tae (2016): Roles of peroxiredoxins in cancer, neurodegenerative diseases and inflammatory diseases. *Pharmacol Ther* (163), 1-23.

Parsonage, Derek; Youngblood, Derek S.; Sarma, Ganapathy N.; Wood, Zachary A.; Karplus, P. Andrew; Poole, Leslie B. (2005): Analysis of the link between enzymatic activity and oligomeric state in AhpC, a bacterial peroxiredoxin. *Biochemistry* 44 (31), 10583–10592.

Pastrana-Mena, Rebecca; Dinglasan, Rhoel R.; Franke-Fayard, Blandine; Vega-Rodríguez, Joel; Fuentes-Caraballo, Mariela; Baerga-Ortiz, Abel *et al*. (2010): Glutathione reductase-null malaria parasites have normal blood stage growth but arrest during development in the mosquito. *J Biol Chem* 285 (35), 27045–27056.

Patzewitz, Eva-Maria; Wong, Eleanor H.; Müller, Sylke (2012): Dissecting the role of glutathione biosynthesis in *Plasmodium falciparum*. *Mol microbio*l 83 (2), 304–318.

Perkins, Arden; Nelson, Kimberly J.; Williams, Jared R.; Parsonage, Derek; Poole, Leslie B.; Karplus, P. Andrew (2013): The sensitive balance between the fully folded and locally unfolded conformations of a model peroxiredoxin. *Biochemistry* 52 (48), 8708–8721.

Perkins, Arden; Poole, Leslie B.; Karplus, P. Andrew (2014): Tuning of peroxiredoxin catalysis for various physiological roles. *Biochemistry* 53 (49), 7693–7705.

Peskin, Alexander V.; Pace, Paul E.; Behring, Jessica B.; Paton, Louise N.; Soethoudt, Marjolein; Bachschmid, Markus M.; Winterbourn, Christine C. (2015): Glutathionylation of the Active Site Cysteines of Peroxiredoxin 2 and Recycling by Glutaredoxin. *J Biol Chem* 291 (6), 3053-3062.

Peterson, Tina M. L.; Gow, Andrew J.; Luckhart, Shirley (2007): Nitric oxide metabolites induced in *Anopheles stephensi* control malaria parasite infection. *Free Radic Biol Med* 42 (1), 132-142.

Pettersen, E. F. *et. al*. (2004): UCSF Chimera-a visualization system for exploratory research and analysis. *J Comput Chem* 25, 1605-1612.

Rahlfs, S.; Becker, K. (2001): Thioredoxin peroxidases of the malarial parasite *Plasmodium falciparum*. *Eur J Biochem* 268 (5), 1404–1409.

Rahlfs, S.; Fischer, M.; Becker, K. (2001): *Plasmodium falciparum* possesses a classical glutaredoxin and a second, glutaredoxin-like protein with a PICOT homology domain. *J Biol Chem* 276 (40), 37133–37140.

Rahlfs, S.; Schirmer, R. H.; Becker, K. (2002): The thioredoxin system of *Plasmodium falciparum* and other parasites. *Cell Mol Life Sci* 59 (6), 1024–1041.

Rahlfs, Stefan; Nickel, Christine; Deponte, Marcel; Schirmer, R. Heiner; Becker, Katja (2003): *Plasmodium falciparum* thioredoxins and glutaredoxins as central players in redox metabolism. *Redox Rep : communications in free radical research* 8 (5), 246–250.

Ranjan, Ravi; Karpurapu, Manjula; Rani, Asha; Chishti, Athar H.; Christman, John W. (2016): Hemozoin Regulates iNOS Expression by Modulating the Transcription Factor NF-κB in Macrophages. *Biochem Mol Biol J* 2 (2).

Reeves, Stacy A.; Parsonage, Derek; Nelson, Kimberly J.; Poole, Leslie B. (2011): Kinetic and thermodynamic features reveal that *Escherichia coli* BCP is an unusually versatile peroxiredoxin. *Biochemistry* 50 (41), 8970-8981.

Richard, Dave; Bartfai, Richard; Volz, Jennifer; Ralph, Stuart A.; Muller, Sylke; Stunnenberg, Hendrik G.; Cowman, Alan F. (2011): A genome-wide chromatin-associated nuclear peroxiredoxin from the malaria parasite *Plasmodium falciparum*. *J Biol Chem* 286 (13), 11746–11755.

Russo Krauss, Irene; Merlino, Antonello; Vergara, Alessandro; Sica, Filomena (2013): An overview of biological macromolecule crystallization. *Int J Mol Sci* 14 (6), 11643-11691.

Salamanca, David Ricardo; Gómez, Marcela; Camargo, Anny; Cuy-Chaparro, Laura; Molina-Franky, Jessica; Reyes, César *et al*. (2019): *Plasmodium falciparum* Blood Stage Antimalarial Vaccines: An Analysis of Ongoing Clinical Trials and New Perspectives Related to Synthetic Vaccines. *Front Microbiol* 10, 2712.

Sannella, Anna Rosa; Casini, Angela; Gabbiani, Chiara; Messori, Luigi; Bilia, Anna Rita; Vincieri, Francesco Franco *et al.* (2008): New uses for old drugs. Auranofin, a clinically established antiarthritic metallodrug, exhibits potent antimalarial effects in vitro: Mechanistic and pharmacological implications. *FEBS Lett* 582 (6), 844–847.

Sarma, Ganapathy N.; Nickel, Christine; Rahlfs, Stefan; Fischer, Marina; Becker, Katja; Karplus, P. Andrew (2005): Crystal structure of a novel *Plasmodium falciparum* 1-Cys peroxiredoxin. *J Mol Biol* 346 (4), 1021–1034.

Schlitzer, Martin (2008): Antimalarial drugs - what is in use and what is in the pipeline. *Archiv der Pharmazie* 341 (3), 149–163.

Schröder, Ewald; Littlechil*, Jennifer A.; Lebedev, Andrey A.; Errington, Neil; Vagin, Alexei A.; Isupov, Michail N. (2000): Crystal structure of decameric 2-Cys peroxiredoxin from human erythrocytes at 1.7Å resolution. *Structure* 8 (6), 605–615.

Söhling, B.; Parther, T.; Rücknagel, K. P.; Wagner, M. A.; Andreesen, J. R. (2001): A selenocysteine-containing peroxiredoxin from the strictly anaerobic organism *Eubacterium acidaminophilum*. *Biol Chem* 382 (6), 979–986.

Stomberski, Colin T.; Hess, Douglas T.; Stamler, Jonathan S. (2019): Protein *S*-Nitrosylation: Determinants of Specificity and Enzymatic Regulation of S-Nitrosothiol-Based Signaling. *Antioxid Redox Sign* 30 (10), 1331-1351.

Ströher, Elke; Millar, A. Harvey (2012): The biological roles of glutaredoxins. *Biochem J* 446 (3), 333-348.

Sturm, Nicole; Jortzik, Esther; Mailu, Boniface M.; Koncarevic, Sasa; Deponte, Marcel; Forchhammer, Karl *et al*. (2009): Identification of proteins targeted by the thioredoxin superfamily in *Plasmodium falciparum*. *PLoS Pathog* 5 (4), e1000383.

Sztajer, H.; Gamain, B.; Aumann, K. D.; Slomianny, C.; Becker, K.; Brigelius-Flohé, R.; Flohé, L. (2001): The putative glutathione peroxidase gene of *Plasmodium falciparum* codes for a thioredoxin peroxidase. *J Biol Chem* 276 (10), 7397–7403.

Tairum, Carlos A.; Oliveira, Marcos A. de; Horta, Bruno B.; Zara, Fernando J.; Netto, Luis E. S. (2012): Disulfide biochemistry in 2-cys peroxiredoxin: requirement of Glu50 and Arg146 for the reduction of yeast Tsa1 by thioredoxin. *J Mol Biol* 424 (1-2), 28–41.

Tairum, Carlos A.; Santos, Melina Cardoso; Breyer, Carlos A.; Geyer, R. Ryan; Nieves, Cecilia J.; Portillo-Ledesma, Stephanie *et al*. (2016): Catalytic Thr or Ser Residue Modulates Structural Switches in 2-Cys Peroxiredoxin by Distinct Mechanisms. *Sci Rep* 6, 33133.

Tehan, Lauren; Taparra, Kekoa; Phelan, Shelley (2013): Peroxiredoxin overexpression in MCF-7 breast cancer cells and regulation by cell proliferation and oxidative stress. *Cancer Invest* 31 (6), 374–384.

Thomas, S.; Anup, R.; Susama, P.; Balasubramanian, K. A. (2001): Nitric oxide prevents intestinal mitochondrial dysfunction induced by surgical stress. *Brit J Surg* 88 (3), 393-399.

Tuteja, Renu (2007): Malaria - an overview. *FEBS J* 274 (18), 4670–4679.

Urig, Sabine; Becker, Katja (2006): On the potential of thioredoxin reductase inhibitors for cancer therapy. *Semin Cancer Biol* 16 (6), 452–465.

Vedadi, M. *et. al*. (2007): Genome-scale protein expression and structural biology of *Plasmodium falciparum* and related apicomplexan organisms. *Mol Biochem Parasitol*. 151, 100-110.

Wang, Lihui; Delahunty, Claire; Prieto, Judith Helena; Rahlfs, Stefan; Jortzik, Esther; Yates, John R.; Becker, Katja (2014): Protein *S*-nitrosylation in *Plasmodium falciparum*. *Antioxid Redox Sign* 20 (18), 2923-2935.

Wassmann, C.; Hellberg, A.; Tannich, E.; Bruchhaus, I. (1999): Metronidazole resistance in the protozoan parasite *Entamoeba histolytica* is associated with increased expression of iron-containing superoxide dismutase and peroxiredoxin and decreased expression of ferredoxin 1 and flavin reductase. *J Biol Chem* 274 (37), 26051–26056.

Wellems, T. E.; Plowe, C. V. (2001): Chloroquine-resistant malaria. *J Infect Dis* 184 (6), 770–776.

Winzeler, Elizabeth Ann (2008): Malaria research in the post-genomic era. *Nature* 455 (7214), 751–756.

Wood, Zachary A.; Poole, Leslie B.; Hantgan, Roy R.; Karplus, P. Andrew (2002): Dimers to doughnuts: redox-sensitive oligomerization of 2-cysteine peroxiredoxins. *Biochemistry* 41 (17), 5493–5504.

Wood, Zachary A.; Poole, Leslie B.; Karplus, P. Andrew (2003a): Peroxiredoxin evolution and the regulation of hydrogen peroxide signaling. *Science* 300 (5619), 650–653.

Wood, Zachary A.; Schröder, Ewald; Robin Harris, J.; Poole, Leslie B. (2003b): Structure, mechanism and regulation of peroxiredoxins. *Trends Biochem Sci* 28 (1), 32–40.

World Health Organisation (2019): *World malaria report.* WHO. Geneva, Switzerland.

Wu, C.; Liu, T.; Chen, W.; Oka, S.; Fu, C.; Jain, M.R.; Parrott, A.M. *et. al.*(2010): Redox regulatory mechanism of transnitrosylation by thioredoxin. *Mol Cell Proteomics* 9, 2262-2275.

Xiong, Ying; Uys, Joachim D.; Tew, Kenneth D.; Townsend, Danyelle M. (2011): *S*-Glutathionylation: From Molecular Mechanisms to Health Outcomes. *Antioxid Redox Sign* 15 (1), 233-270.

Yano, Kazuhiko; Komaki-Yasuda, Kanako; Kobayashi, Tamaki; Takemae, Hitoshi; Kita, Kiyoshi; Kano, Shigeyuki; Kawazu, Shin-ichiro (2005): Expression of mRNAs and proteins for peroxiredoxins in *Plasmodium falciparum* erythrocytic stage. *Parasitol Int* 54 (1), 35–41.

Yano, Kazuhiko; Komaki-Yasuda, Kanako; Tsuboi, Takafumi; Torii, Motomi; Kano, Shigeyuki; Kawazu, Shin-ichiro (2006): 2-Cys Peroxiredoxin TPx-1 is involved in gametocyte development in *Plasmodium berghei*. *Mol Biochem Parasitol* 148 (1), 44-51.

Young, M. D.; Moore, D. V. (1961): Chloroquine resistance in *Plasmodium falciparum*. *Am J Trop Med Hyg* 10, 317–320.

Zhou, Y.; Kok, K. H.; Chun, A. C.; Wong, C. M.; Wu, H. W.; Lin, M. C. *et al*. (2000): Mouse peroxiredoxin V is a thioredoxin peroxidase that inhibits p53-induced apoptosis. *Biochem Biophys Res Commun* 268 (3), 921–927.